Approximate methods for nuclei (I)

Artur M. Ankowski
SLAC National Accelerator Laboratory

NuSTEC Training in Neutrino-Nucleus Scattering Physics
Fermilab, November 7–15, 2017

Outline

1) **Introduction**
- Neutrino oscillations in a nutshell
- Accurate neutrino-energy reconstruction requires an accurate modeling of nuclear effects

2) **Impulse approximation**
- Why to test nuclear models using electron scattering data
- Fermi gas model
- Shell model
- Spectral function approach
- Final-state interactions in the spectral function approach

3) **Summary**

Neutrino oscillations in a nutshell

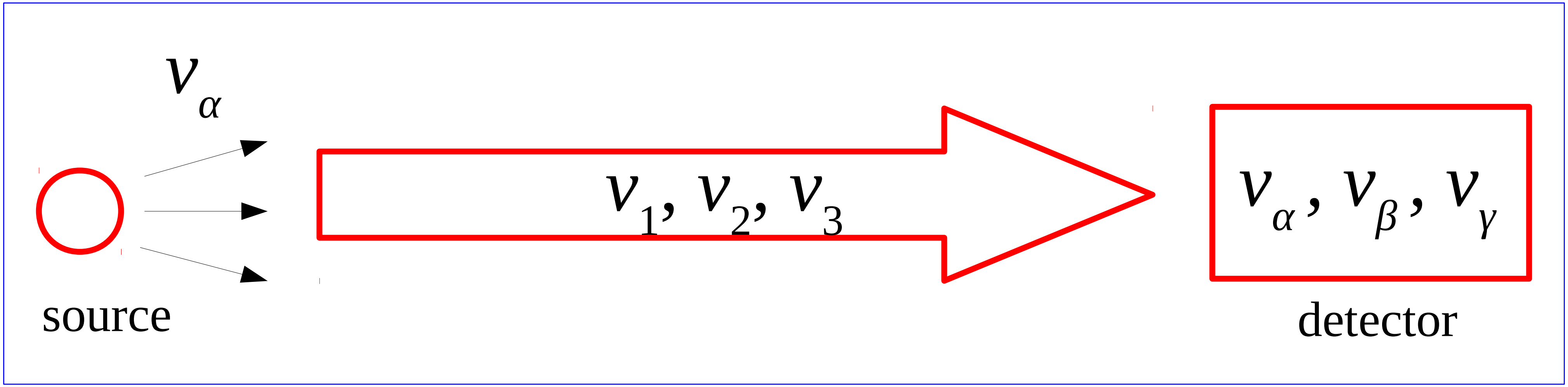

- ν's produced in a given flavor α, **mixture of mass eigenstates**
- different masses propagate with **different phases**, e^{-itE_i}

$$tE_i = t\sqrt{m_i^2 + \mathbf{p}^2} = t|\mathbf{p}|\left(1 + \frac{m_i^2}{2|\mathbf{p}|^2}\right) = |\mathbf{p}|t + \frac{m_i^2 L}{2E_\nu}$$

- detected mixture of mass eigenstates is, in general, different; appearance of **another flavors**, β and γ

Neutrino oscillations in a nutshell

In the simplest case of 2 flavors

$$P(\nu_\alpha \to \nu_\alpha) = 1 - \sin^2 2\theta \sin^2\left(\frac{\Delta m^2 L}{4E_\nu}\right)$$

Example [K. Abe *et al.* (T2K Collaboration), PRD 91, 072010 (2015)]

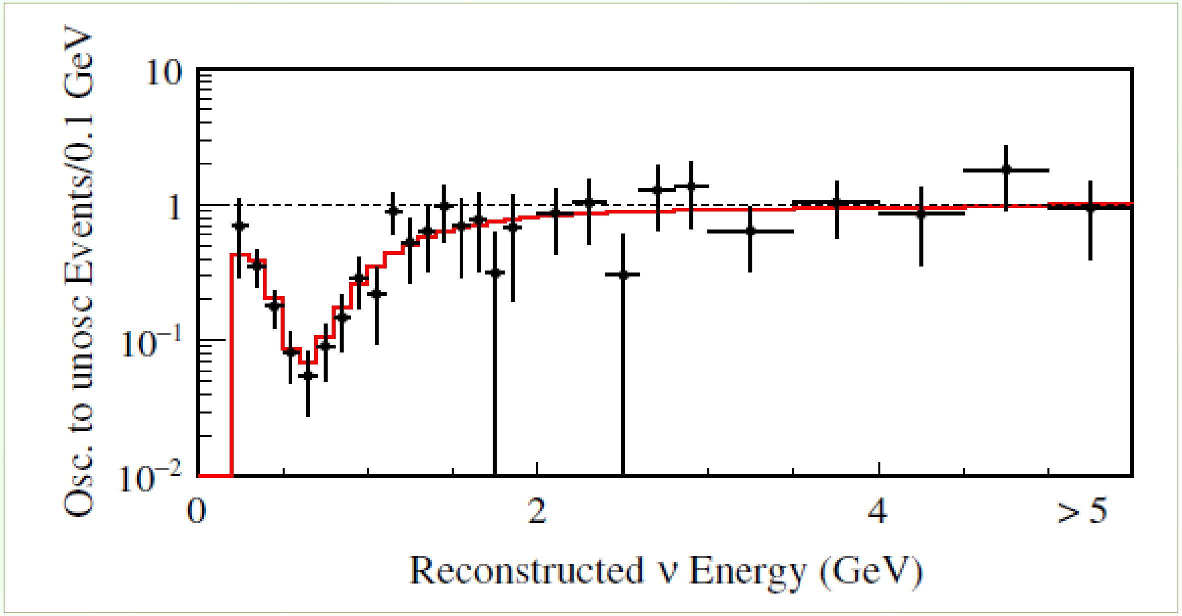

Neutrino oscillations in a nutshell

In the simplest case of 2 flavors

$$P(\nu_\alpha \to \nu_\alpha) = 1 - \boxed{\sin^2 2\theta} \sin^2\left(\frac{\Delta m^2 L}{4E_\nu}\right)$$

Example [K. Abe *et al.* (T2K Collaboration), PRD 91, 072010 (2015)]

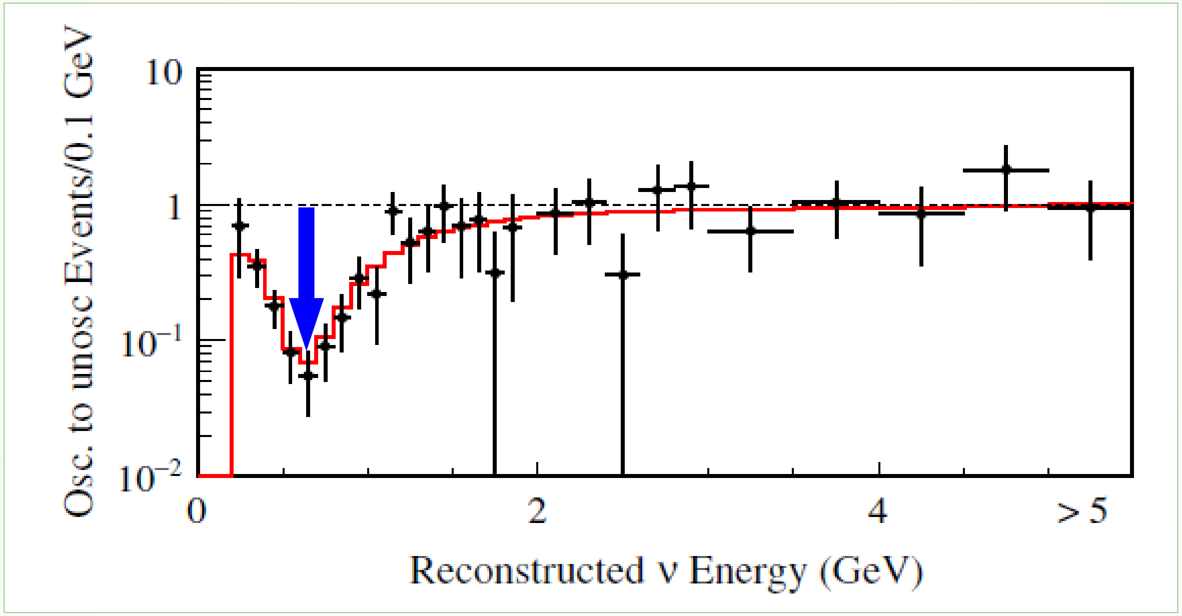

Neutrino oscillations in a nutshell

In the simplest case of 2 flavors

$$P(\nu_\alpha \to \nu_\alpha) = 1 - \sin^2 2\theta \sin^2 \left(\frac{\boxed{\Delta m^2} L}{4E_\nu} \right)$$

Example [K. Abe *et al.* (T2K Collaboration), PRD 91, 072010 (2015)]

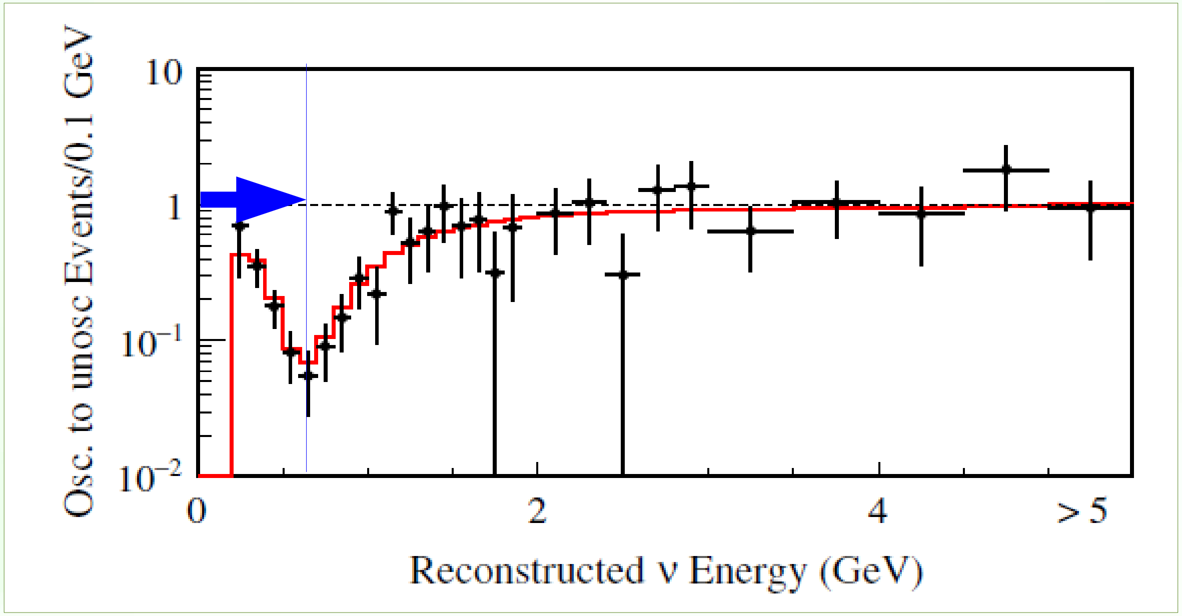

Energy reconstruction

Neutrino beams

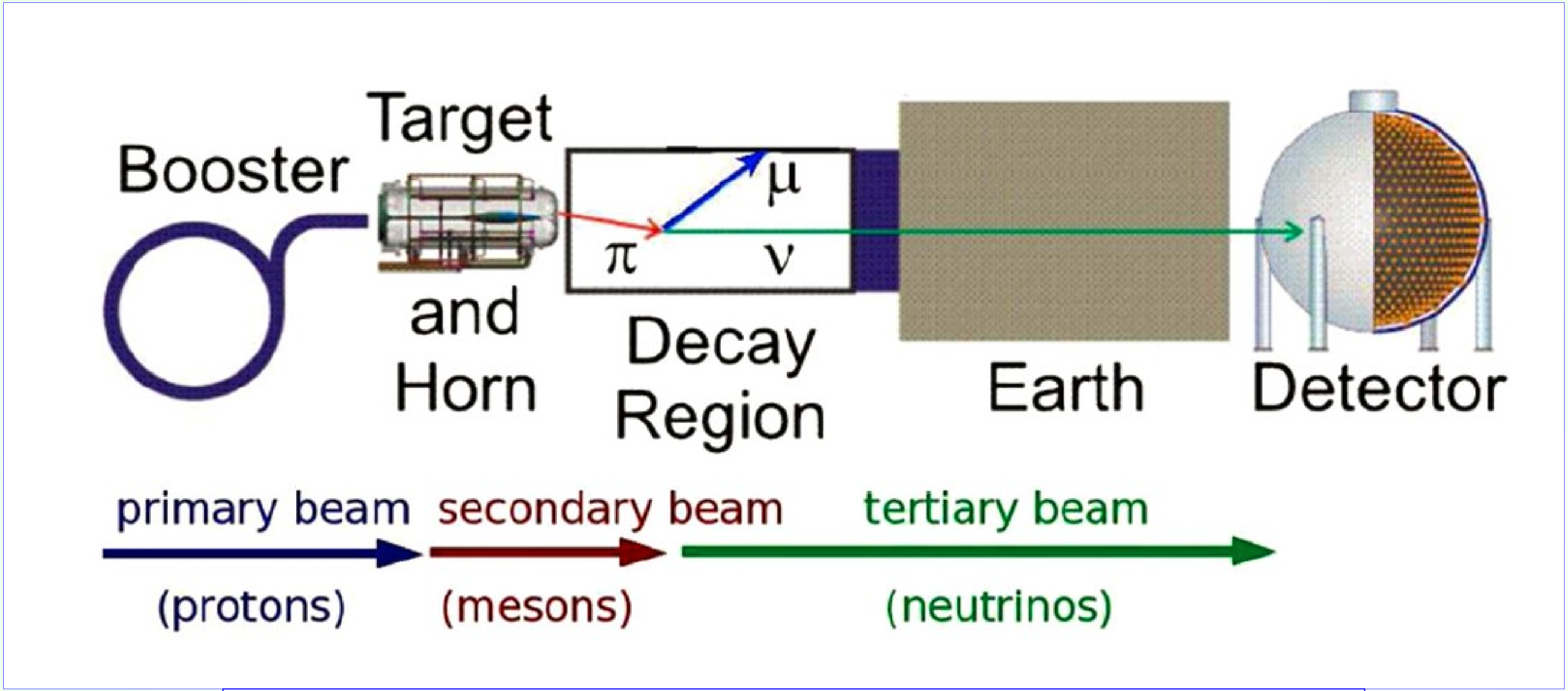

Aguilar-Arevalo et al. (MiniBooNE), D 81, 092005 (2010)

What precision are we reaching?

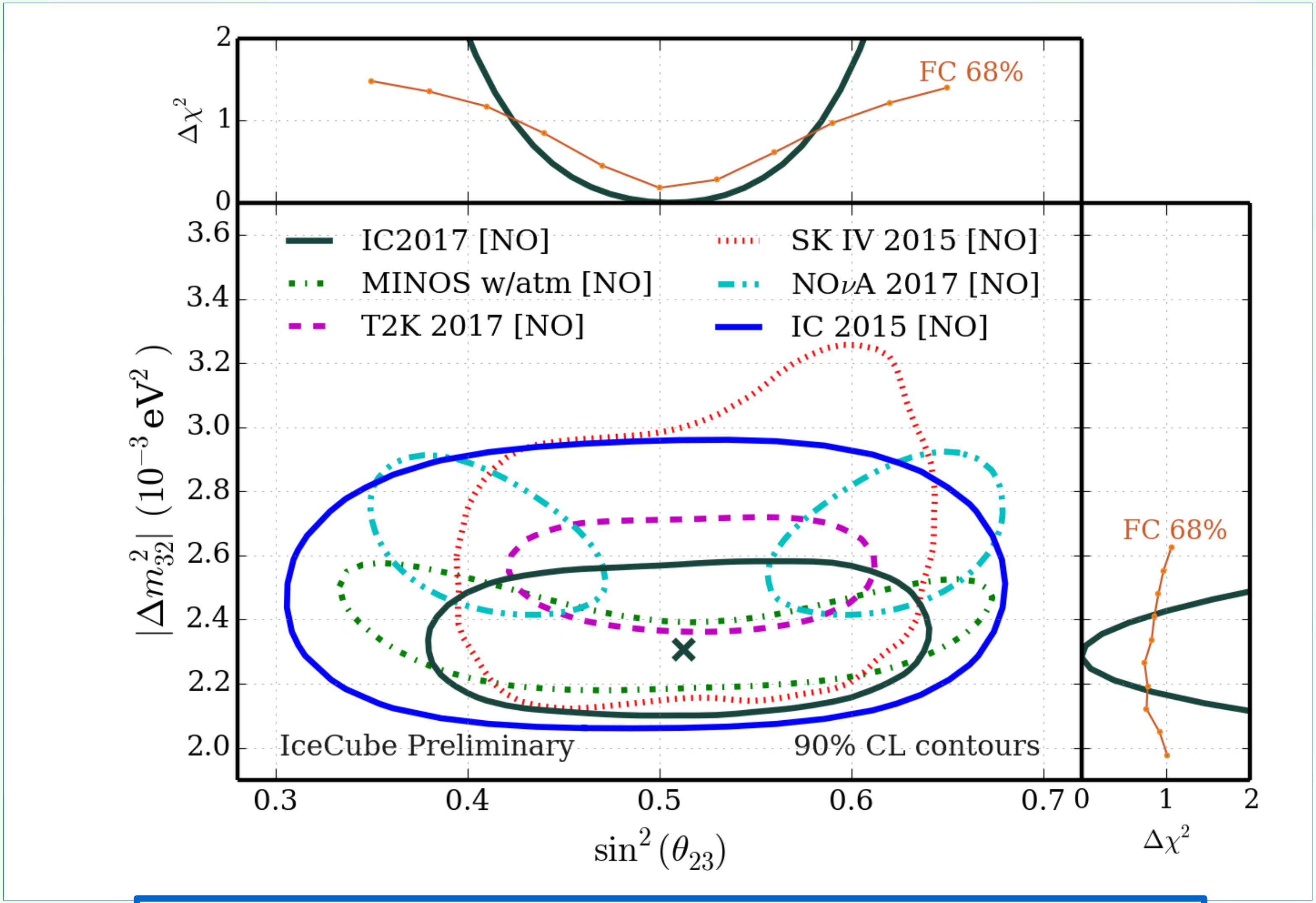

J. Hignight (IceCube), APS April Meeting, 2017

What precision are we reaching?

At neutrino energy ~600 MeV (T2K kinematics),

- 10% uncertainty (current T2K), ~60 MeV
- 2% uncertainty (current global fits), ~10 MeV

At the NOvA and DUNE kinematics, values x4−5.

DUNE and **T2HK** aim at uncertainties < 1%,
requiring ~**25 MeV** and ~**5 MeV** precision.

Effects considered to be “small” need to be accounted for accurately to avoid biases.

Neutrino scattering

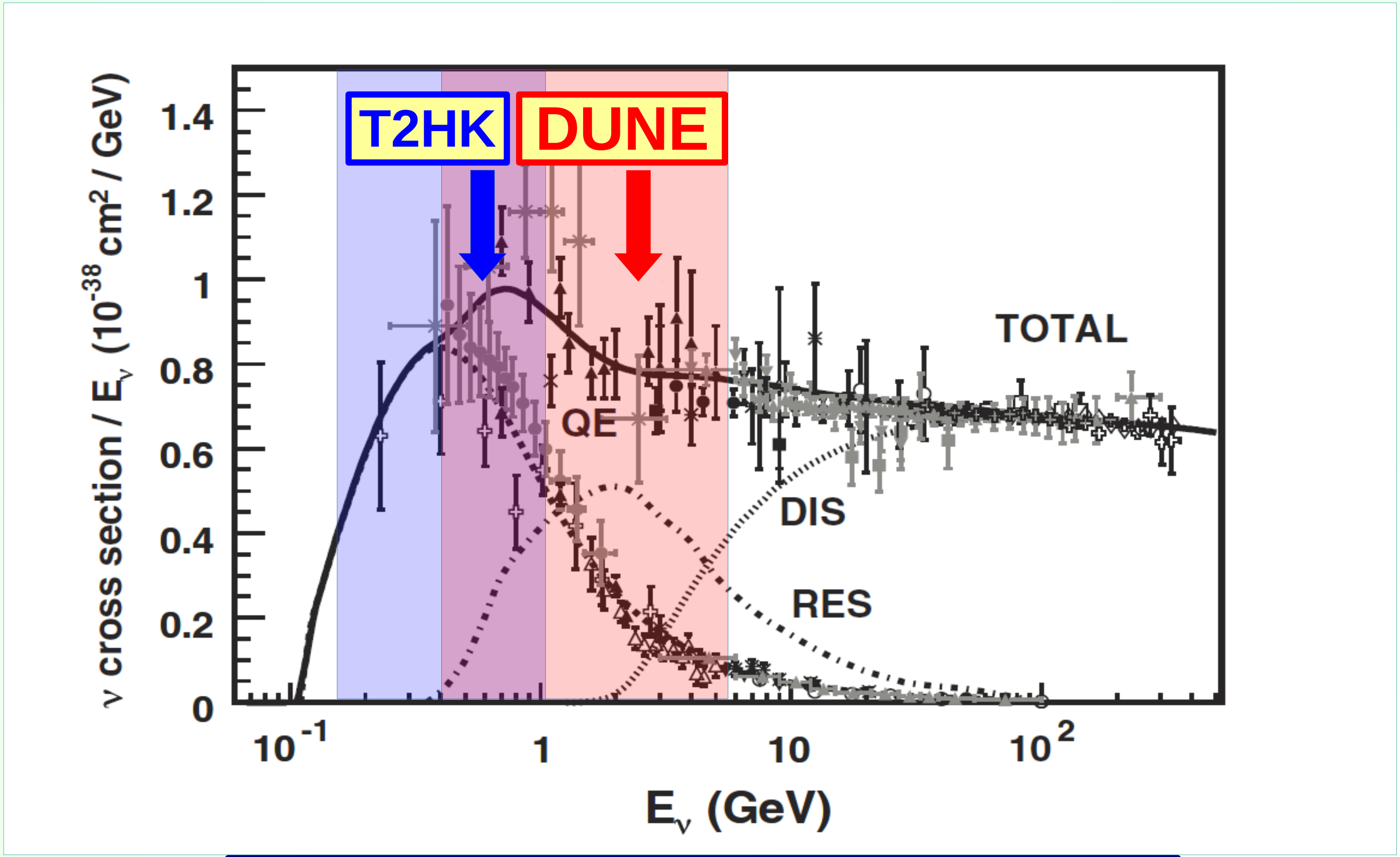

adopted from
Formaggio & Zeller, RMP 84, 1307 (2013)

Electron scattering

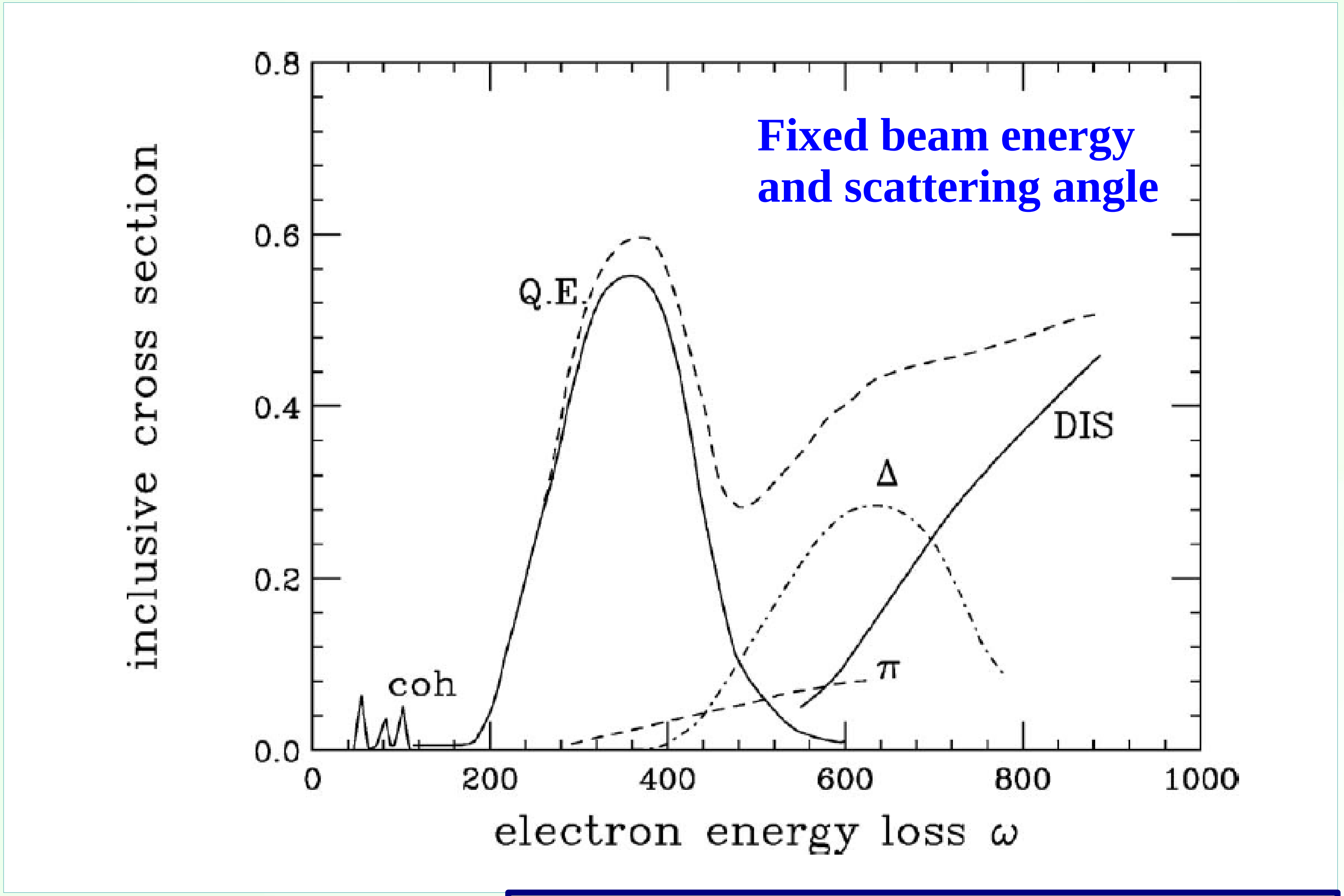

Benhar *et al.*, RMP 80, 189 (2008)

Target dependence

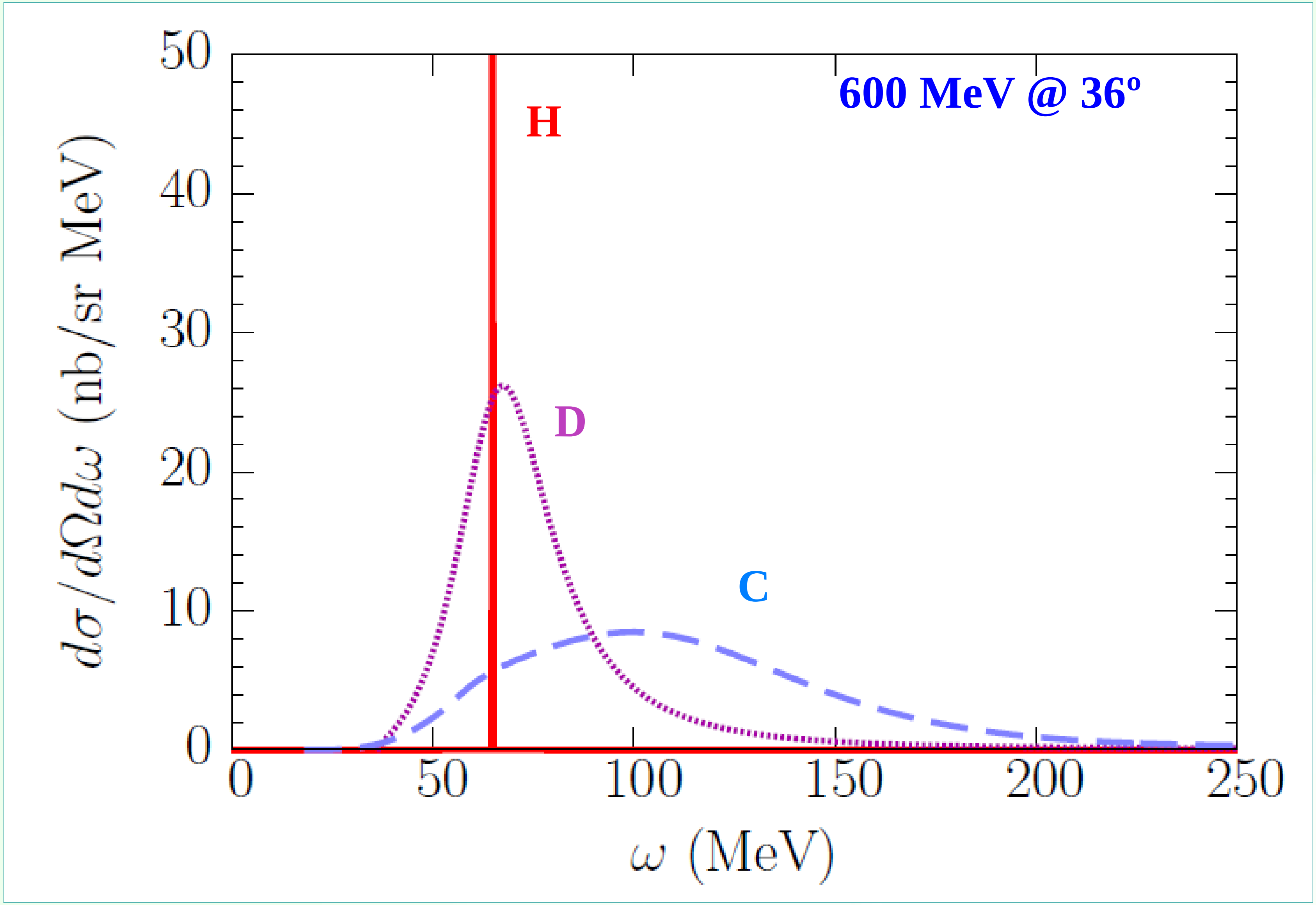

Kinematic reconstruction

In quasielastic scattering off free nucleons, $\bar{\nu} + p \rightarrow l + n$ and $\nu + n \rightarrow l + p$, we can deduce the neutrino energy from the charged lepton's kinematics.

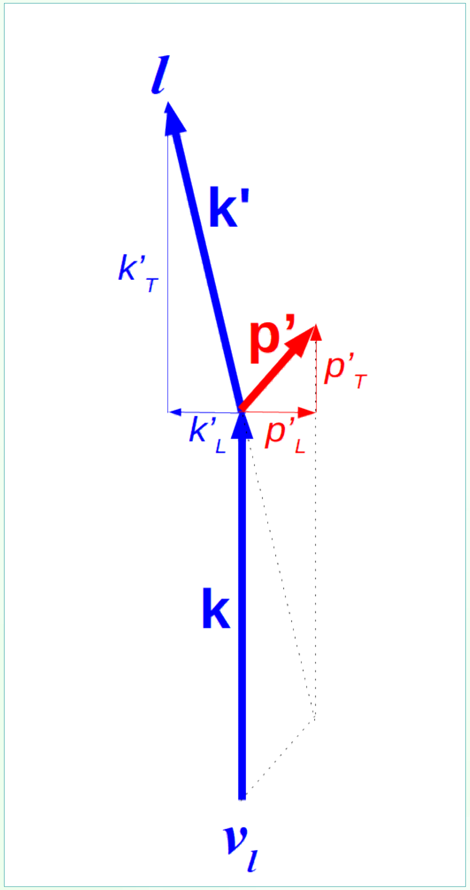

Energy conservation

$$E + M = E' + \sqrt{M^2 + p_L'^2 + p_T'^2}$$

Momentum conservation

$$E = |k'| \cos\theta + p_L'$$

$$0 = |k'| \sin\theta + p_T'$$

Kinematic reconstruction

In quasielastic scattering off free nucleons, $\bar{\nu} + p \to l + n$ and $\nu + n \to l + p$, we can deduce the neutrino energy from the charged lepton's kinematics.

No need to reconstruct the nucleon kinematics.

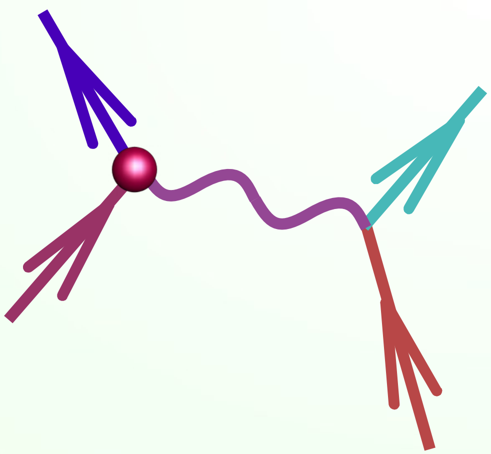

E' and θ known

$$E = \frac{ME' + \text{const}}{M - E' + |\boldsymbol{k}'| \cos\theta}$$

Kinematic reconstruction

In nuclei an exact reconstruction would require knowledge of the recoil momentum and the energy of (A−1) nucleons, as the struck nucleon's energy is $E_p = M_A - E_{A-1}$.

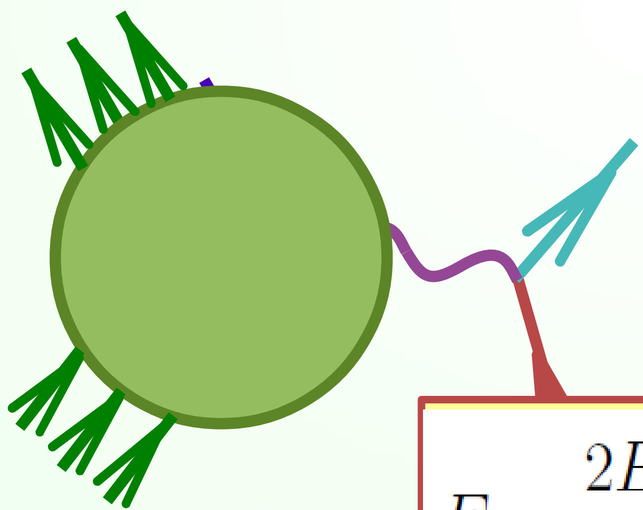

E' and θ known

$$E = \frac{2E_pE' - 2\mathbf{p}\cdot\mathbf{k}' + M'^2 - E_p^2 + \mathbf{p}^2 - m^2}{2(E_p - |\mathbf{p}|\cos\theta_h - E' + |\mathbf{k}'|\cos\theta)}$$

Kinematic reconstruction

In nuclei the reconstruction becomes an approximation due to the binding energy, Fermi motion, final-state interactions, two-body interactions etc.

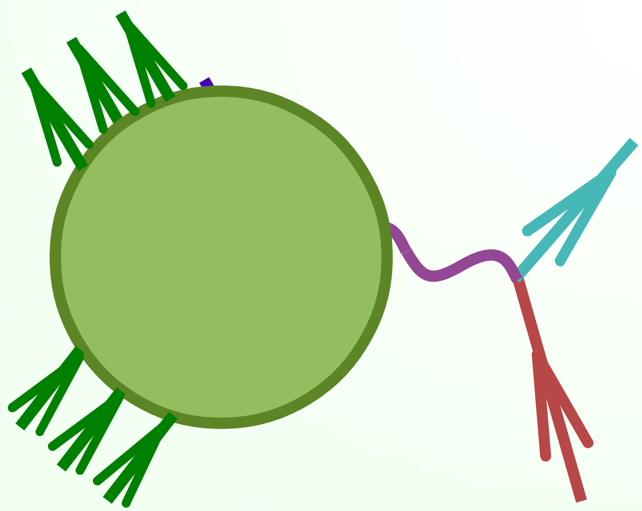

E' and θ known

$$E \simeq \frac{(M-\epsilon)E' + \mathrm{const}}{M-\epsilon-E'+|\boldsymbol{k}'|\cos\theta}$$

Free-proton events

For targets containing H, the (ν and $\bar{\nu}$) pion-production events on free protons could be separated out, based on the balance of the transverse momentum.

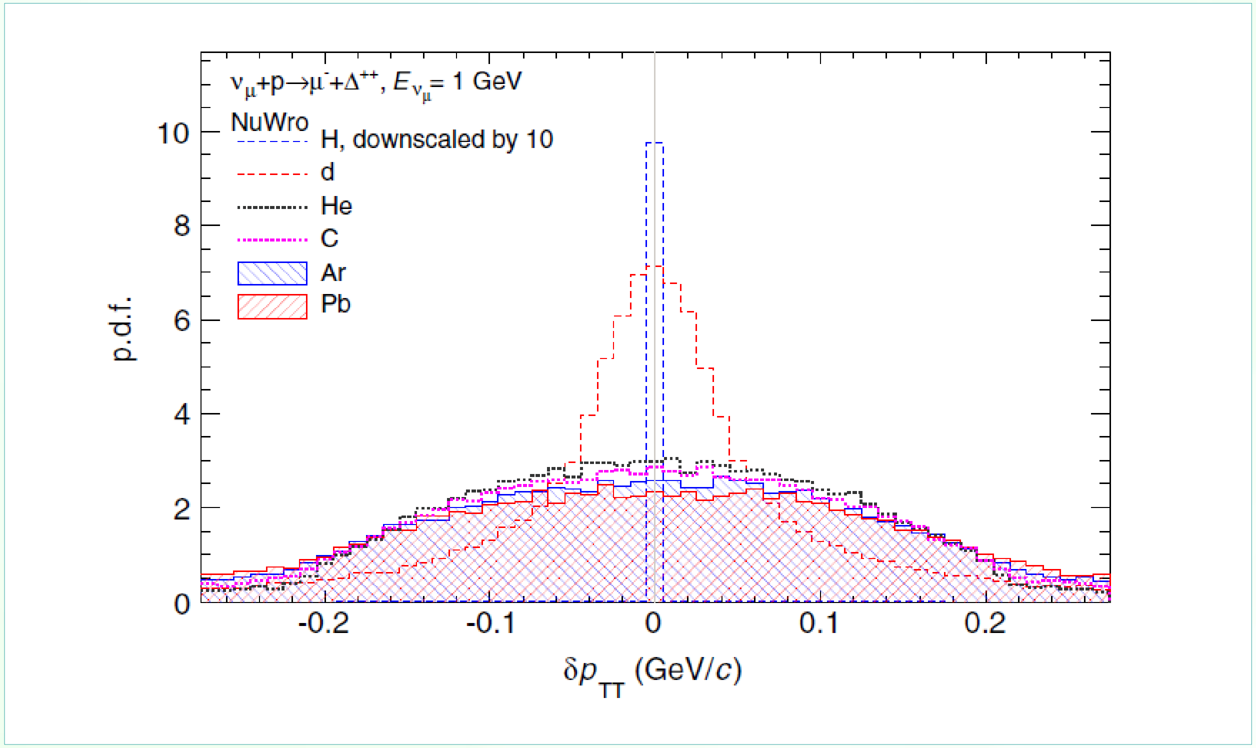

Lu *et al.*, PRD 92, 051302 (2015)

Unknown monochromatic beam

Consider the simplest (unrealistic) case:

the beam is monochromatic but its energy is unknown and has to be reconstructed

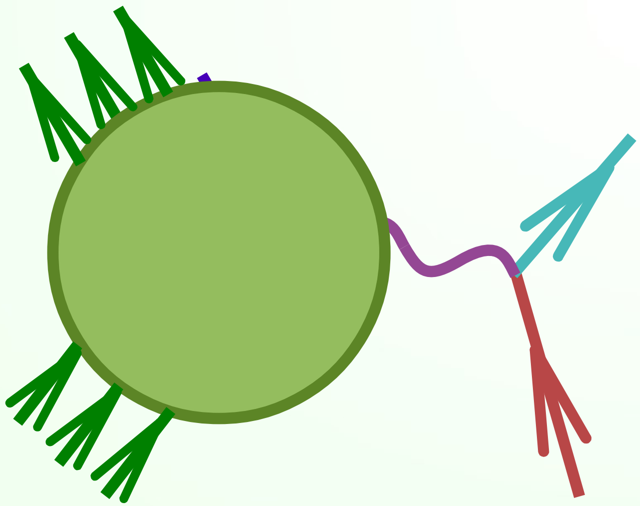

E' and θ known

$E = ?$

"Unknown" monochromatic e^- beam

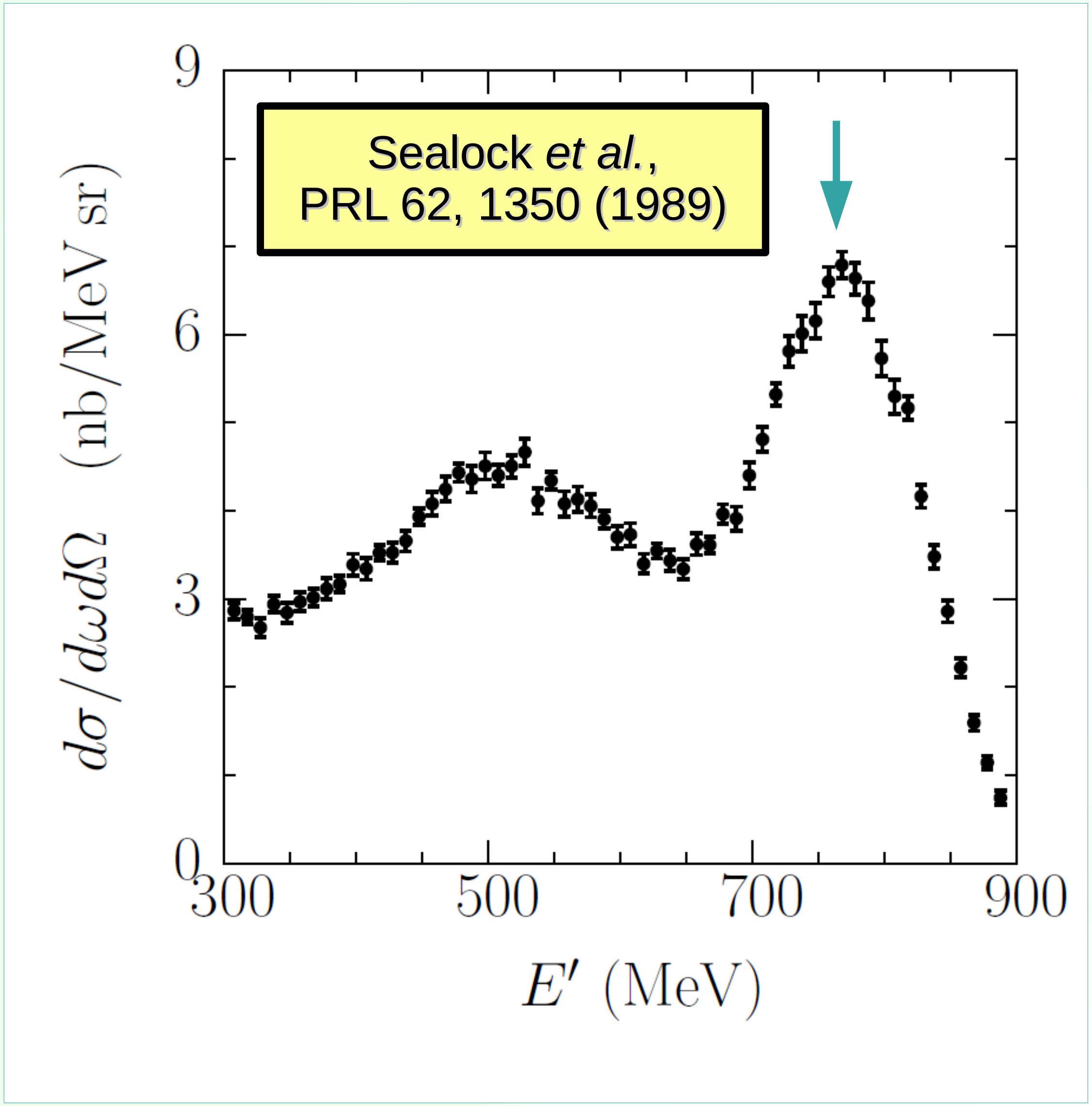

$E' = 768$ MeV
$\theta = 37.5$ deg
$\Delta E' = 5$ MeV

“Unknown” monochromatic e^- beam

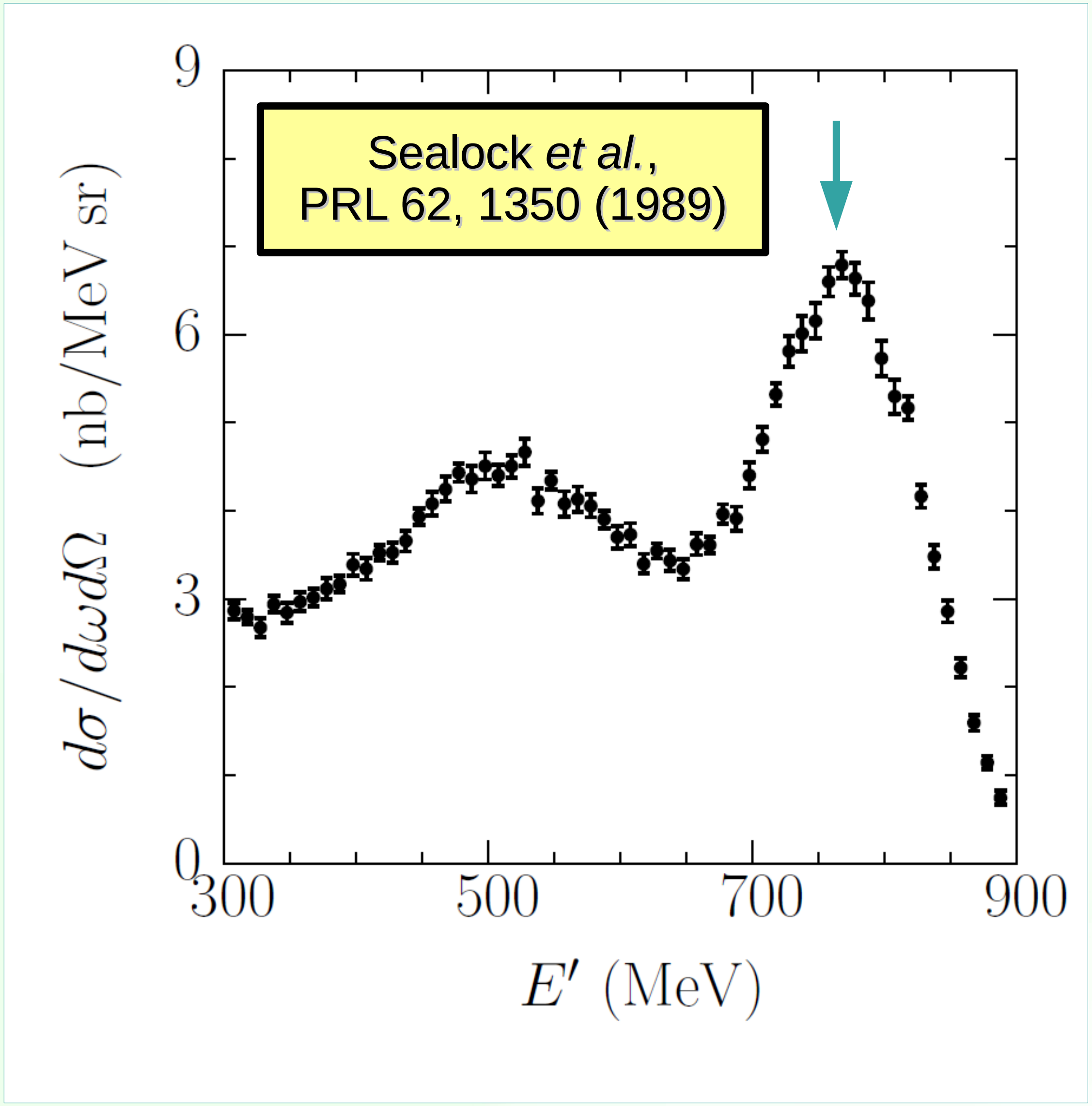

$E' = 768$ MeV
$\theta = 37.5$ deg
$\Delta E' = 5$ MeV

for $\epsilon = 25$ MeV
$E = 960$ MeV
$\Delta E = 7$ MeV

“Unknown” monochromatic e^- beam

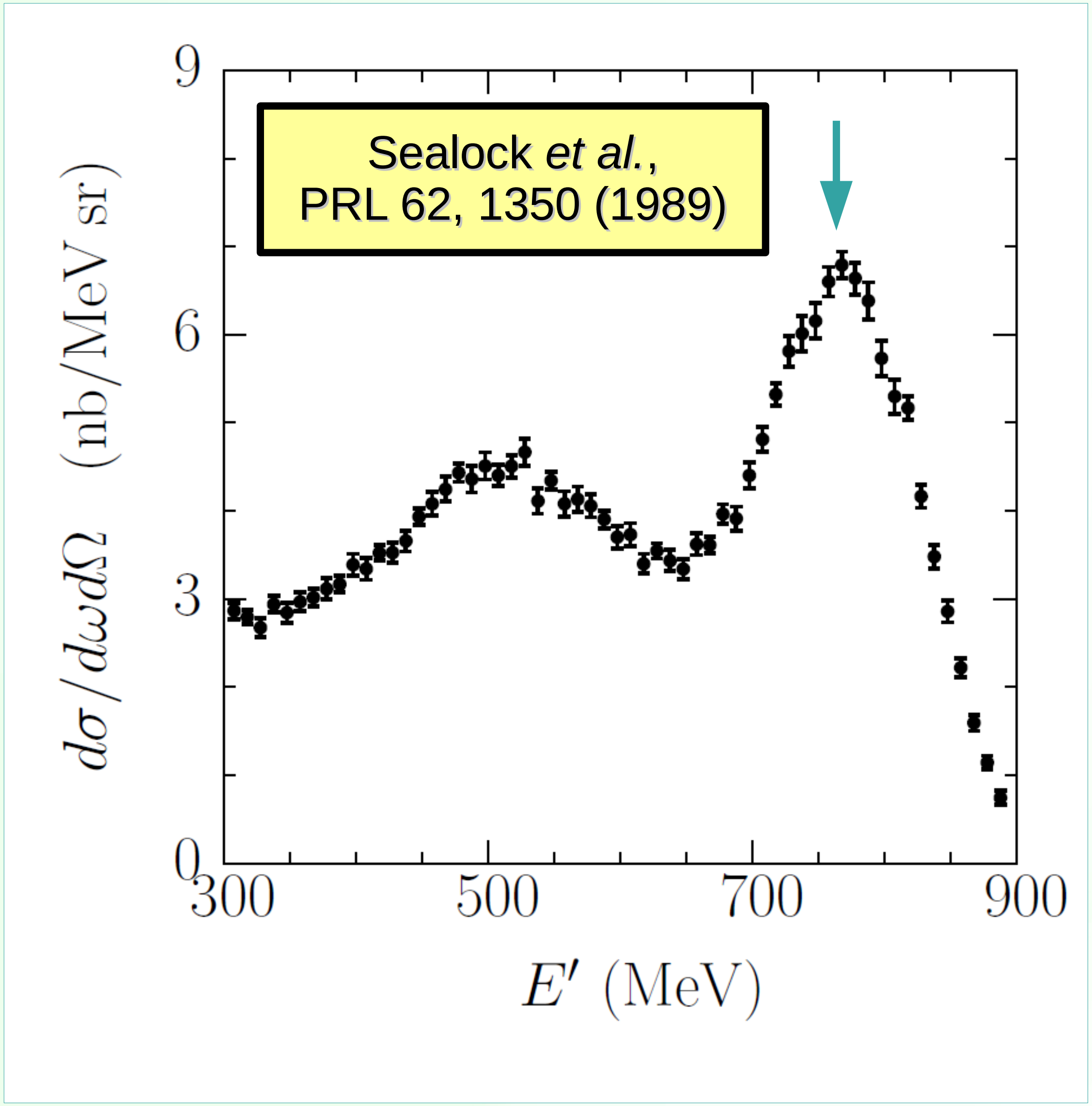

$E' = 768$ MeV
$\theta = 37.5$ deg
$\Delta E' = 5$ MeV

for $\epsilon = 25$ MeV
$E = 960$ MeV
$\Delta E = 7$ MeV

true value
$E = 961$ MeV

"Unknown" monochromatic e^- beam

θ (deg)	37.5	37.5	37.1	36.0	36.0
E' (MeV)	976	768	615	487.5	287.5
$\Delta E'$ (MeV)	5	5	5	5	2.5

Assuming $\epsilon = 25$ MeV

rec. E	1285 ± 8	960 ± 7	741 ± 7	571 ± 6	333 ± 3
true E	1299	961	730	560	320

“Unknown” monochromatic e^- beam

θ (deg)	37.5	37.5	37.1	36.0	36.0
E' (MeV)	976	768	615	487.5	287.5
$\Delta E'$ (MeV)	5	5	5	5	2.5

Appropriate ϵ value?

true E	**1299**	**961**	**730**	**560**	**320**
ϵ	**33 ± 5**	**26 ± 5**	**16 ± 5**	**16 ± 3**	**13 ± 3**

Sealock et al., PRL 62, 1350 (1989)

O'Connell *et al.*, PRC 35, 1063 (1987)

Barreau *et al.*, NPA 402, 515 (1983)

"Unknown" monochromatic e^- beam

θ (deg)	37.5	37.5	37.1	36.0	36.0
E' (MeV)	976	768	615	487.5	287.5
$\Delta E'$ (MeV)	5	5	5	5	2.5

Appropriate ϵ value?

true E	**1299**	**961**	**730**	**560**	**320**
$\boldsymbol{\epsilon}$	**33 ± 5**	**26 ± 5**	**16 ± 5**	**16 ± 3**	**13 ± 3**

different E ≡ different Q^2 ≡ different θ
→ different ϵ

“Unknown” monochromatic e^- beam

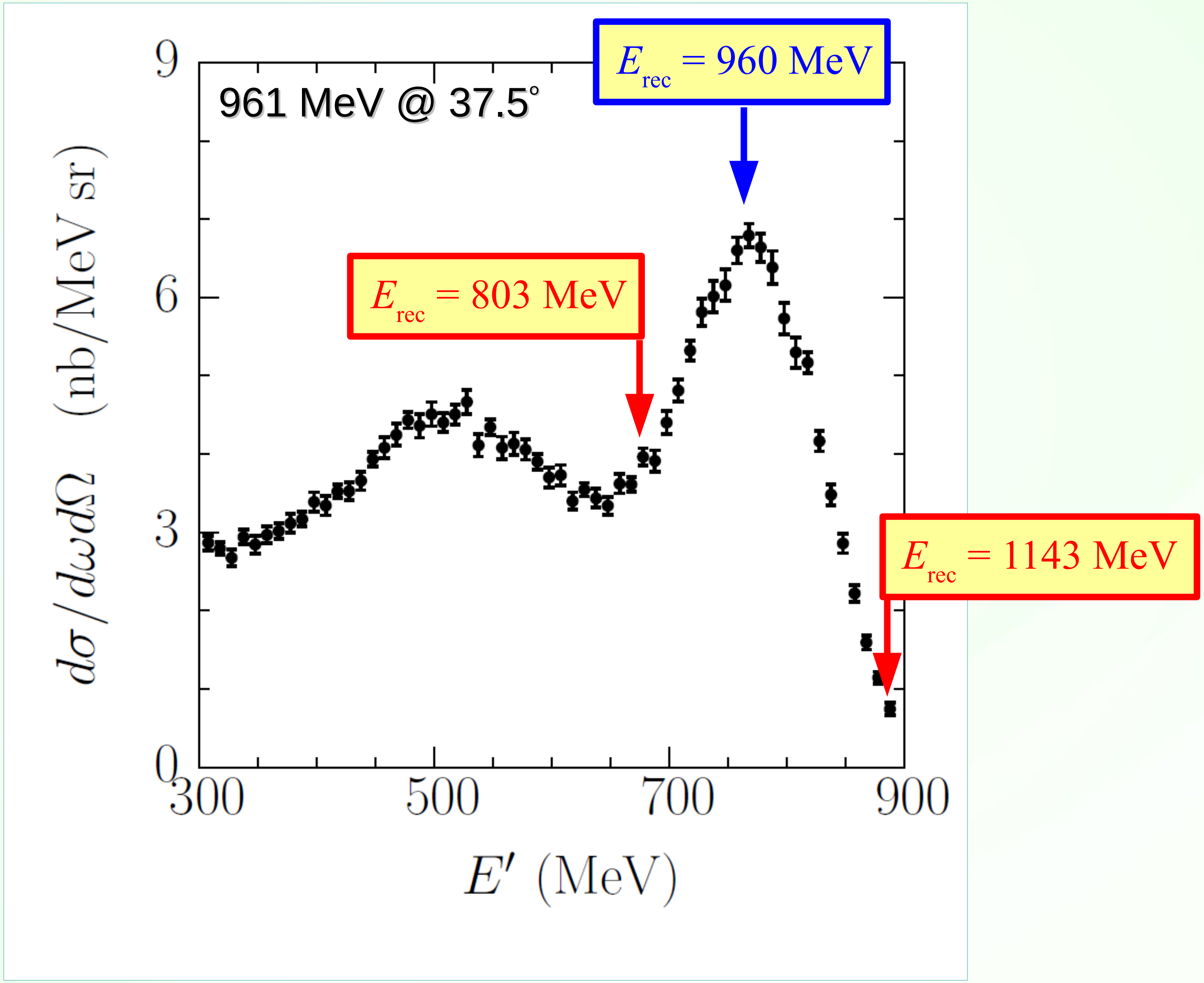

Realistic calculations vs E_{rec}

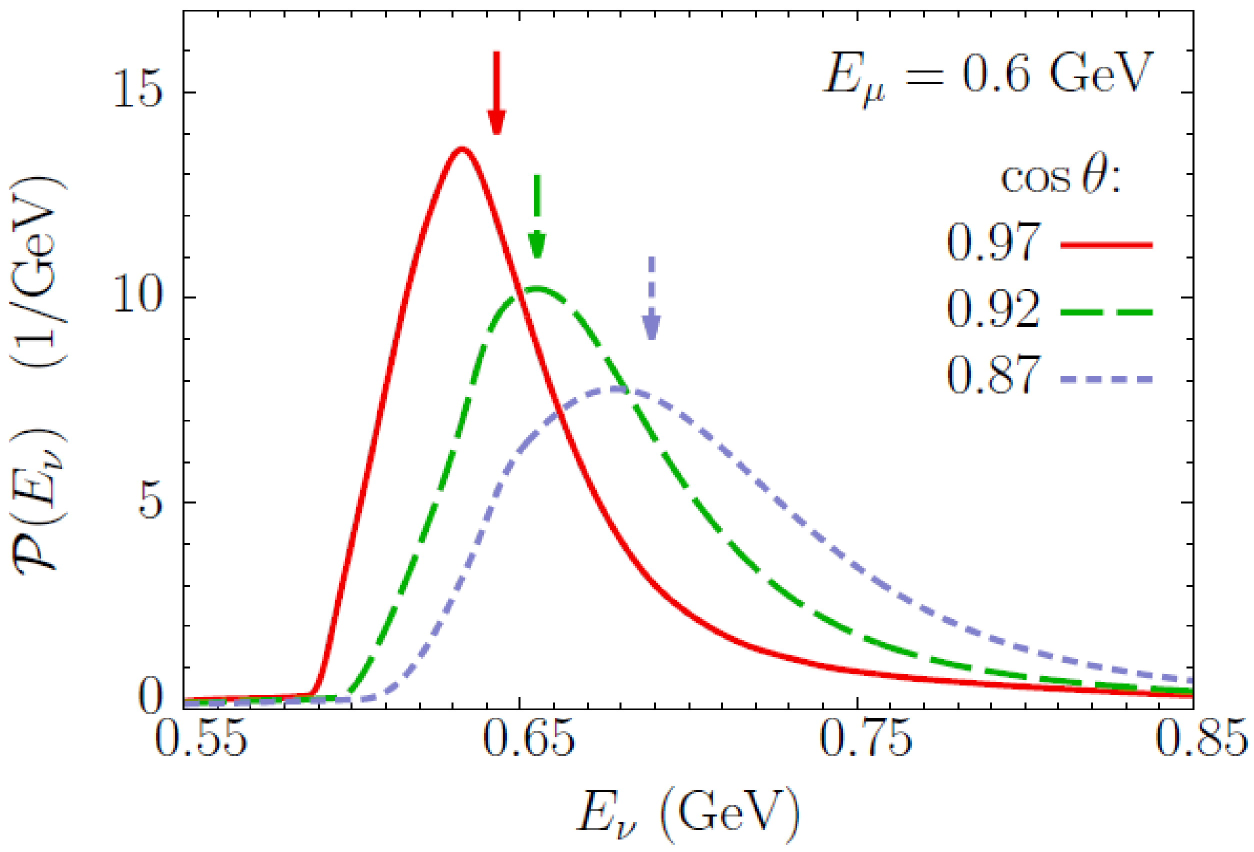

Realistic calculations vs E_{rec}

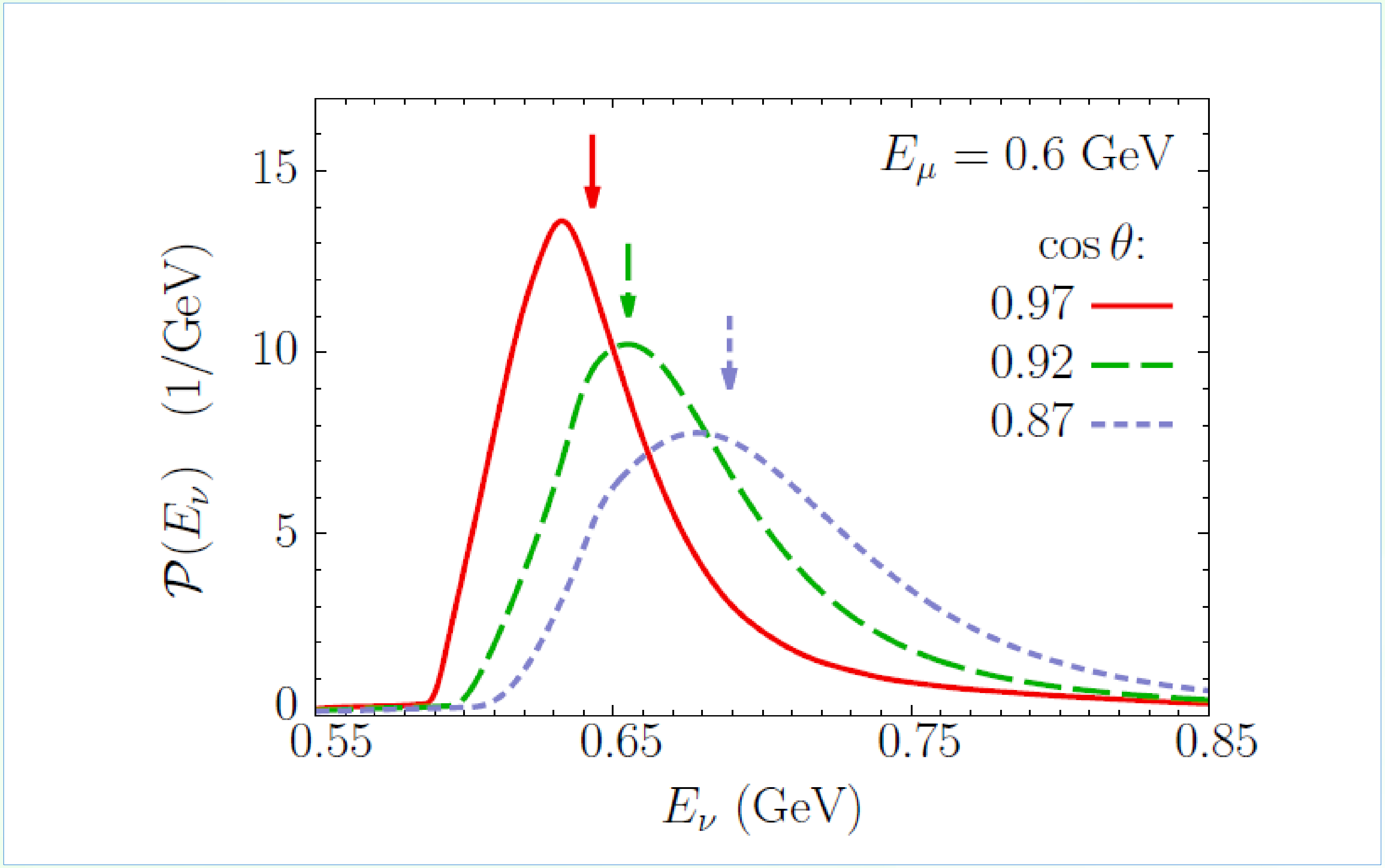

Same physics drives the QE peak position
and relates the kinematics to neutrino energy

Polychromatic beam

In modern experiments, the neutrino beams are not monochromatic, and the energy must be reconstructed from the observables, typically E' and $\cos\theta$ under the CCQE event hypothesis.

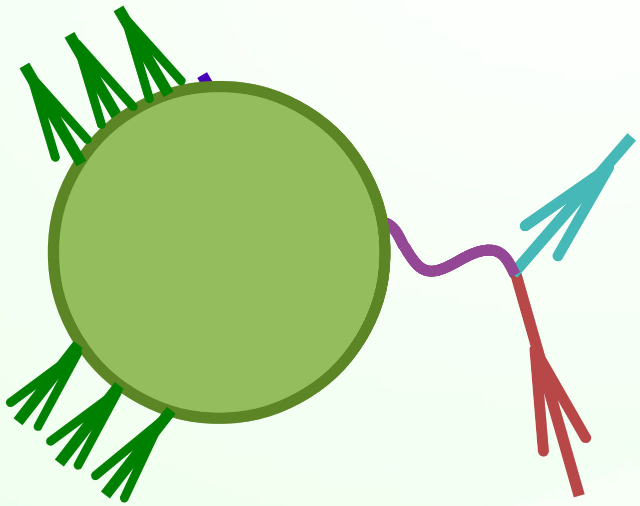

E' and θ known

$E = ?$

CCQE events

In practice, CCQE event candidates are defined as containing **no pions observed**.

CCQE (any number of nucleons)

\+ pion production and followed by absorption

undetected pions

− CCQE with pions from FSI

0π events

Recall the monochromatic-beam case

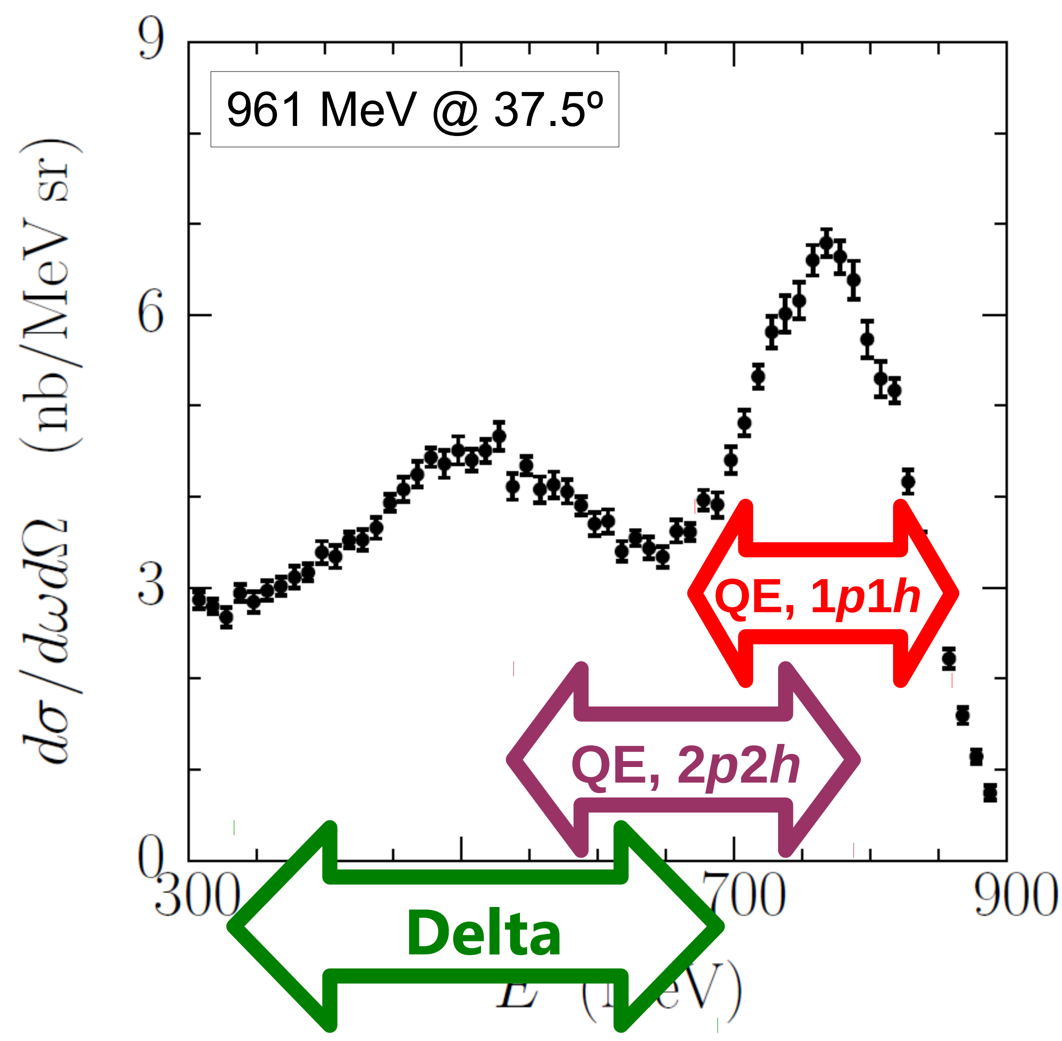

CCQE events of given $l^{\pm}$ kinematics

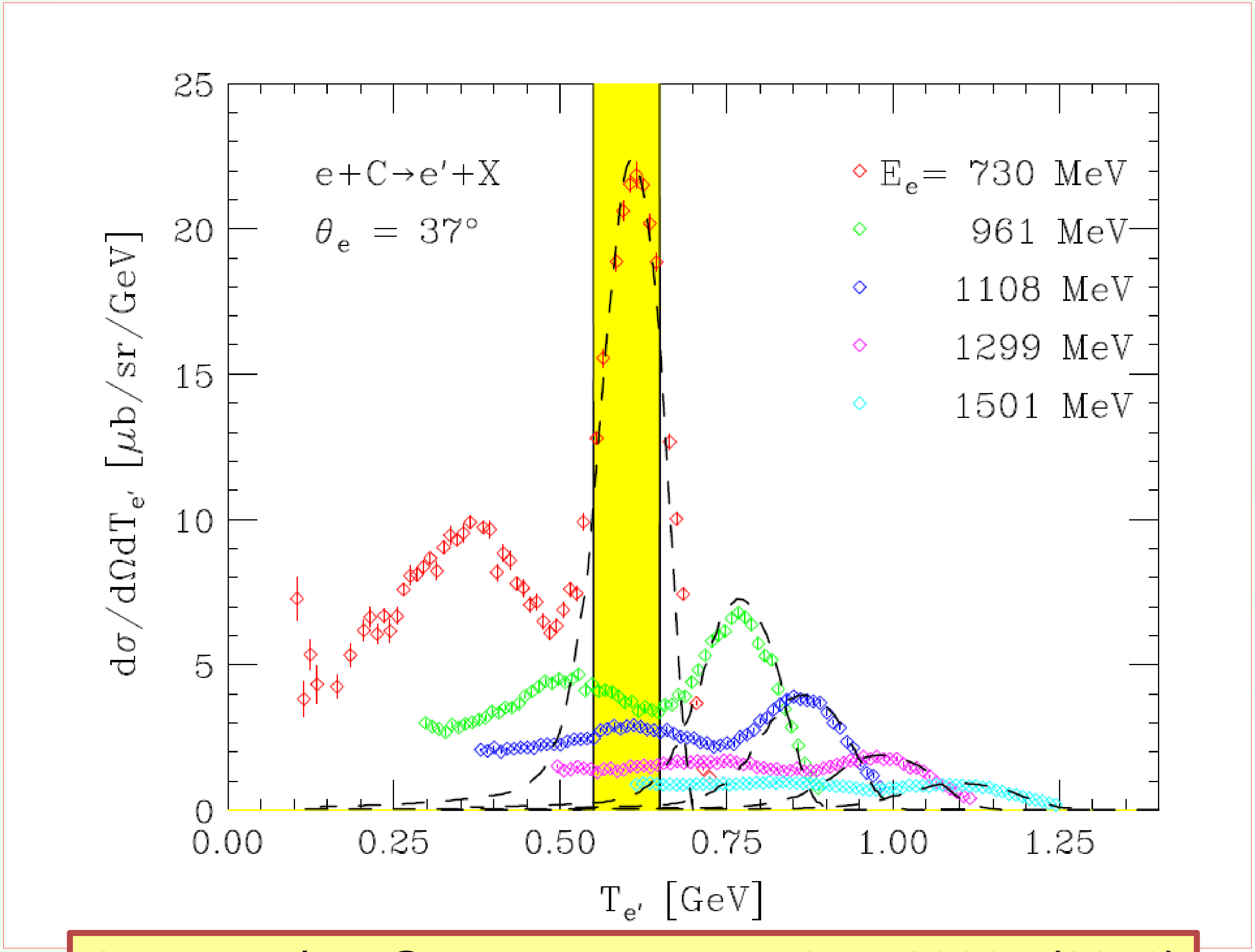

Omar Benhar @ NuFact11, PRL 105, 132301 (2010)

CCQE events of given $l^{\pm}$ kinematics

Very different **processes** and **neutrino energies** contribute to CCQE-like events of a given E' and $\cos\theta$.

An undetected pion typically lowers the reconstructed energy by **~300–350 MeV**.

Note that in the reconstruction formula, $M_\Delta = 1232$ MeV would be more suitable than $M' = 939$ MeV.

$$E_\nu^{\text{rec}} = \frac{2(M-\varepsilon)E_\ell + M'^2 - (M-\varepsilon)^2 - m_\ell^2}{2(M-\varepsilon-E_\ell+|\mathbf{k}_\ell|\cos\theta)}.$$

$$\frac{M_\Delta^2 - M'^2}{2M} \approx 340 \text{ MeV}$$

Absorbed or undetected pions

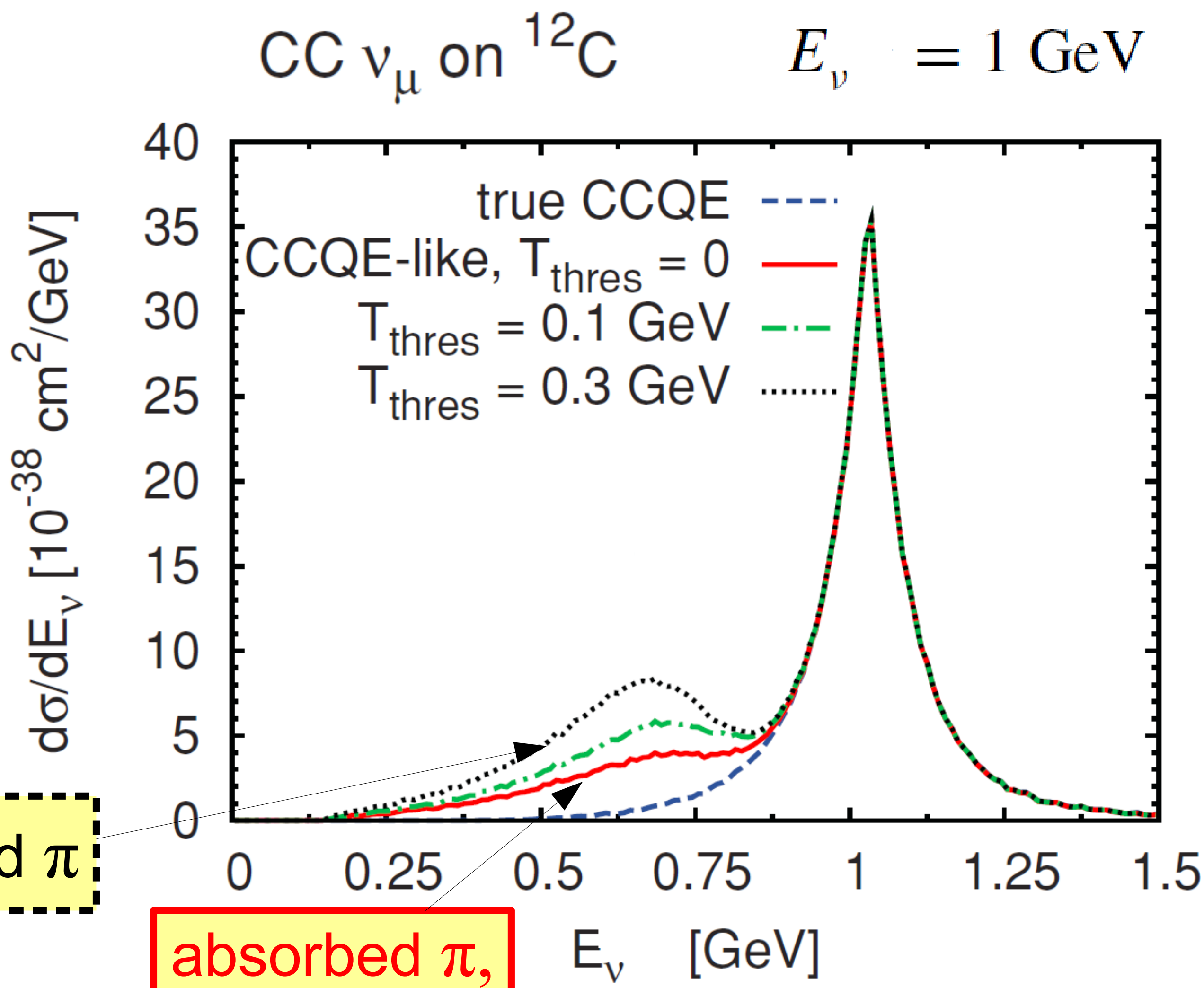

undetected π

absorbed π, irreducible

T. Leitner & U. Mosel
PRC 81, 064614 (2010)

Calorimetric energy reconstruction

- Seemingly simple procedure: add all energy depositions in the detector related to the neutrino event
- Advantages: (i) applicable to any final states, (ii) in an ideal detector, the reconstruction would be exact and insensitive to nuclear effects

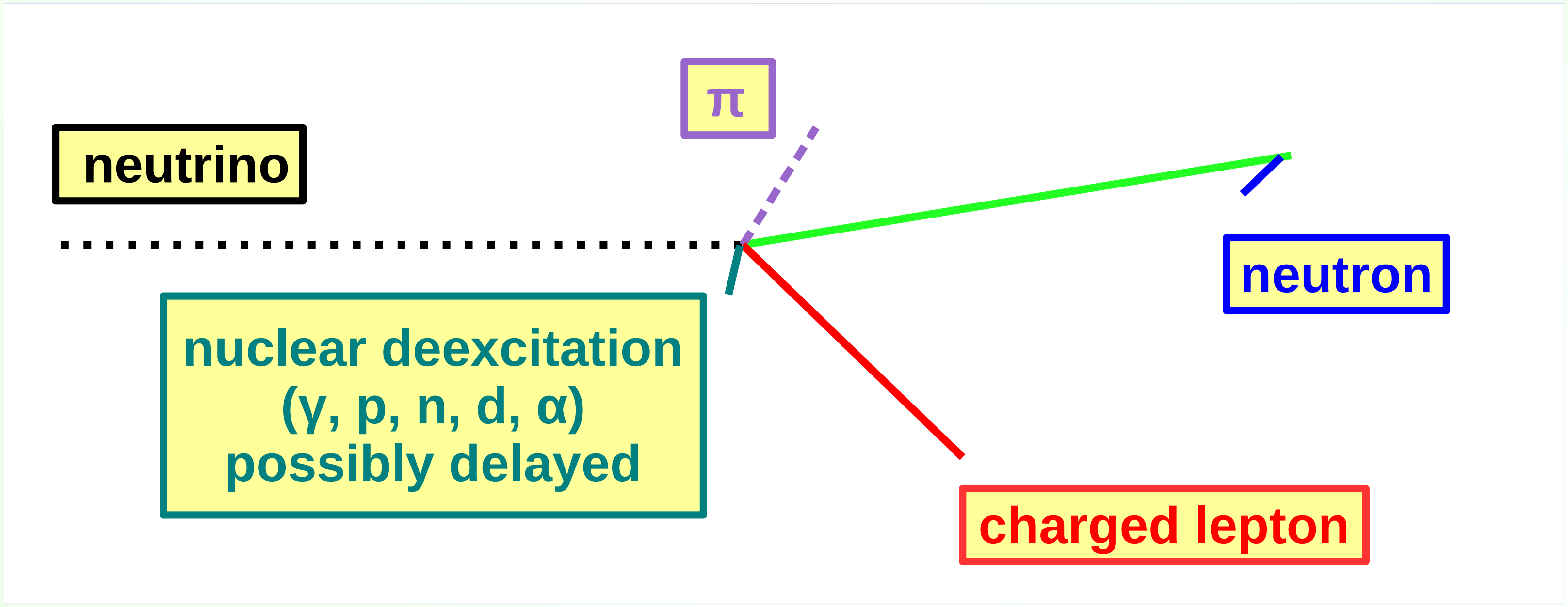

Calorimetric energy reconstruction

- In a real detector the method is only insensitive to nuclear effects when

missing energy « neutrino energy

- Otherwise, requires input from nuclear models
- Correction for the missing energy may be significant:
  - undetected pion at least m_π = 140 MeV
  - neutrons are hard to associate with the event

To achieve ~25 MeV accuracy in DUNE, accurate predictions of exclusive cross sections are required.

A.M.A., arXiv:1704.07835

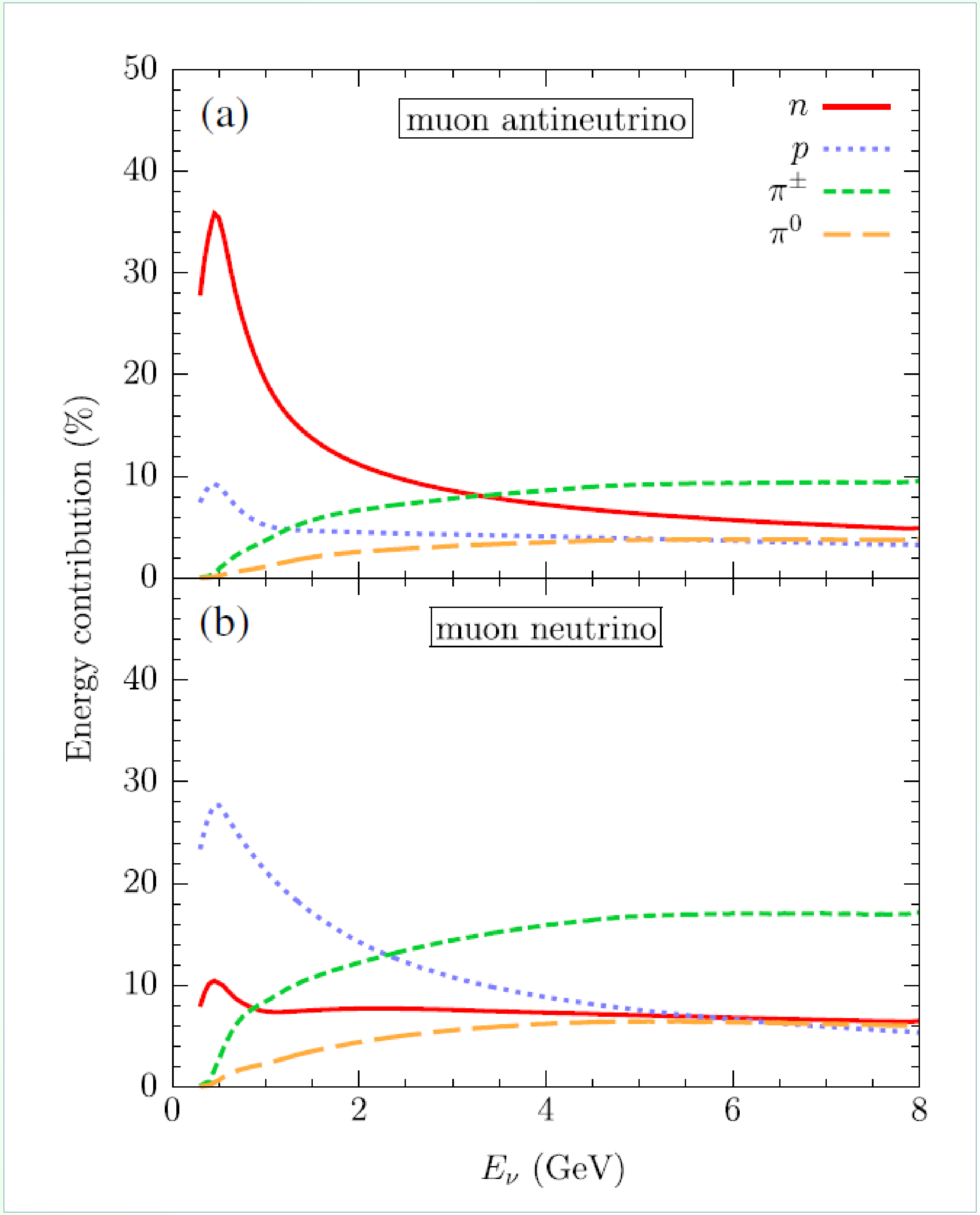

AMA *et al.*
PRD 92,
073014 (2015)

Impulse approximation

Impulse approximation

Assumption: the dominant process of lepton-nucleus interaction is **scattering off a single nucleon**, with the remaining nucleons acting as a spectator system.

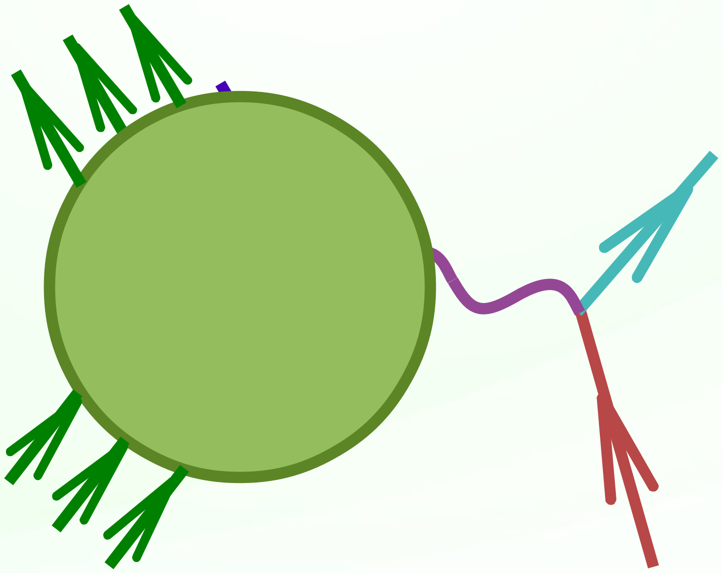

Impulse approximation

Assumption: the dominant process of lepton-nucleus interaction is **scattering off a single nucleon**, with the remaining nucleons acting as a spectator system.

It is valid when the momentum transfer |**q**| is high enough, as the probe's spatial resolution is ~1/|**q**|.

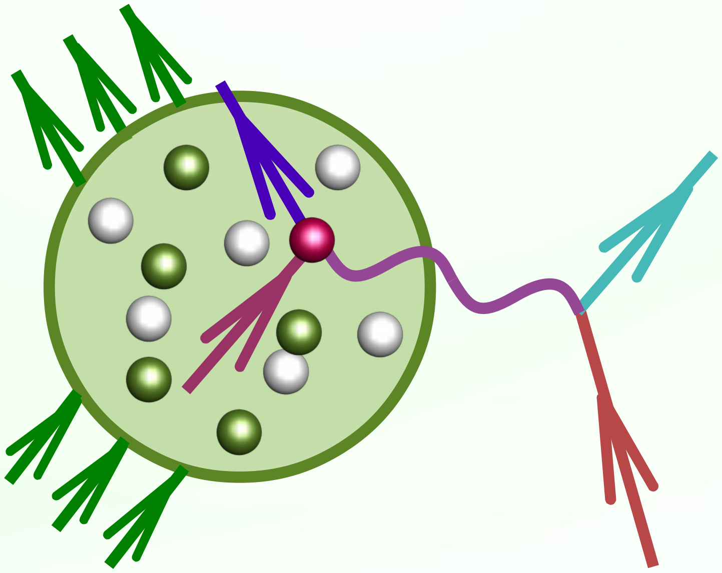

Impulse approximation

$$\frac{d\sigma_{\ell A}}{d\omega d\Omega} = \sum_N \int d\omega'\, d^3p\, dE\, \underline{P^N_{\text{hole}}(\mathbf{p}, E)}\, \underline{\frac{M}{E_{\mathbf{p}}} \frac{d\sigma^{\text{elem}}_{\ell N}}{d\omega' d\Omega}}\, \underline{P^N_{\text{part}}(\mathbf{p}', \mathcal{T}', \omega')}$$

Hole spectral function

Particle spectral function

Elementary cross section

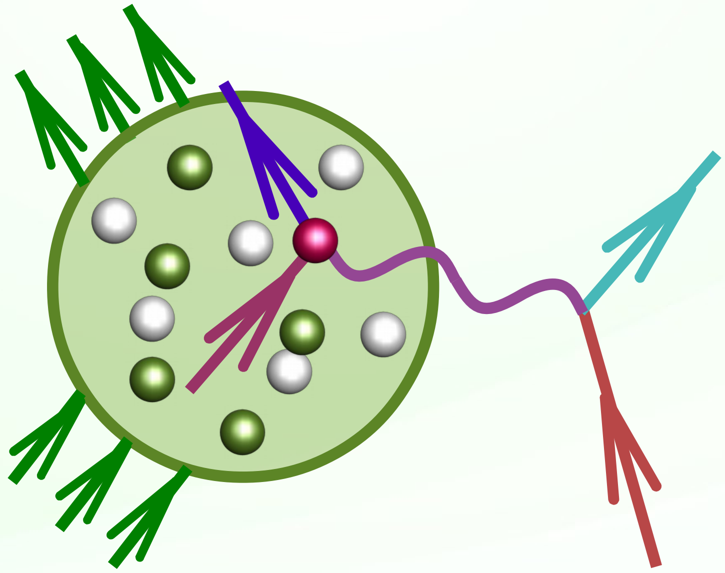

Impulse approximation

$$\frac{d\sigma_{\ell A}}{d\omega d\Omega} = \sum_N \int d\omega'\, d^3p\, dE\, P^N_{\text{hole}}(\mathbf{p}, E)\, \frac{M}{E_{\mathbf{p}}} \frac{d\sigma^{\text{elem}}_{\ell N}}{d\omega' d\Omega}\, P^N_{\text{part}}(\mathbf{p}', \mathcal{T}', \omega')$$

Describes the ground-state properties of the target nucleus

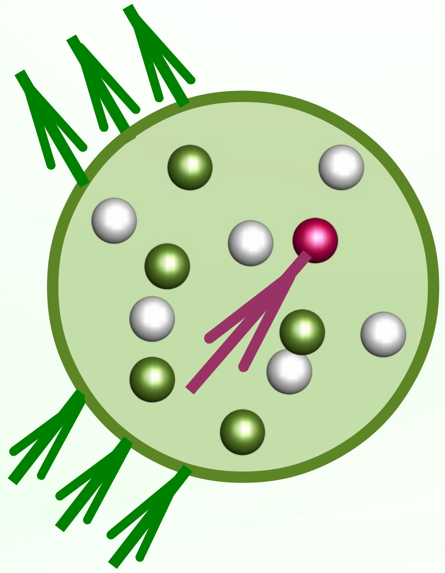

Impulse approximation

$$\frac{d\sigma_{\ell A}}{d\omega d\Omega} = \sum_N \int d\omega'\, d^3p\, dE\, P^N_{\text{hole}}(\mathbf{p}, E)\, \underline{\frac{M}{E_{\mathbf{p}}} \frac{d\sigma^{\text{elem}}_{\ell N}}{d\omega' d\Omega}}\, P^N_{\text{part}}(\mathbf{p}', \mathcal{T}', \omega')$$

Characterizes the interaction vertex

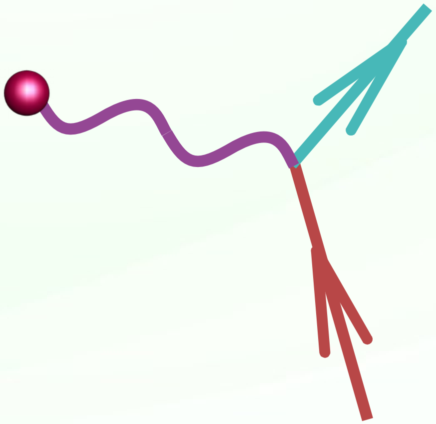

Impulse approximation

$$\frac{d\sigma_{\ell A}}{d\omega d\Omega} = \sum_N \int d\omega' \, d^3p \, dE \, P^N_{\text{hole}}(\mathbf{p}, E) \, \frac{M}{E_{\mathbf{p}}} \frac{d\sigma^{\text{elem}}_{\ell N}}{d\omega' d\Omega} \, \underline{P^N_{\text{part}}(\mathbf{p}', \mathcal{T}', \omega')}$$

Ensures the energy conservation and Pauli blocking

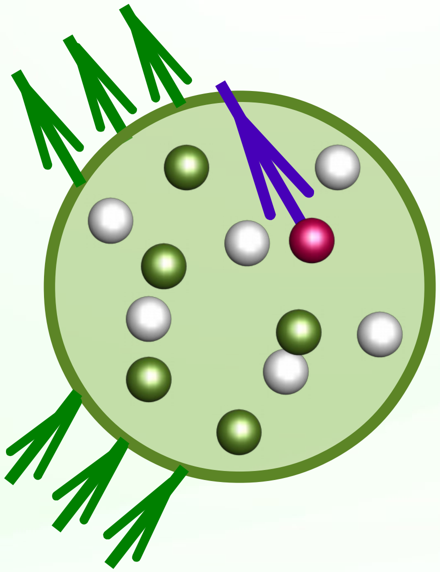

Impulse approximation

$$\frac{d\sigma_{\ell A}}{d\omega d\Omega} = \sum_N \int d\omega'\, d^3p\, dE\, \underline{P^N_{\text{hole}}(\mathbf{p}, E)}\, \underline{\frac{M}{E_\mathbf{p}} \frac{d\sigma^{\text{elem}}_{\ell N}}{d\omega' d\Omega}}\, \underline{P^N_{\text{part}}(\mathbf{p}', \mathcal{T}', \omega')}$$

Hole spectral function

Elementary cross section

Particle spectral function

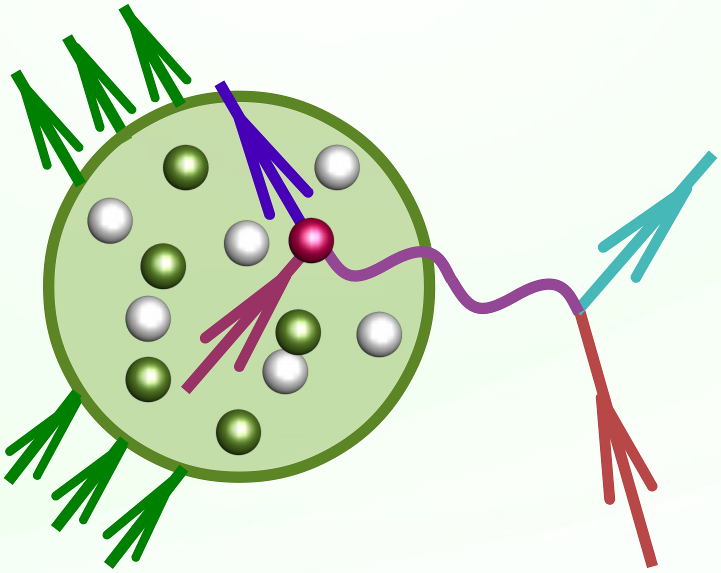

Impulse approximation

For scattering in a given angle, neutrinos and electrons differ only due to **the elementary cross section**.

In neutrino scattering, uncertainties come from (i) interaction dynamics and (ii) **nuclear effects.**

It is **highly improbable** that theoretical approaches unable to reproduce *(e,e′)* data would describe nuclear effects in neutrino interactions at similar kinematics.

Much more than the vector part...

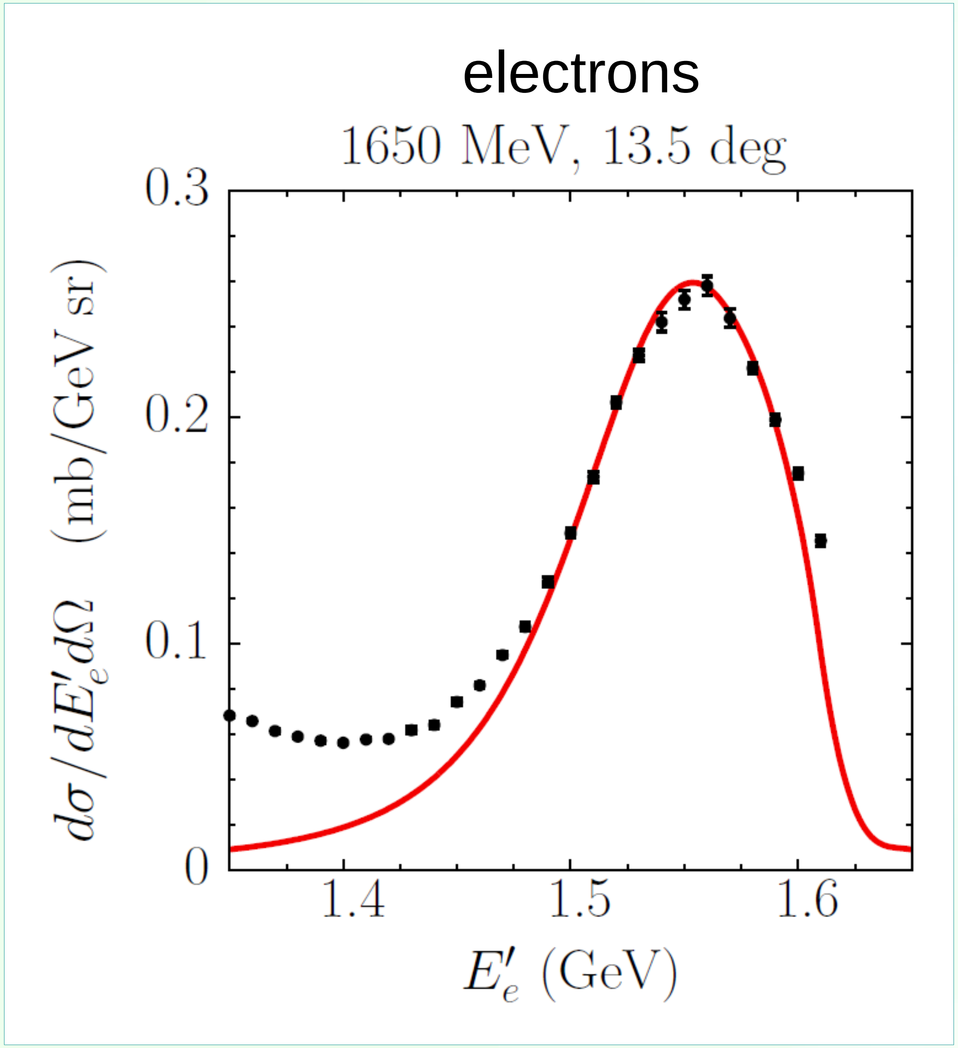

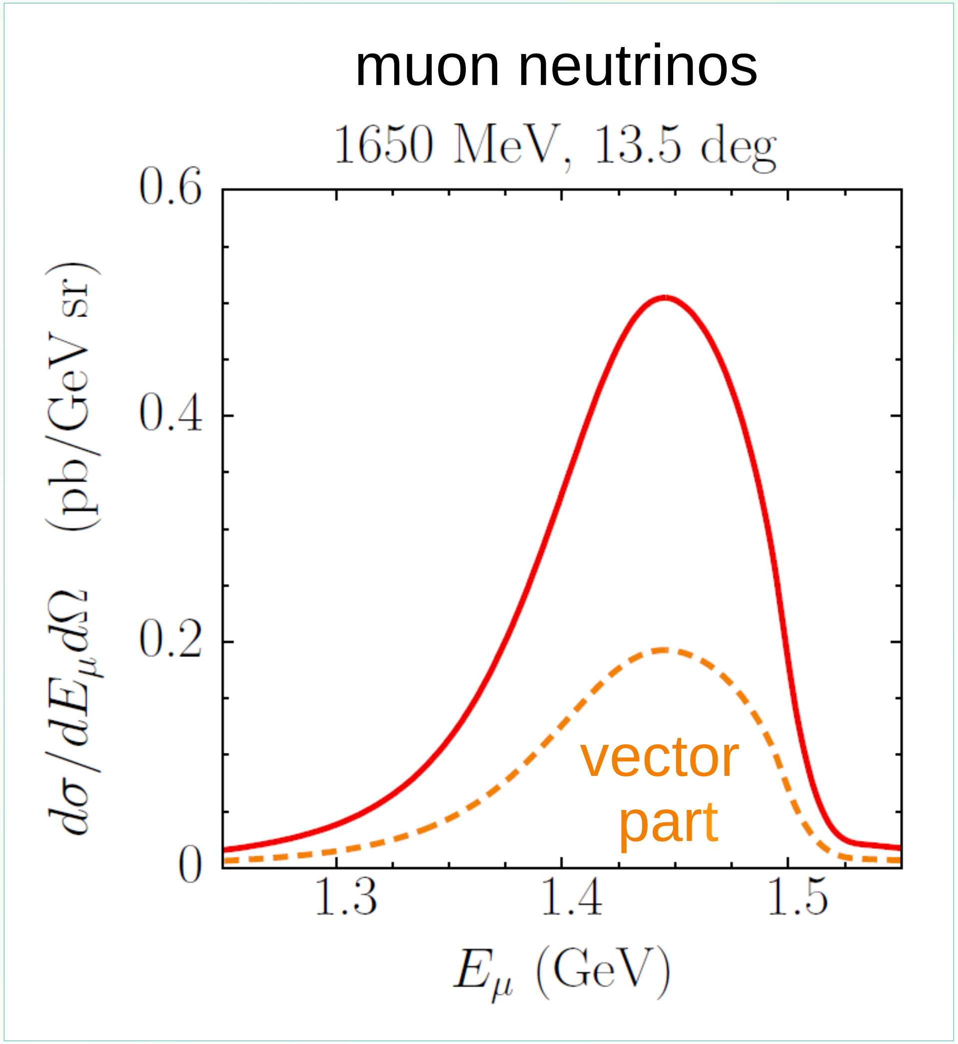

How relevant is the precision?

Expected sensitivity of DUNE to CP violation as a function of exposure for a ν_e signal normalization uncertainties between 5% + 1% and 5% + 3%.

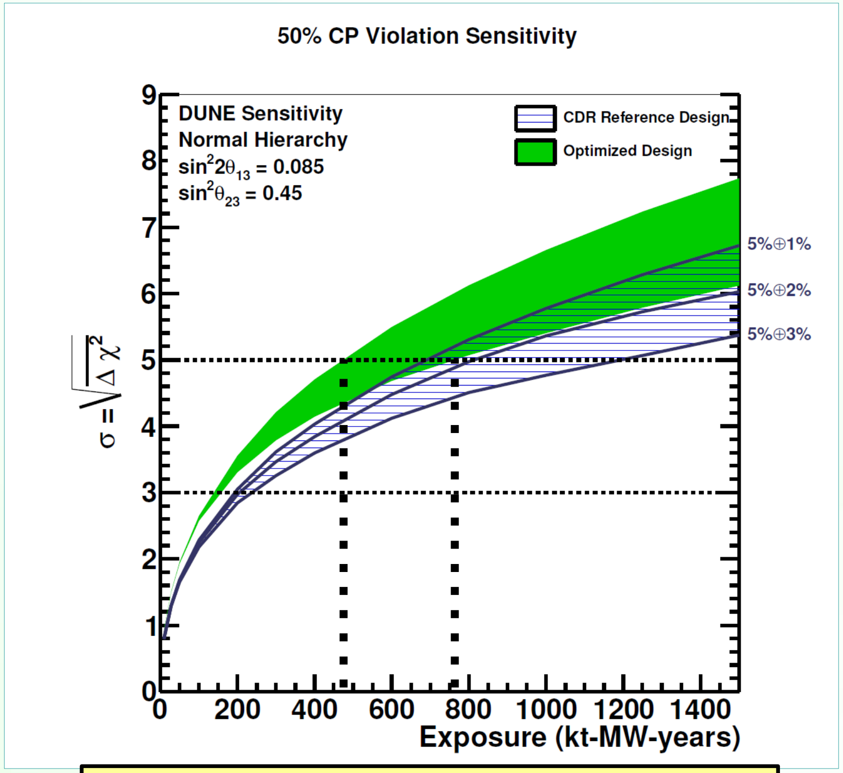

Acciari *et al.*, arXiv:1512.06148

Off-shell effects

Consider a nucleus stable against emission of nucleons.

As in its ground state, $E_A = M_A$, the energy cannot be decreased by emission of a nucleon

$$E_A = E_{A\text{-}1} + E_p < E_{A\text{-}1} + M$$

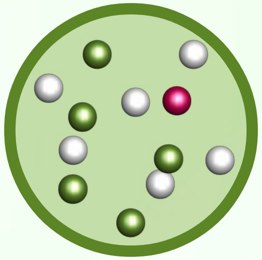

so the energy of a nucleon in the nucleus is lower than M.

V.R. Pandharipande, Nucl. Phys. B (Proc. Suppl.) 112, 51 (2002)

Off-shell effects

In a nuclear model, the initial nucleon's energy may

- differ from the on-shell energy by a constant

$$\boxed{E_p = \sqrt{M^2 + |\mathbf{p}|^2} - \epsilon}$$

- be a function of the momentum

$$\boxed{E_p = \sqrt{M^2 + |\mathbf{p}|^2} - \varepsilon(|\mathbf{p}|)}$$

- lack 1:1 correspondence with momentum

increasing sophistication

Off-shell effects

The elementary cross section,

$$\boxed{\frac{d\sigma_{\ell N}^{\mathrm{elem}}}{dE_{\mathbf{k}'}d\Omega dE_{\mathbf{p}'}d\Omega_{\mathbf{p}'}} \propto L_{\mu\nu}H^{\mu\nu}}$$

contains two tensors

$$\boxed{L_{\mu\nu} \propto j_{\mu}^{\mathrm{lept}} j_{\nu}^{\mathrm{lept}*} \quad \text{and} \quad H^{\mu\nu} \propto j_{\mathrm{hadr}}^{\mu} j_{\mathrm{hadr}}^{\nu*}}$$

with **only the hadron one** affected by off-shell effects.

Off-shell effects

The current appearing in the hadron tensor is known on the mass shell,

$$j^{\mu}_{\mathrm{hadr}} = \overline{u}(\mathbf{p}', s') \left(\gamma^{\mu} F_1 + i\sigma^{\mu\kappa} \frac{q_{\kappa}}{2M} F_2 + \dots \right) u(\mathbf{p}, s)$$

or equivalently

$$j^{\mu}_{\mathrm{hadr}} = \overline{u}(\mathbf{p}', s') \left(\gamma^{\mu} (F_1 + F_2) - \frac{(p + p')^{\mu}}{2M} F_2 + \dots \right) u(\mathbf{p}, s)$$

Off-shell effects

The prescription of de Forest [NPA 392, 232 (1983)]:

to approximate the off-shell hadron tensor, one can use the on-shell expression with the same momentum transfer and a modified energy transfer,

$$\boxed{H^{\mu\nu}_{\text{off-shell}}(p,q) \to H^{\mu\nu}_{\text{off-shell}}(\tilde{p},\tilde{q})}$$

with

$$\boxed{\tilde{p} = (\sqrt{M^2+\mathbf{p}^2}, \mathbf{p}) \quad \text{and} \quad \tilde{q} = (\tilde{\omega}, \mathbf{q})}$$

Off-shell effects

The prescription of de Forest [NPA 392, 232 (1983)]:

as the initial nucleon's energy is now $E_{\boldsymbol{p}} = \sqrt{M^2 + \boldsymbol{p}^2}$
in our calculations, and the final energy is an observable,
the energy transfer has to be

$$\boxed{\tilde{\omega} = \sqrt{M^2 + (\mathbf{p} + \mathbf{q})^2} - \sqrt{M^2 + \mathbf{p}^2}}$$

the difference between the “lepton” ω and “hadron” $\widetilde{\omega}$
is transferred to the spectator system of (A-1) nucleons.

Off-shell effects

Examples of an oversimplified treatment:

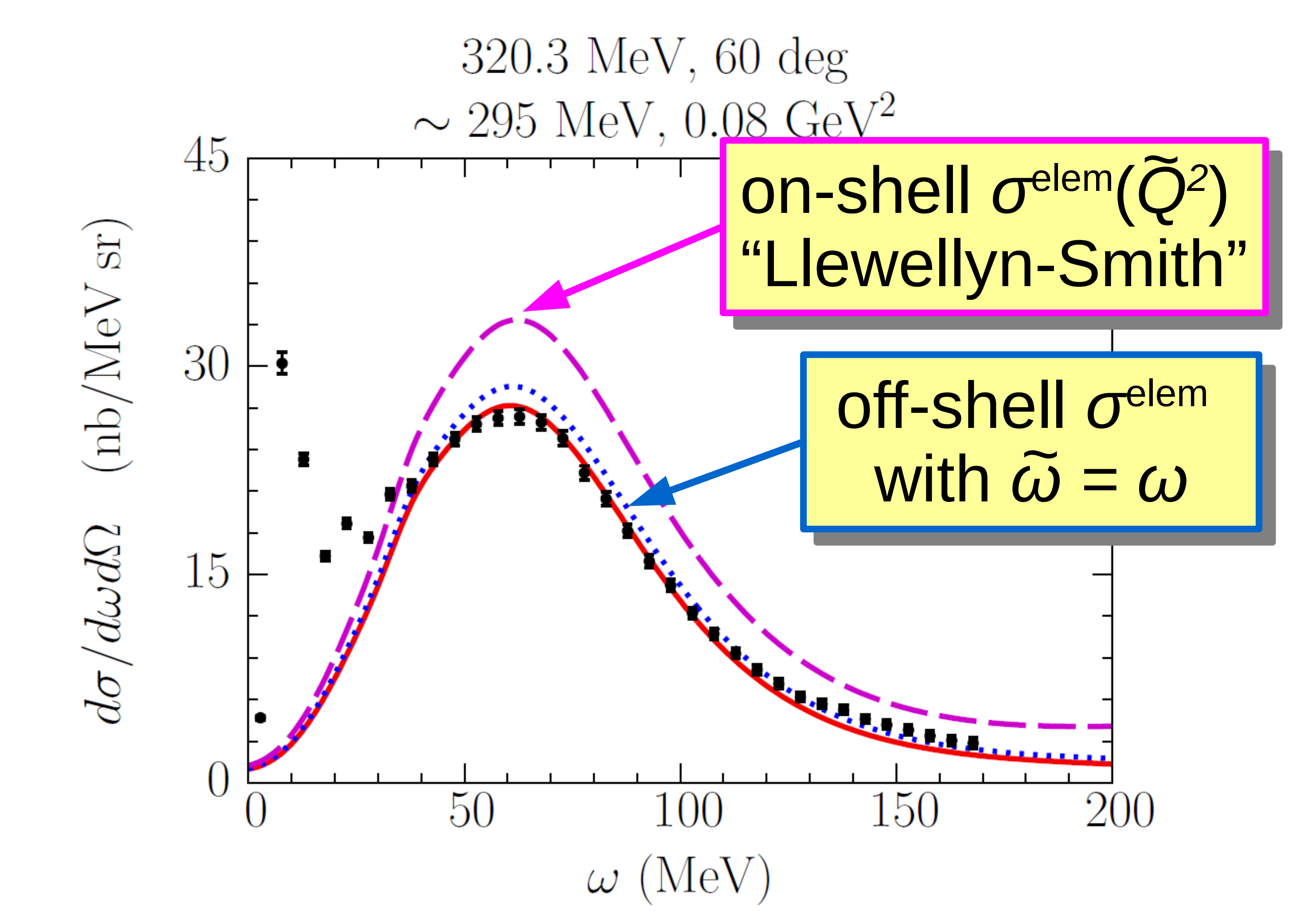

Coulomb effects

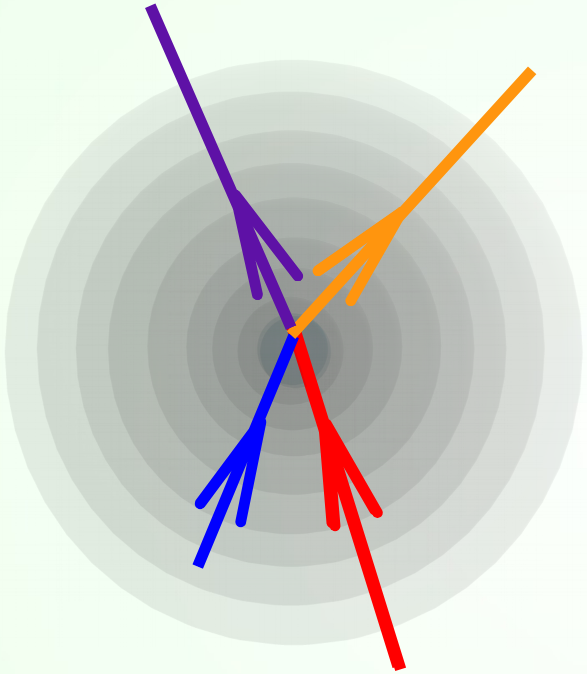

deeper binding

deceleration

$$\nu_\ell + n \to \ell^- + p,$$

$$\bar{\nu}_\ell + p \to \ell^+ + n,$$

acceleration

deeper potential

Coulomb effects

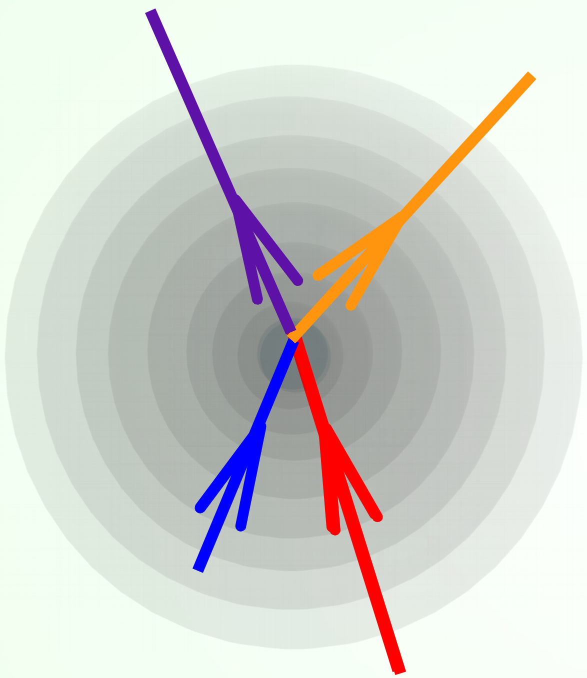

deeper binding

deceleration

$$\nu_\ell + n \to \ell^- + p,$$
$$\bar{\nu}_\ell + p \to \ell^+ + n,$$

acceleration

deeper potential

For ^{12}C, it gives 2.8 + 3*3.5 ≈ 13 MeV,
the difference relevant for ~~CP~~ measurements

Questions

Target dependence

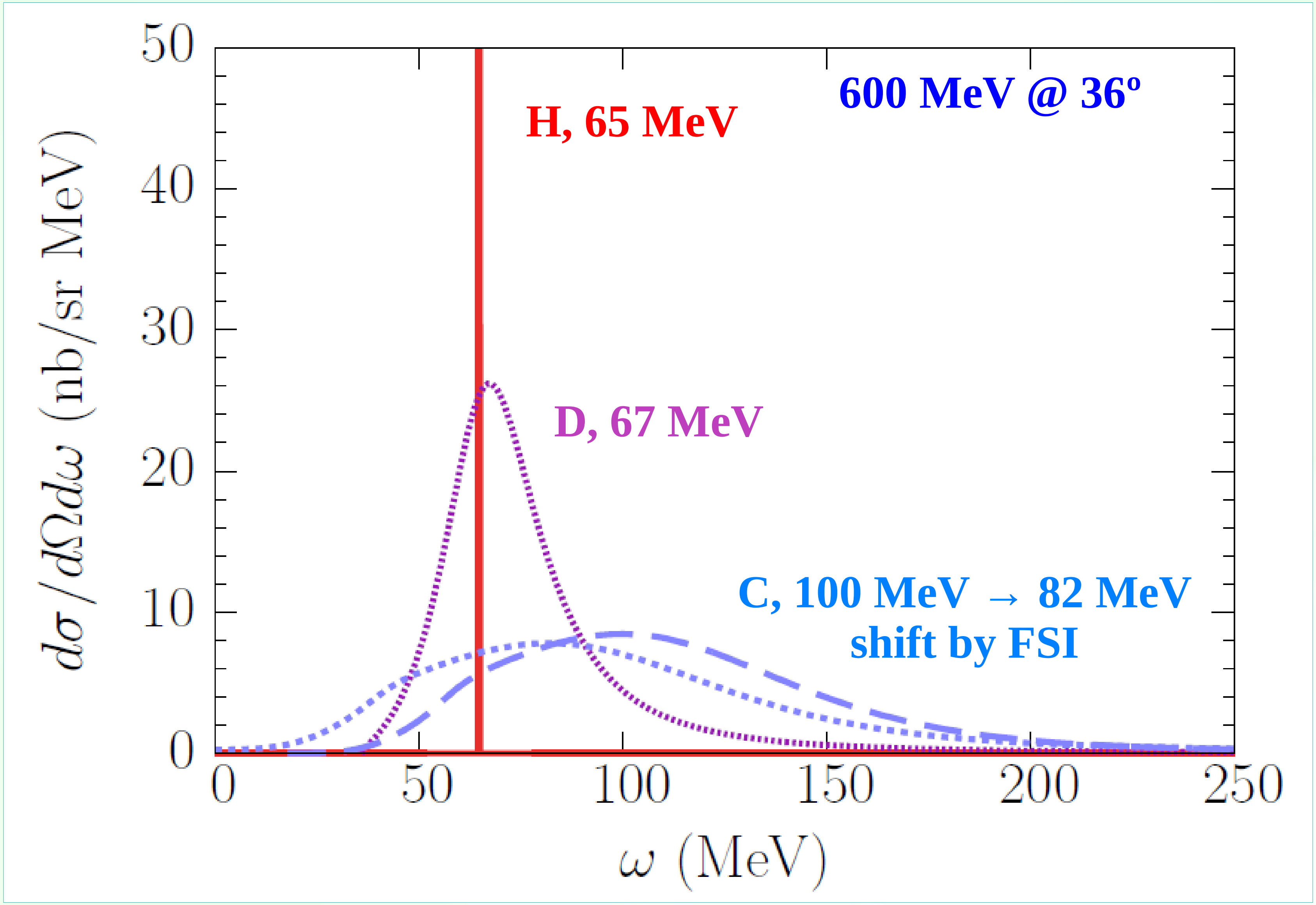

(Quasi)elastic scattering

- **Free nucleon**

$$E_p'^2 - \boldsymbol{p}'^2 = M^2$$

$$(M+\omega)^2 - \boldsymbol{q}^2 = M^2$$

$$2M\omega = Q^2$$

$$Q^2/(2M\omega) = 1$$

- **Bound nucleon**

$$E_p'^2 - \boldsymbol{p}'^2 = M^2$$

$$(M-E+\omega)^2 - (\boldsymbol{p}+\boldsymbol{q})^2 = M^2$$

$$2M\omega + E[E-2(\omega+M)] - \boldsymbol{p}(\boldsymbol{p}+2\boldsymbol{q}) = Q^2$$

$$Q^2/(2M\omega) = 1 + \frac{E}{M}(\ldots) + \frac{\boldsymbol{p}}{M}(\ldots)$$

Energy conservation

$$E_k + M_A = E_{k'} + E_{A-1} + E_{p'}$$

$$E_{A-1} = \sqrt{(M_A - M + E)^2 + \mathbf{p}^2}$$

removal energy

Calorimetric energy reconstruction

- In real detectors the method is only insensitive to nuclear effects when missing energy « neutrino energy
- Otherwise, requires input from nuclear models

To achieve ~25 MeV accuracy in DUNE, accurate predictions of exclusive cross sections are required.

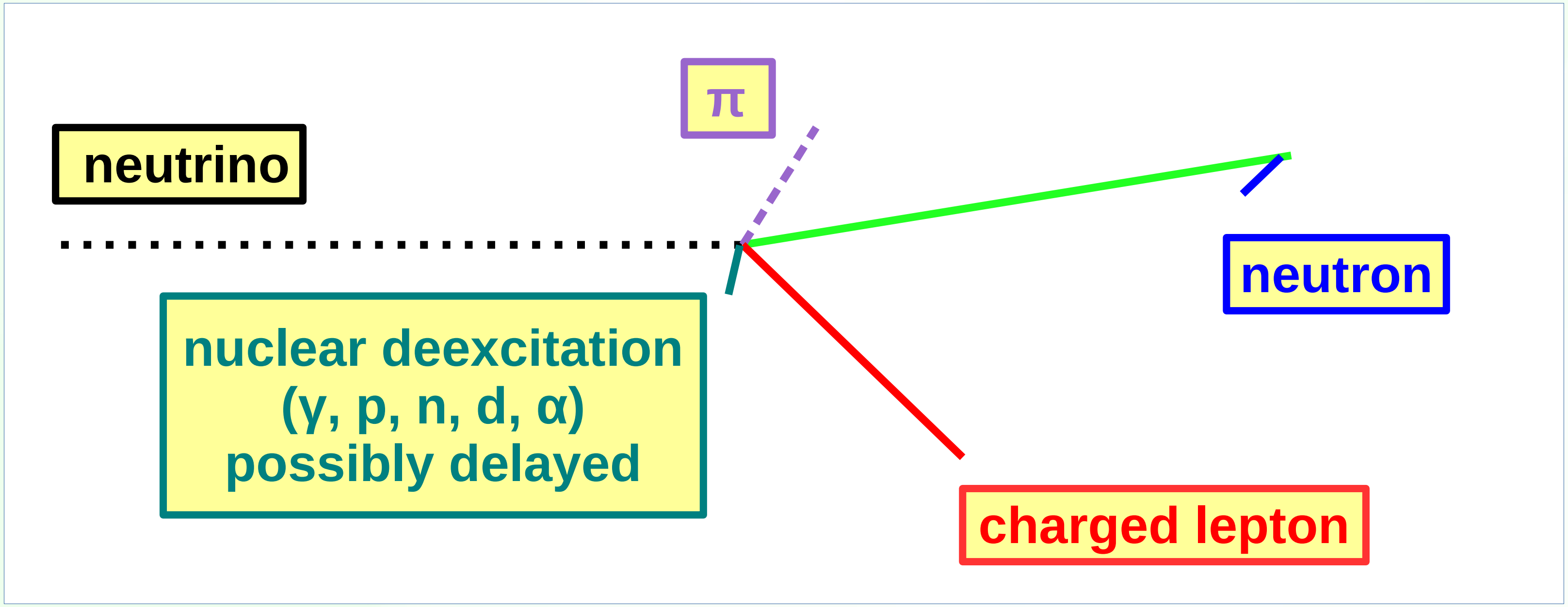

Impulse approximation

$$\frac{d\sigma_{\ell A}}{d\omega d\Omega} = \sum_N \int d\omega'\, d^3p\, dE\, \underbrace{P^N_{\text{hole}}(\mathbf{p}, E)}_{\text{Hole spectral function}}\, \underbrace{\frac{M}{E_{\mathbf{p}}} \frac{d\sigma^{\text{elem}}_{\ell N}}{d\omega' d\Omega}}_{\text{Elementary cross section}}\, \underbrace{P^N_{\text{part}}(\mathbf{p}', \mathcal{T}', \omega')}_{\text{Particle spectral function}}$$

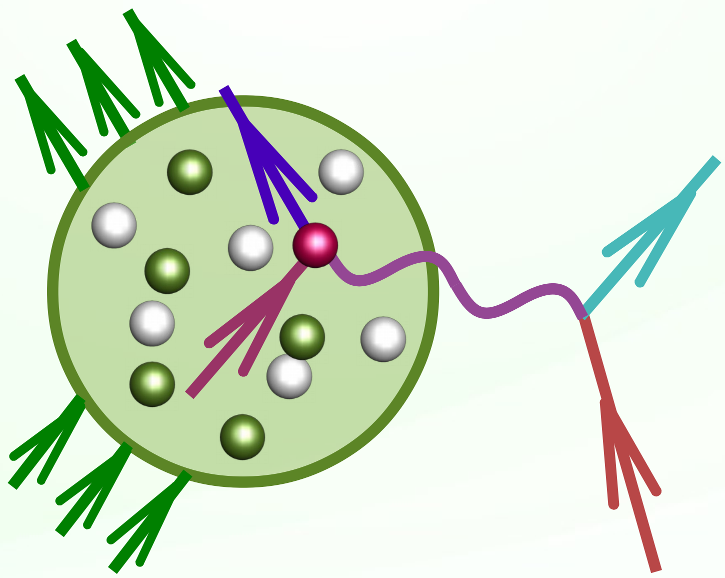

Fermi gas model

Fermi gas model

Imagine an infinite space filled uniformly with nucleons

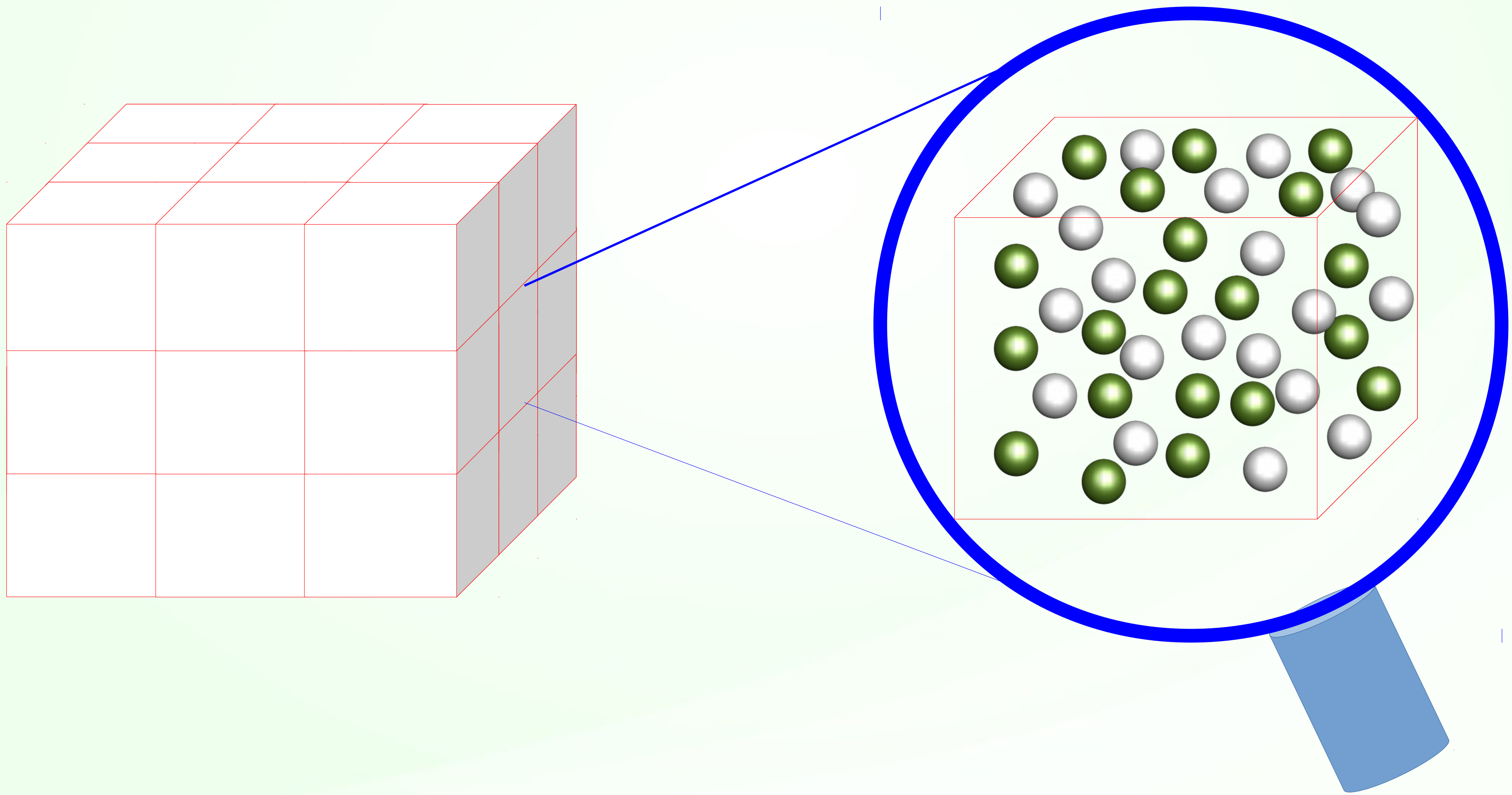

Fermi gas model

Due to the translational invariance, the eigenstates can be labeled using momentum, $\psi(x)=C e^{-i\boldsymbol{p}\boldsymbol{x}}$.

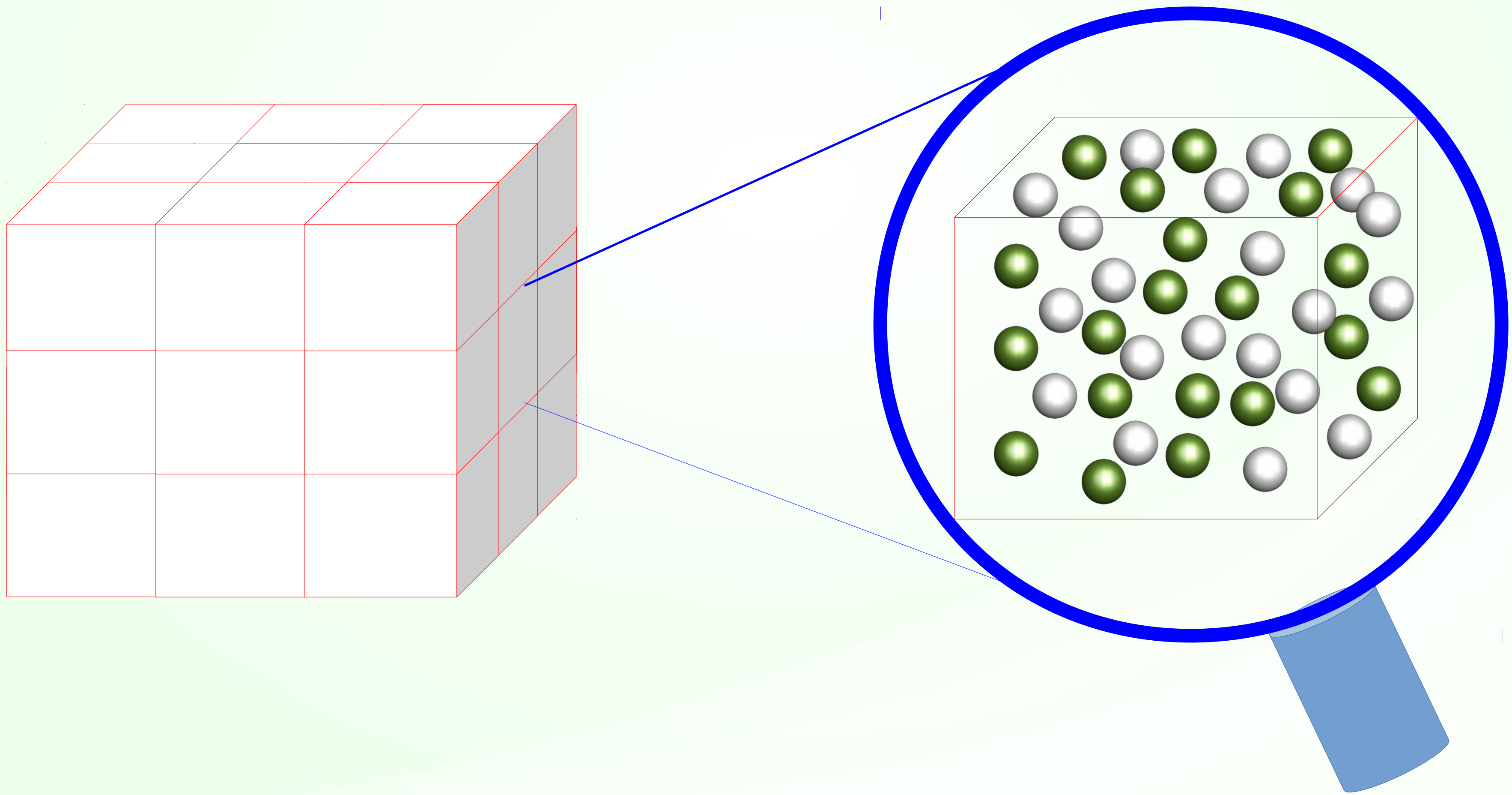

Fermi gas model

Due to the boundary conditions, $p_i \frac{L}{2} = \frac{\pi}{2} + n\pi$

every state occupies $(2\pi/L)^3$ in the momentum space

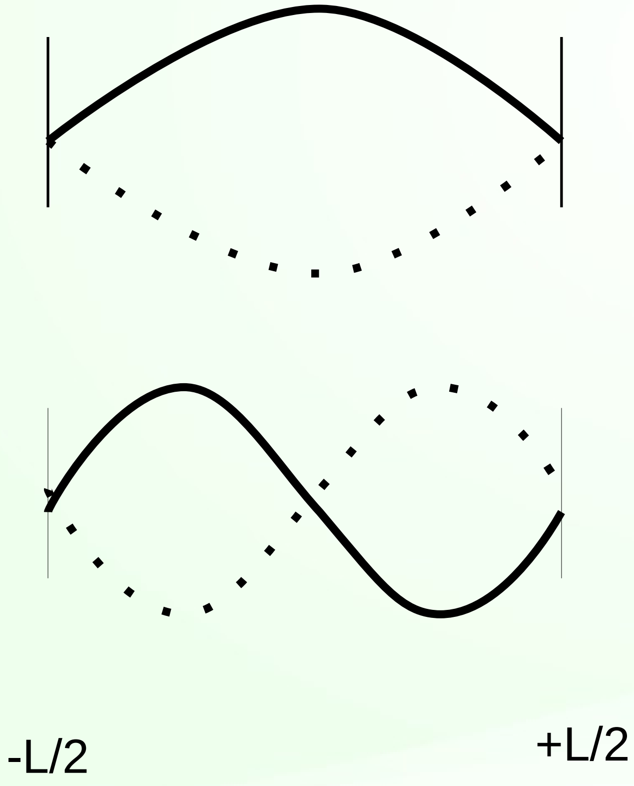

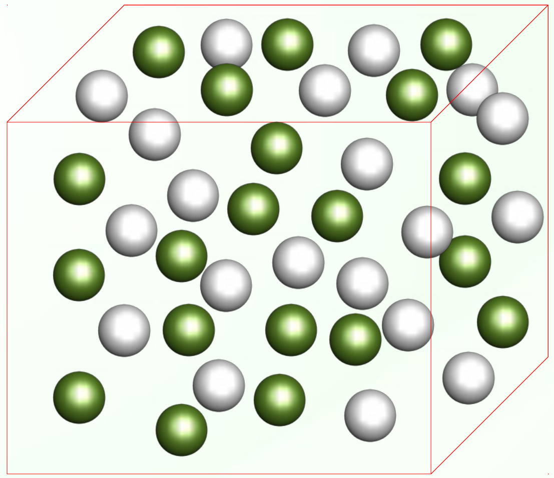

Fermi gas model

Due to the boundary conditions, $p_i \frac{L}{2} = \frac{\pi}{2} + n\pi$

every state occupies $(2\pi/L)^3$ in the momentum space

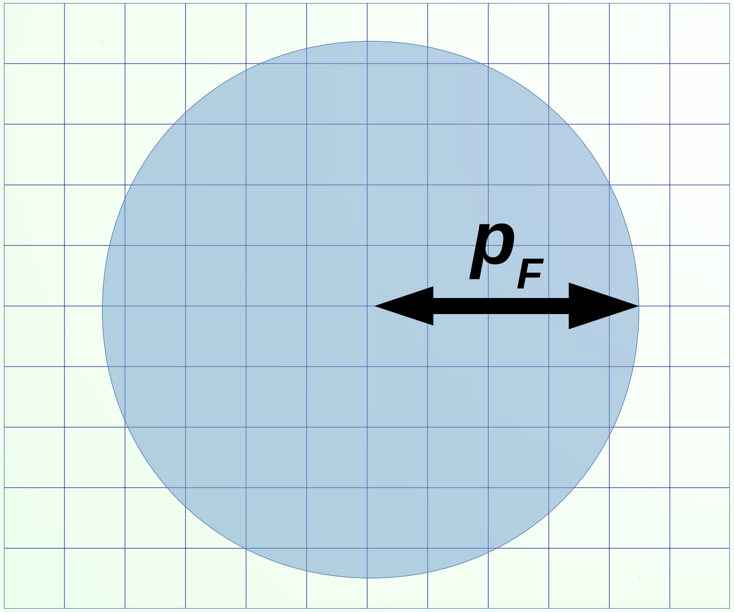

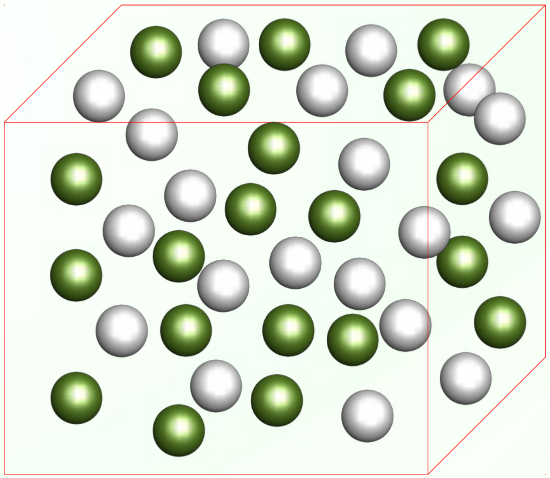

Momentum space

Coordinate space

Electron scattering off carbon, 500 MeV, 60 deg

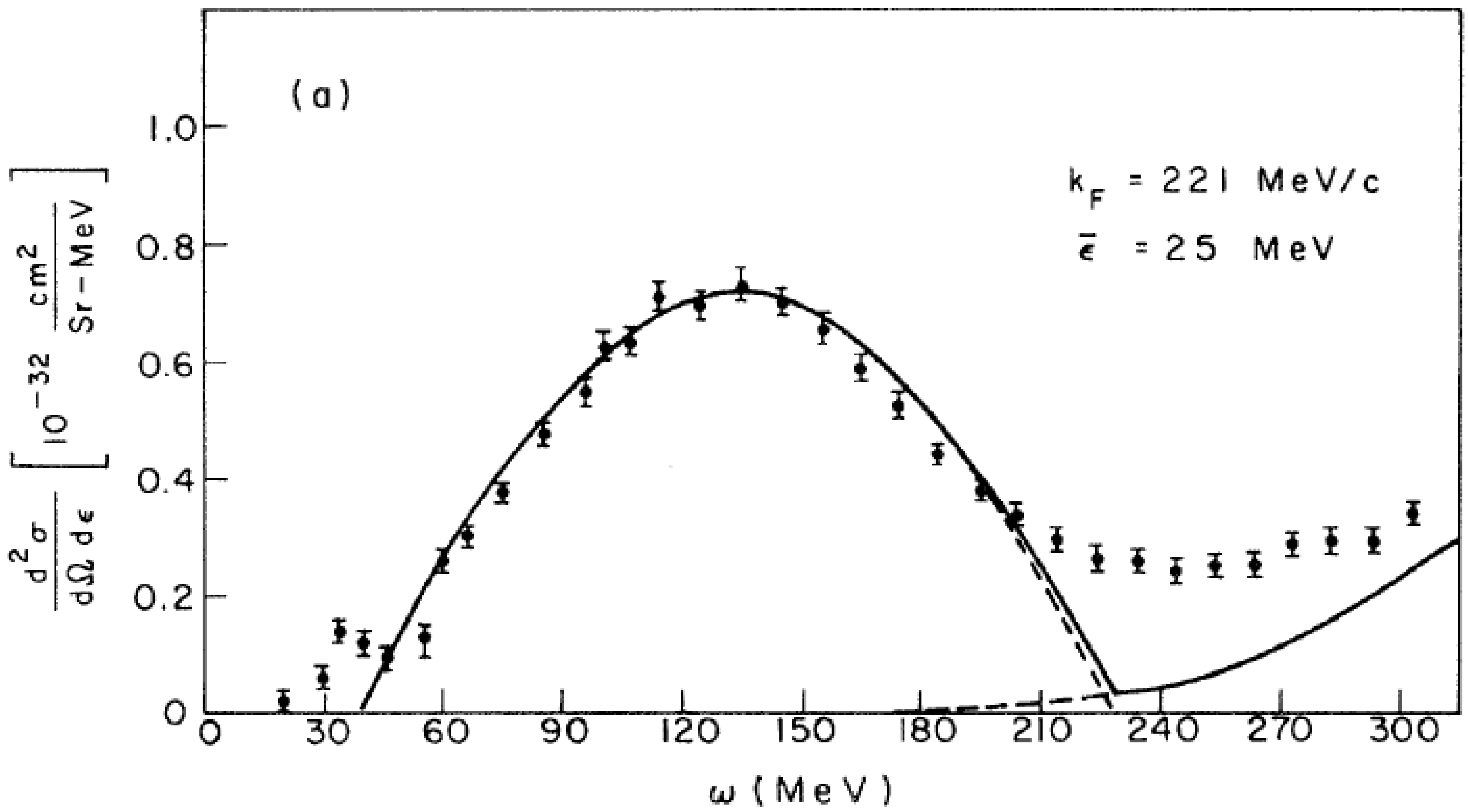

Moniz *et al.*, PRL 26, 445 (1971)

Electron scattering off carbon, 500 MeV, 60 deg

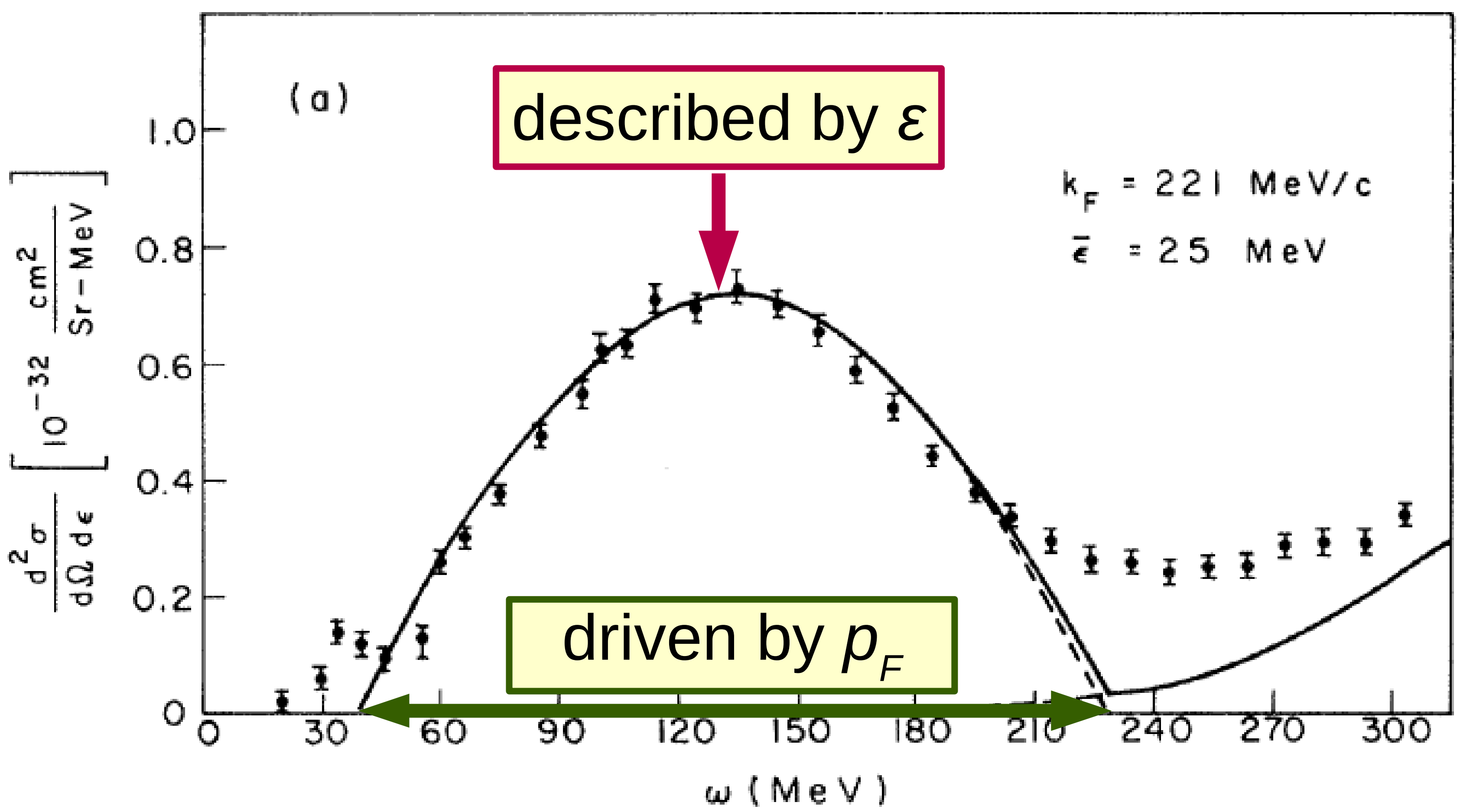

Moniz *et al.*, PRL 26, 445 (1971)

Fermi gas model

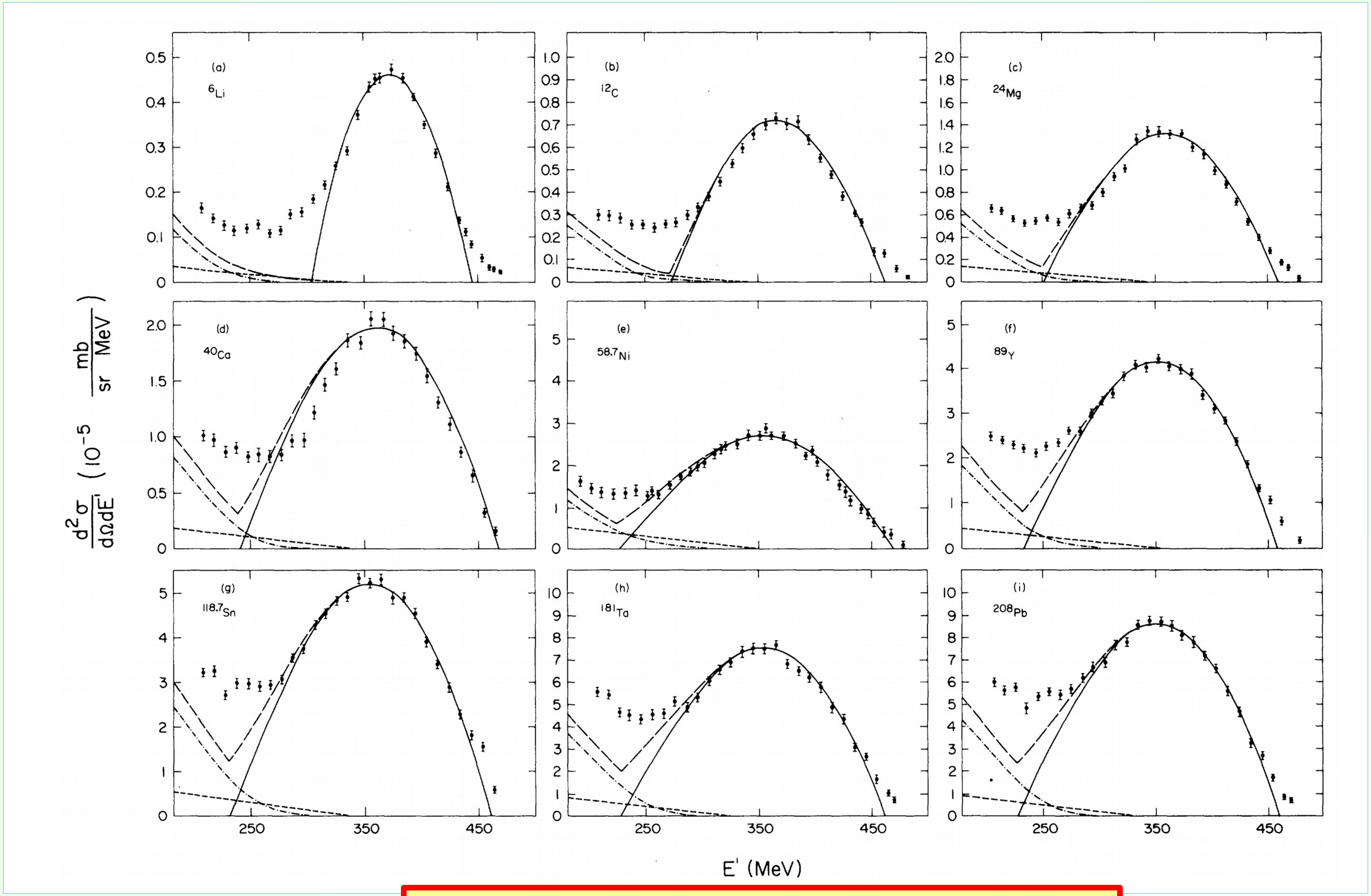

Whitney *et al.*, PRC 9, 2230 (1974)

Fermi gas model

What happens at kinematics other than 500 MeV, 60 deg?

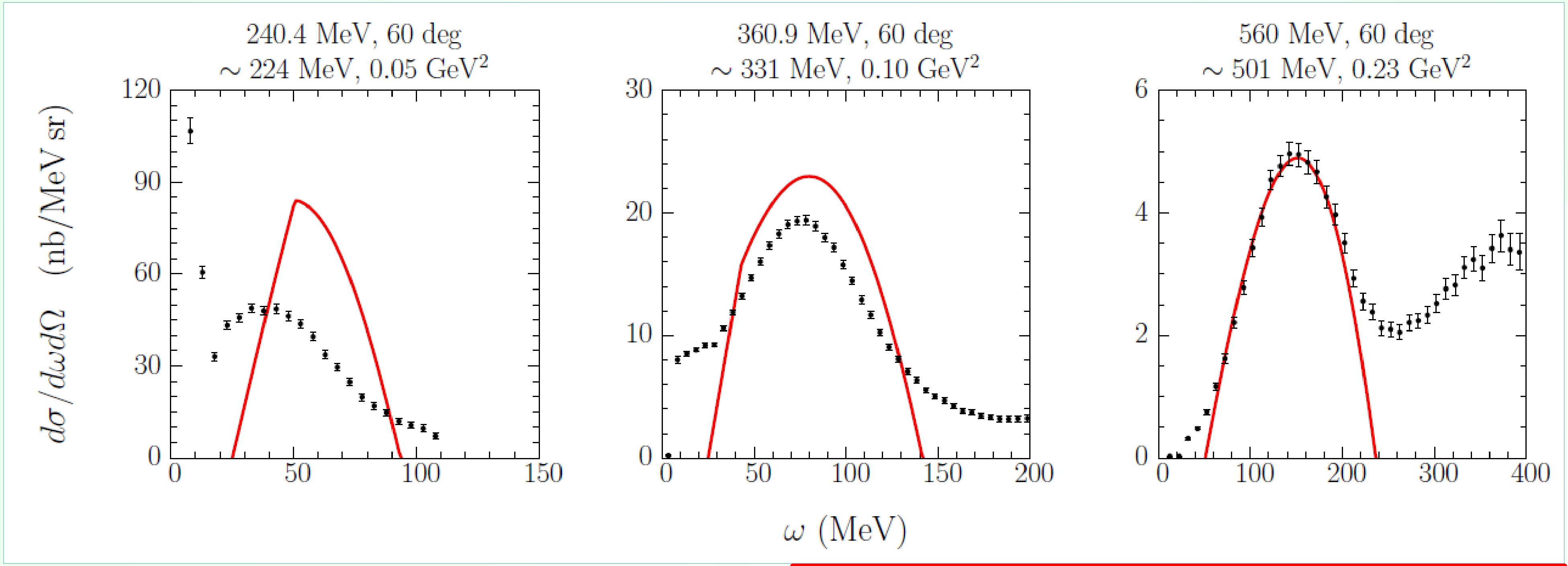

Barreau *et al.*, NPA 402, 515 (1983)

Shell model

Shell model

In a spherically symmetric potential, the eigenstates can be labeled using the total angular momentum.

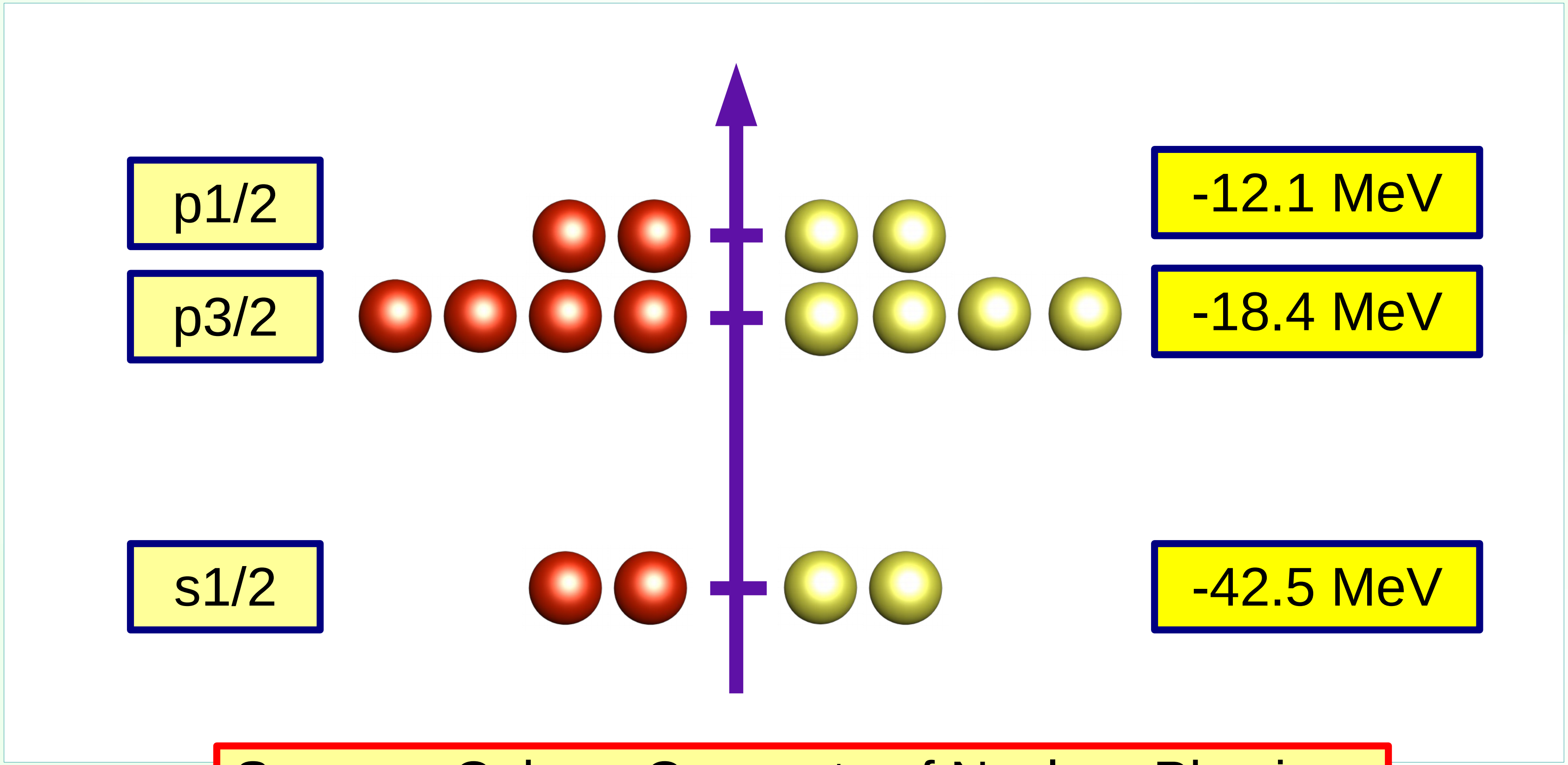

See e.g. Cohen, Concepts of Nuclear Physics, McGraw-Hill, 1971

Example: oxygen nucleus

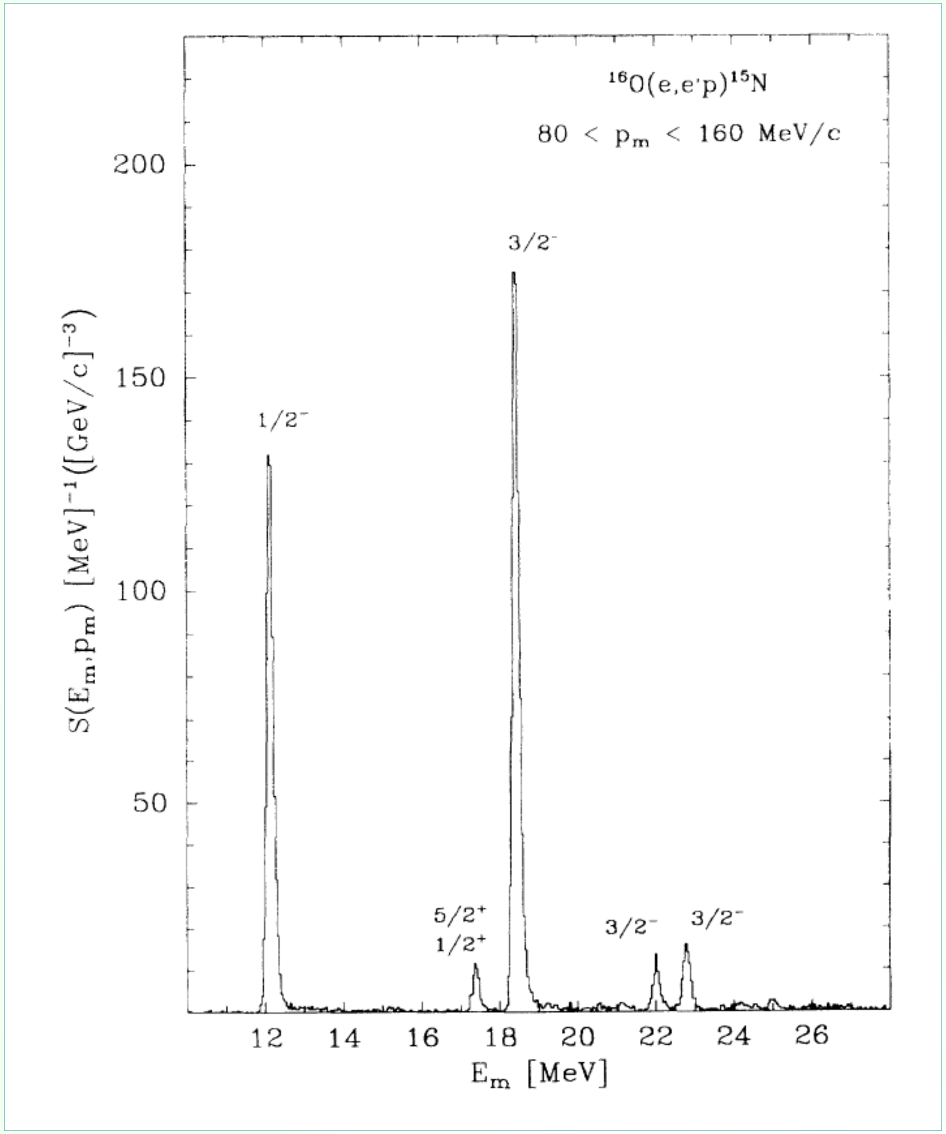

Leuschner *et al.*, PRC 49, 955 (1994)

Example: oxygen spectral function

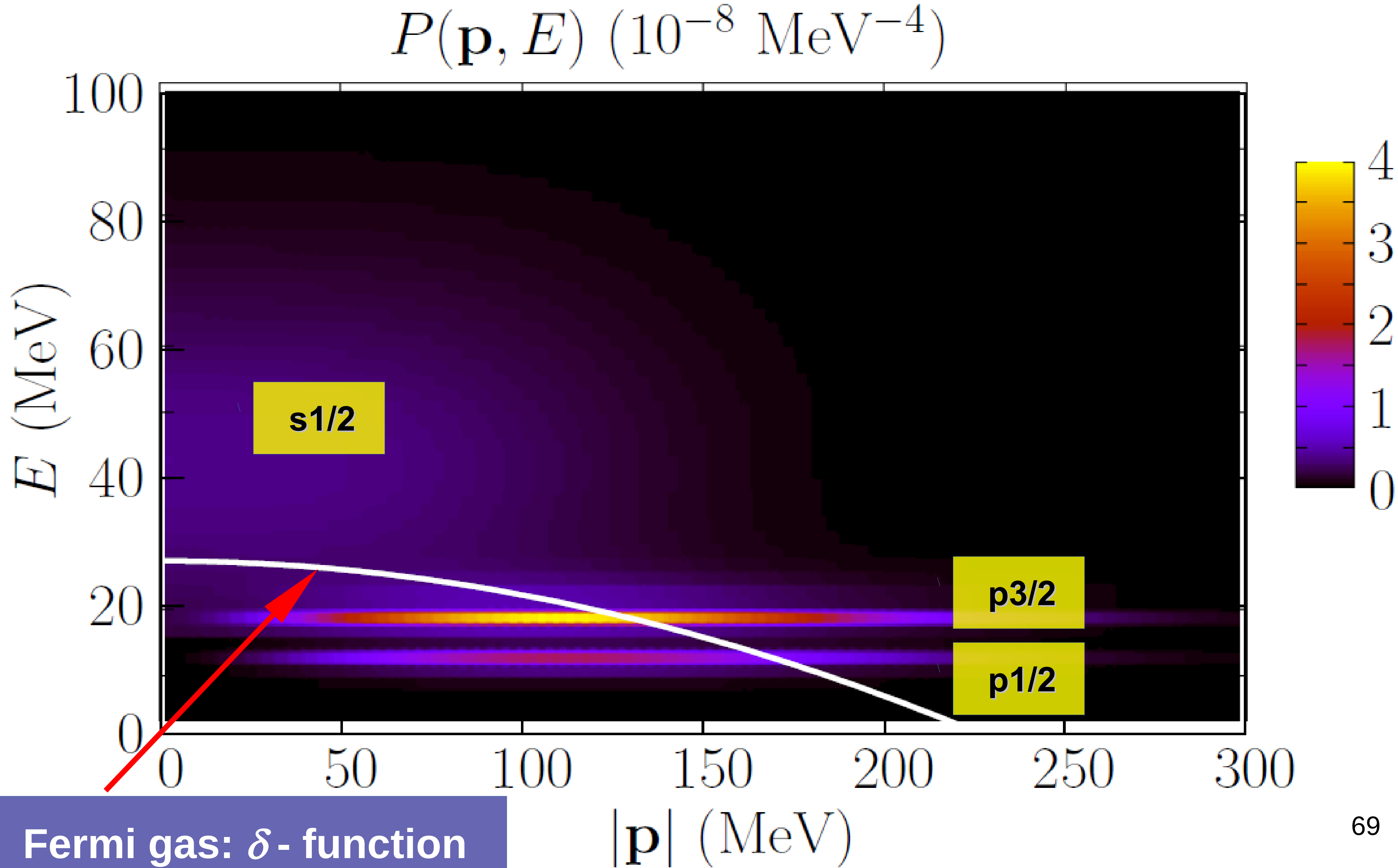

Fermi gas: δ - function

Depletion of the shell-model states

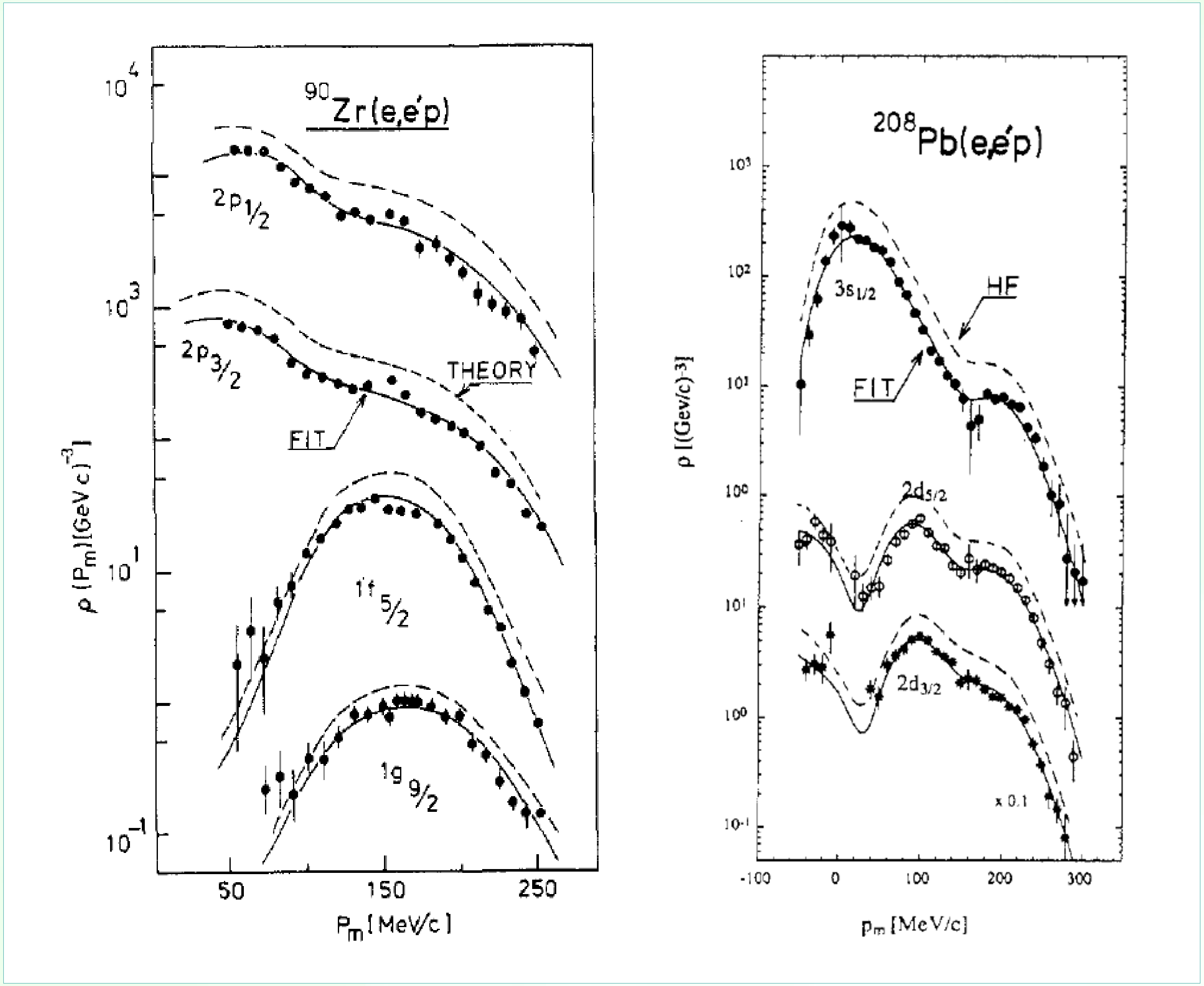

De Witt Huberts, JPG 16, 507 (1990)

Depletion of the shell-model states

The observed depletion is ~35% for the valence shells (LRC and SRC) and ~20% when higher missing energy is probed (SRC).

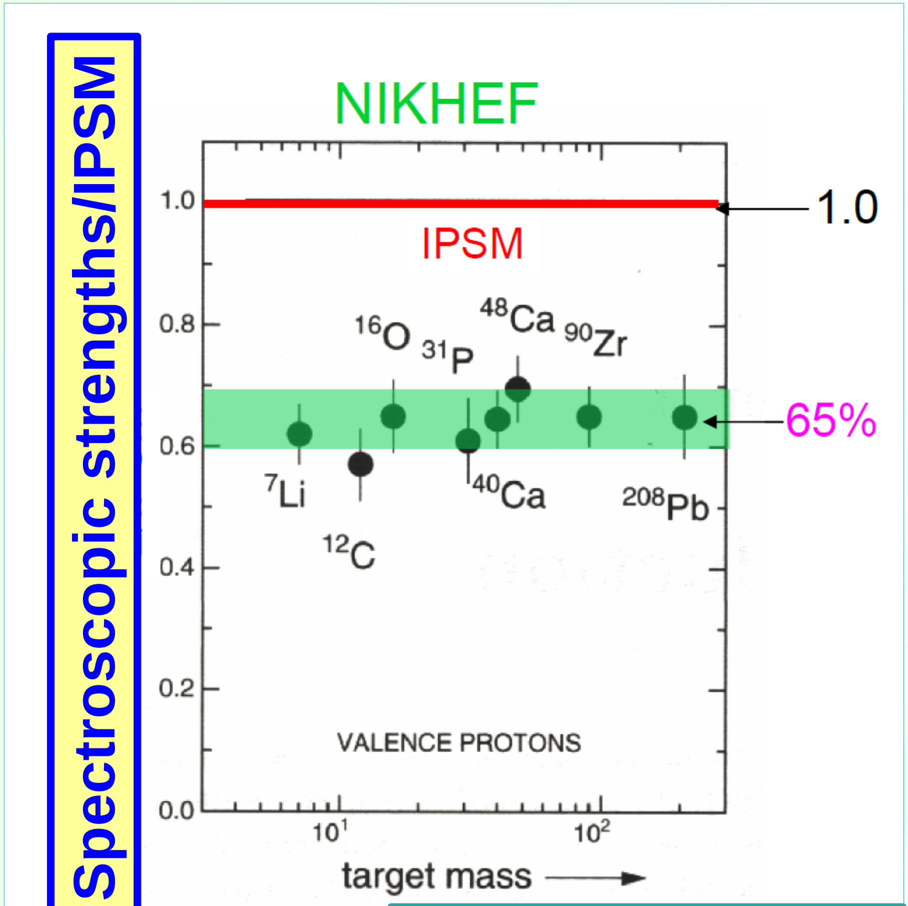

D. Rohe, NuInt05

NIKHEF: ^{208}Pb(e,e'p)^{207}Tl

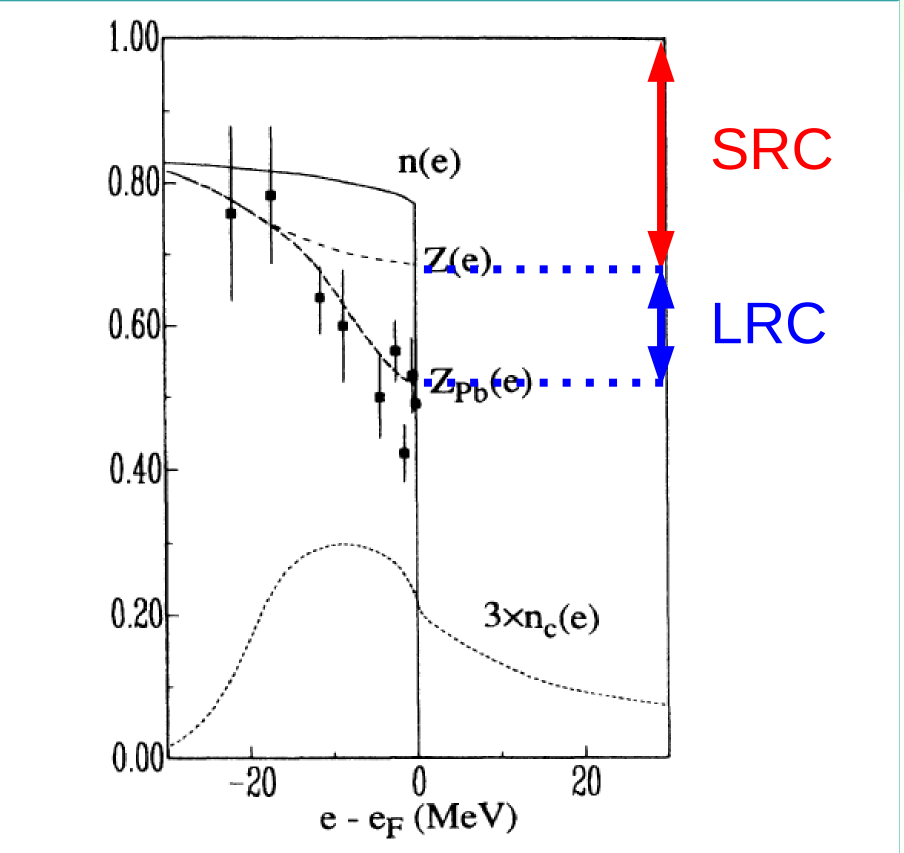

Benhar et al, PRC 41, R24 (1990)

Spectral function approach

Short-range correlations

The main source of the depletion of the shell-model states at high *E* are **short-range nucleon-nucleon correlations**.

Yielding NN pairs (typically pn pairs) with high relative momentum, they move ~20% of nucleons to the states of high removal energies.

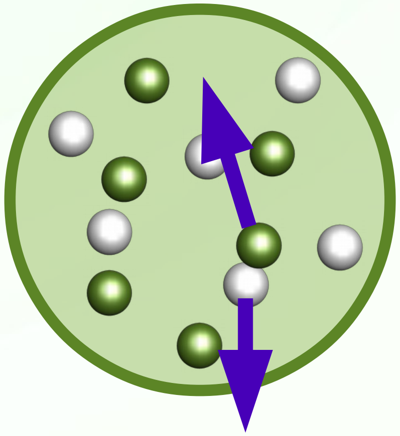

Short-range correlations

The hole spectral function can be expressed as

$$P_N(\mathbf{p}, E) = \sum_\alpha \underline{n_\alpha |\phi_\alpha|^2 f_\alpha (E - E_\alpha^N)} + \underline{P_{\text{corr}}^N(\mathbf{p}, E)},$$

describes the contribution of the shell-model states, vanishes at high |p| or high *E*

relevant only at high |p| **and** *E*

Short-range correlations

Momentum distributions

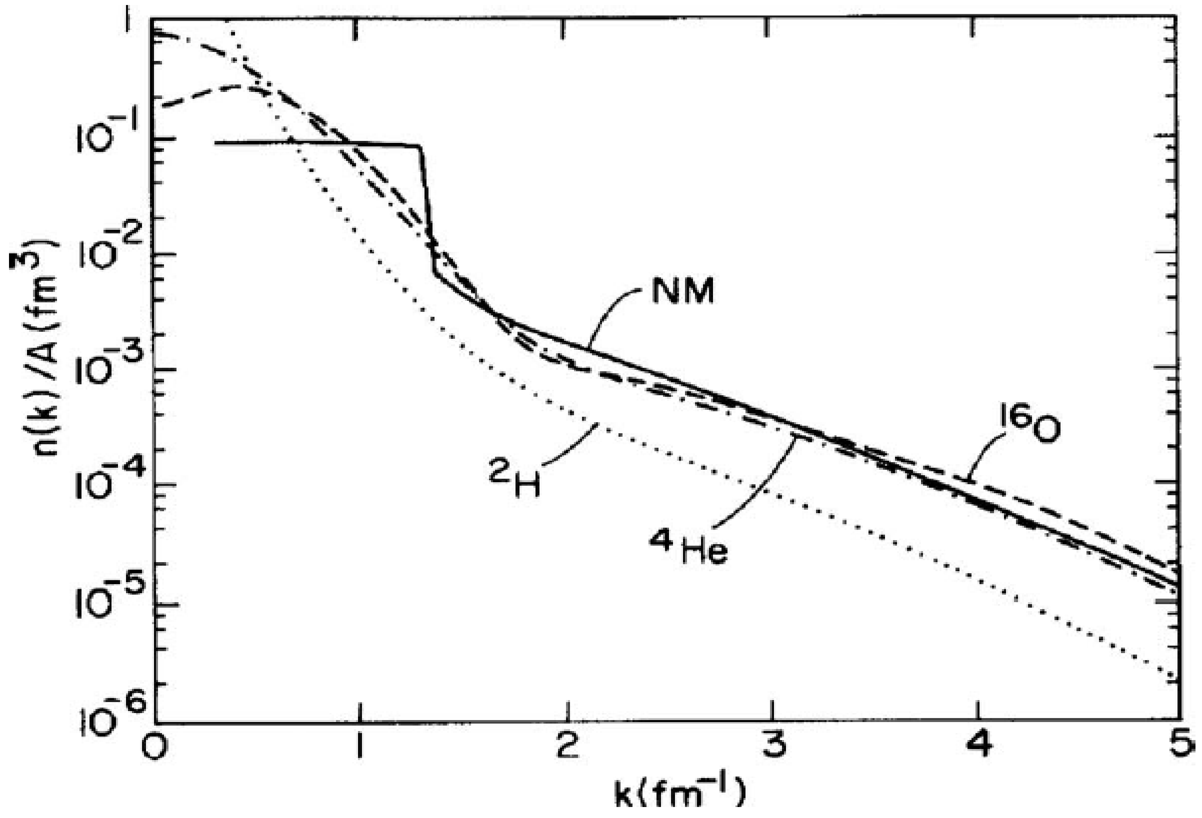

Benhar&Pandharipande, RMP 65, 817 (1993)

Short-range correlations

Momentum distributions

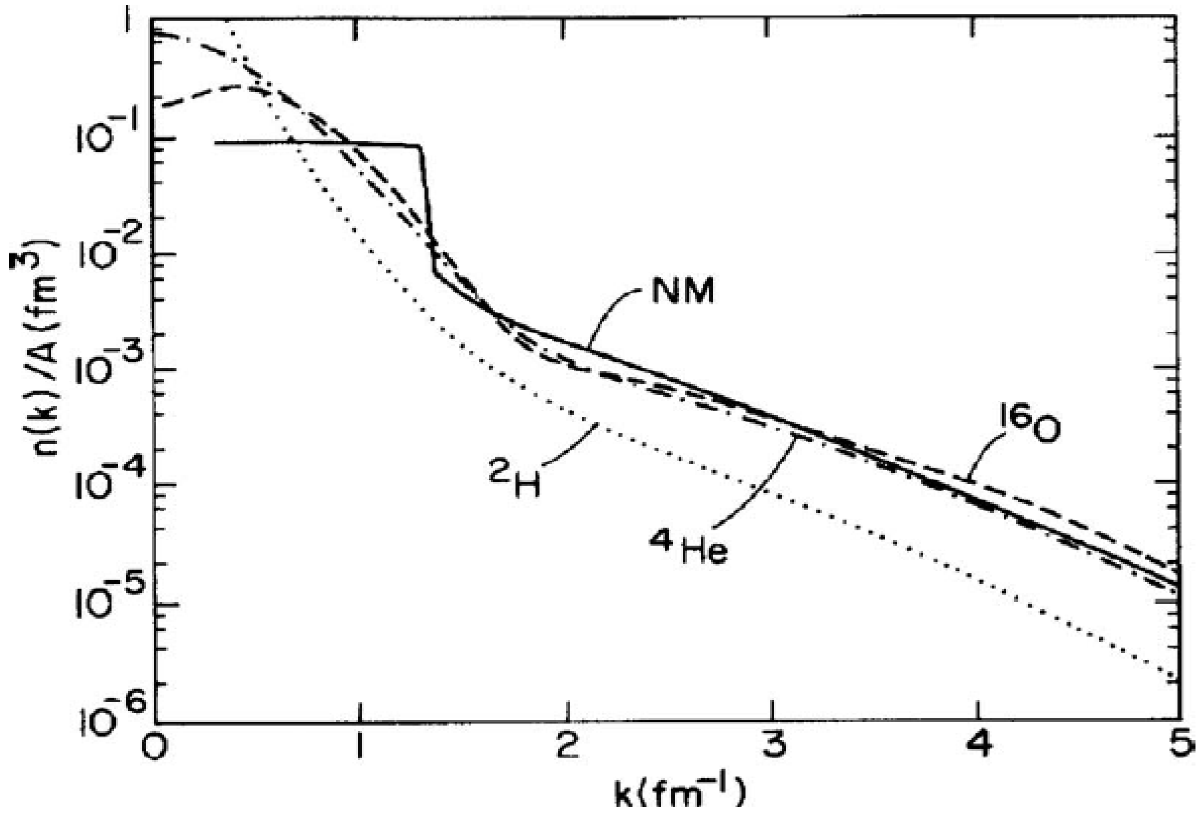

SRC don't depend on the shell structure or finite-size effects, only on the density

Local-density approximation

The correlation component in nuclei can be obtained combining the results for infinite nuclear matter obtained at different densities:

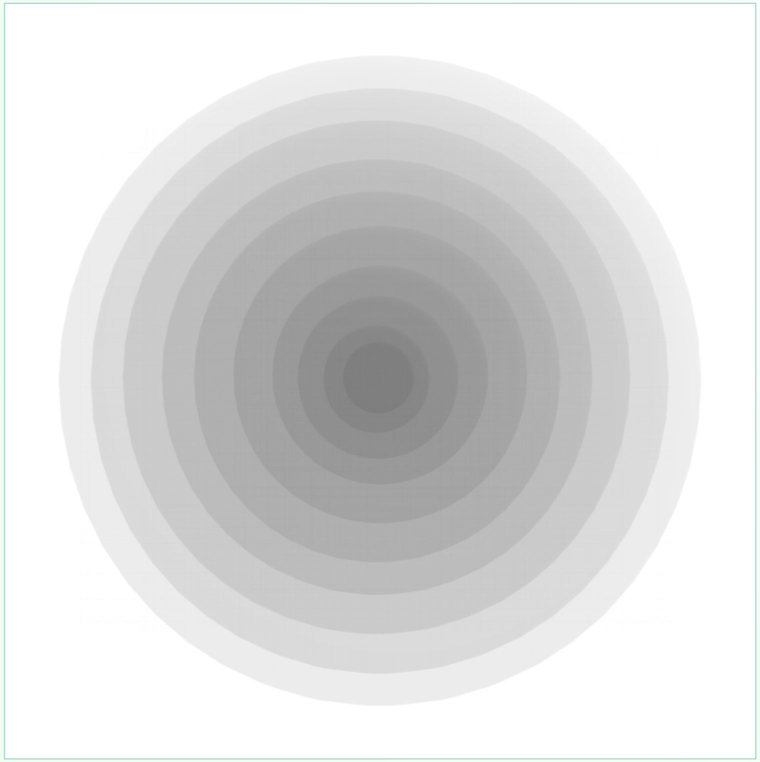

$$P^{N}_{\rm corr}(\mathbf{p}, E) = \int dR \rho(R) P^{NM,N}_{\rm corr}(\rho, \mathbf{p}, E).$$

Benhar *et al.*, NPA 579 493, (1994), included Urbana v_{14} NN interactions and 3N interactions [Lagaris & Pandharipande]

Side remark: relativistic kinematics

A.M.A. & O. Benhar, PRC 83, 054616 (2011)

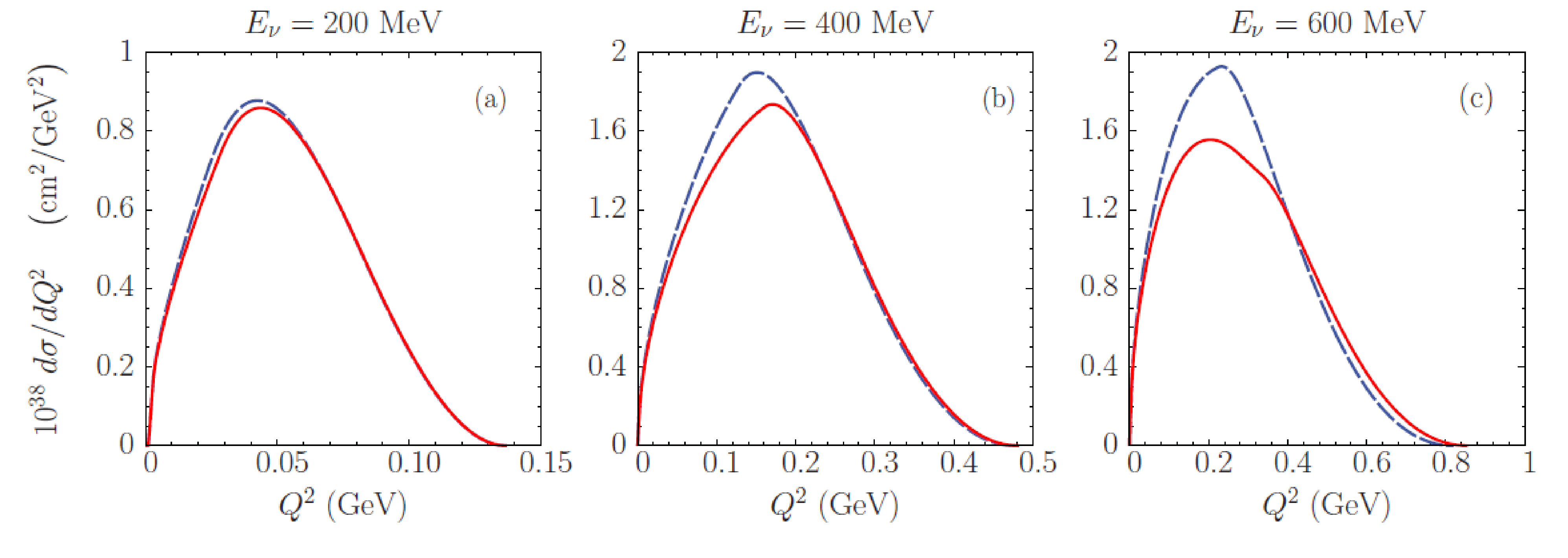

Sizable differences between the **relativistic** and **nonrelativistic** results at neutrino energies ~500 MeV.

Side remark: relativistic kinematics

A.M.A. & O. Benhar, PRC 83, 054616 (2011)

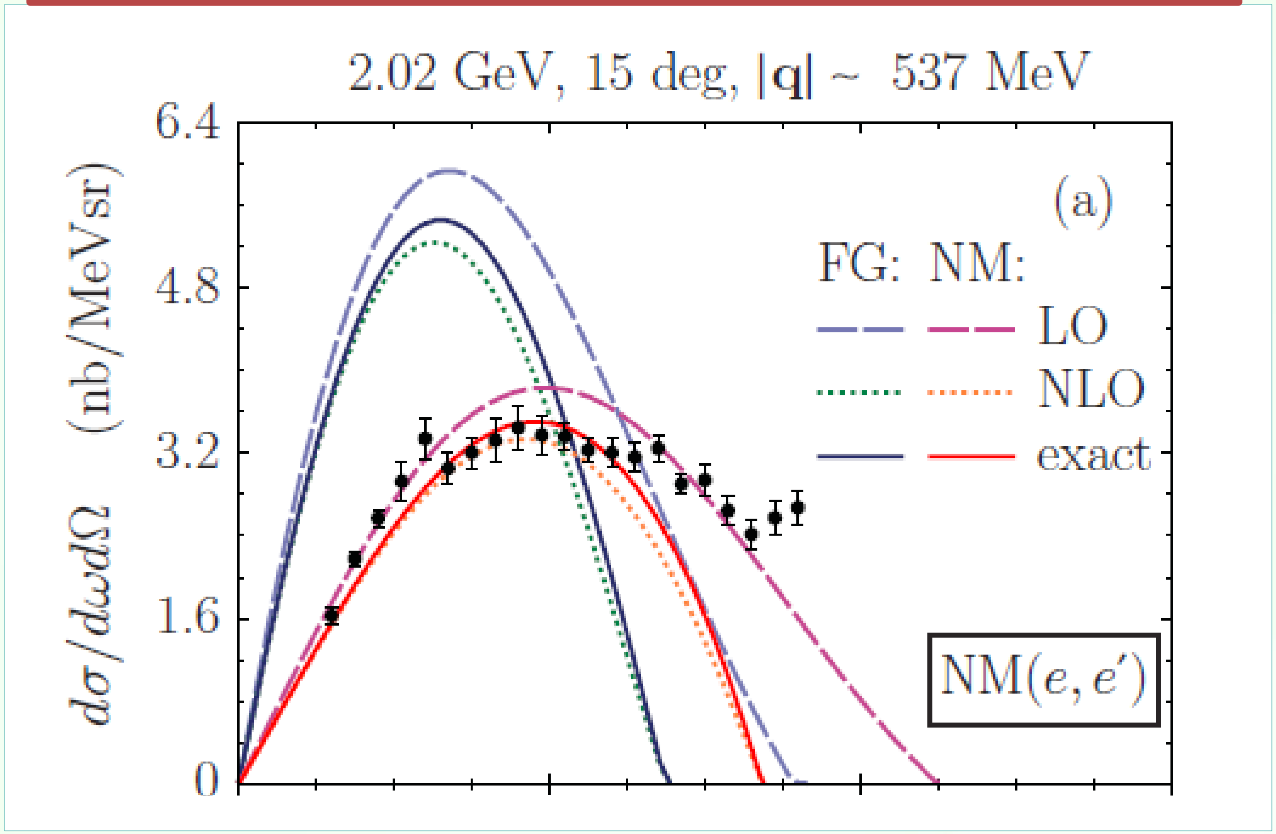

At |q|~540 MeV, semi-relativistic result is **5% lower** than the exact cross section.

Comparison to C(e, e') data

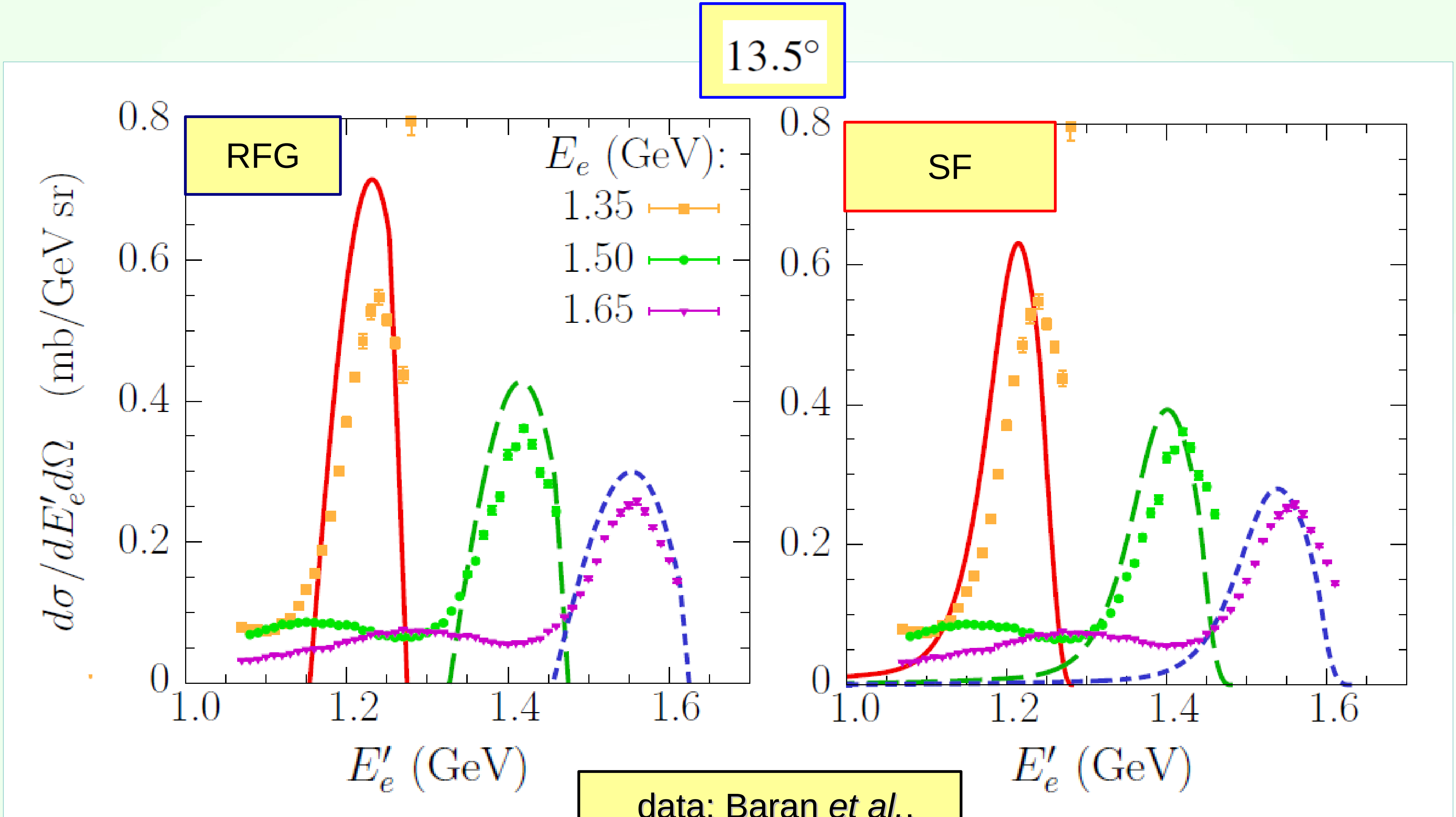

data: Baran *et al.*, PRL 61, 400 (1988)

Energy conservation

$$E_{\mathbf{k}} + M_A = E_{\mathbf{k}'} + E_{A-1} + E_{\mathbf{p}'}$$

Energy conservation

$$E_{\mathbf{k}} + M_A = E_{\mathbf{k}'} + E_{A-1} + E_{\mathbf{p}'}$$

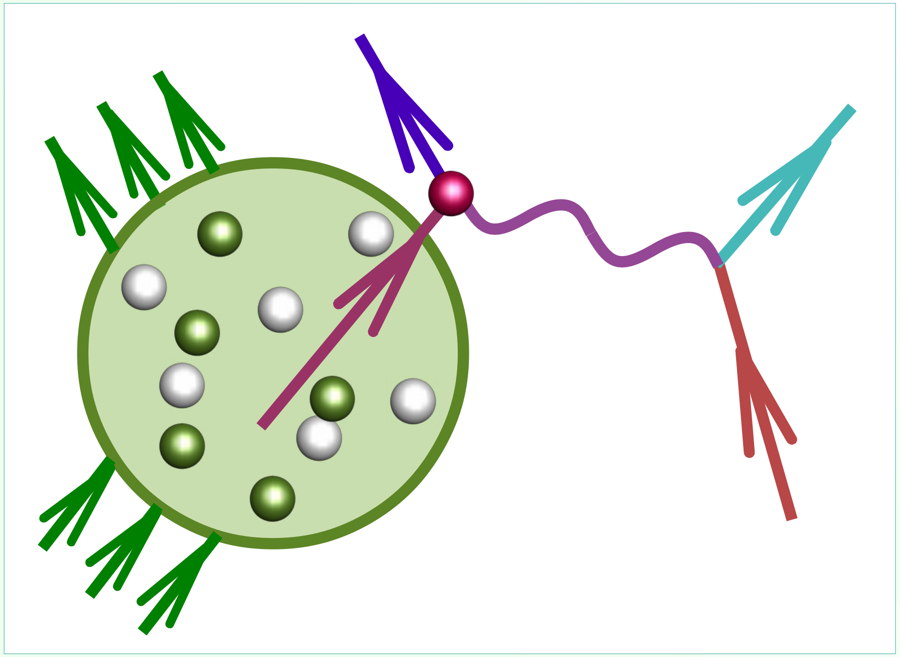

Energy conservation

$$E_{\mathbf{k}} + M_A = E_{\mathbf{k}'} + E_{A-1} + E_{\mathbf{p}'}$$

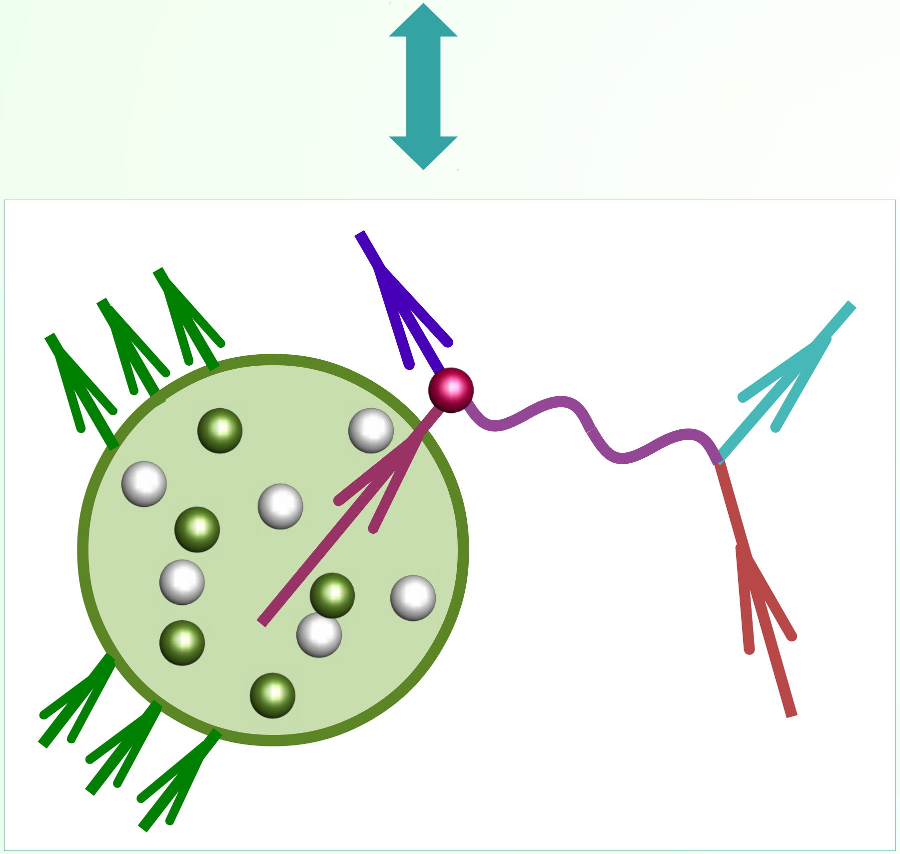

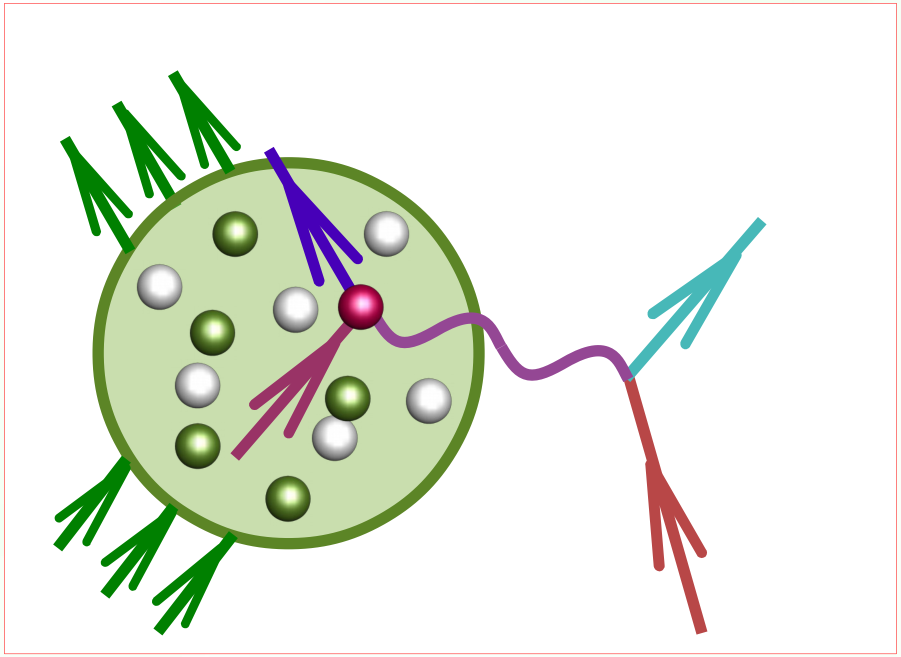

Energy conservation

$$E_{\mathbf{k}} + M_A = E_{\mathbf{k}'} + E_{A-1} + E_{\mathbf{p}'}$$

$$E_{\mathbf{k}} + M_A = E_{\mathbf{k}'} + E_{A-1} + E_{\mathbf{p}'} + U_V(\mathbf{p}')$$

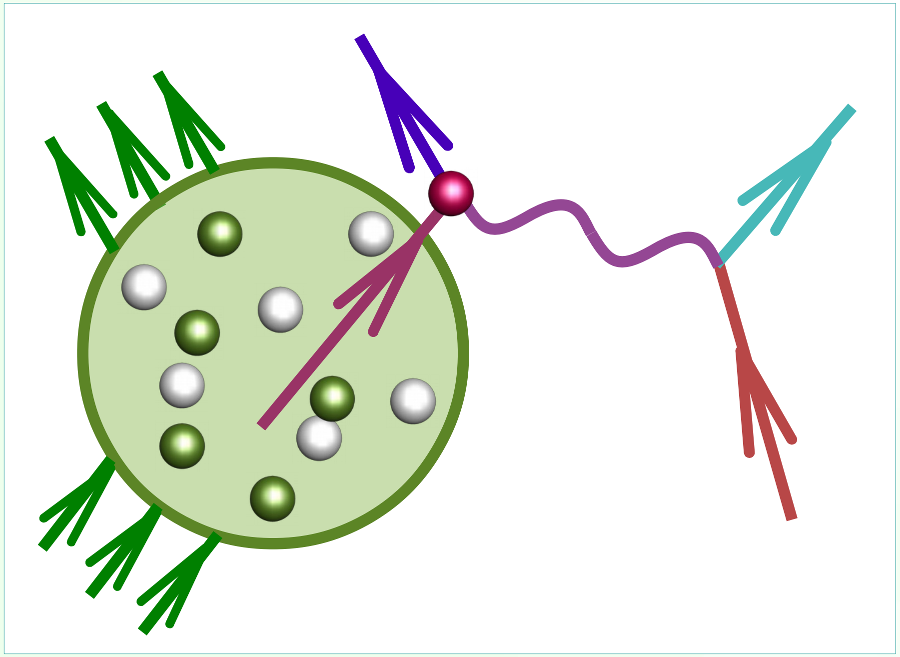

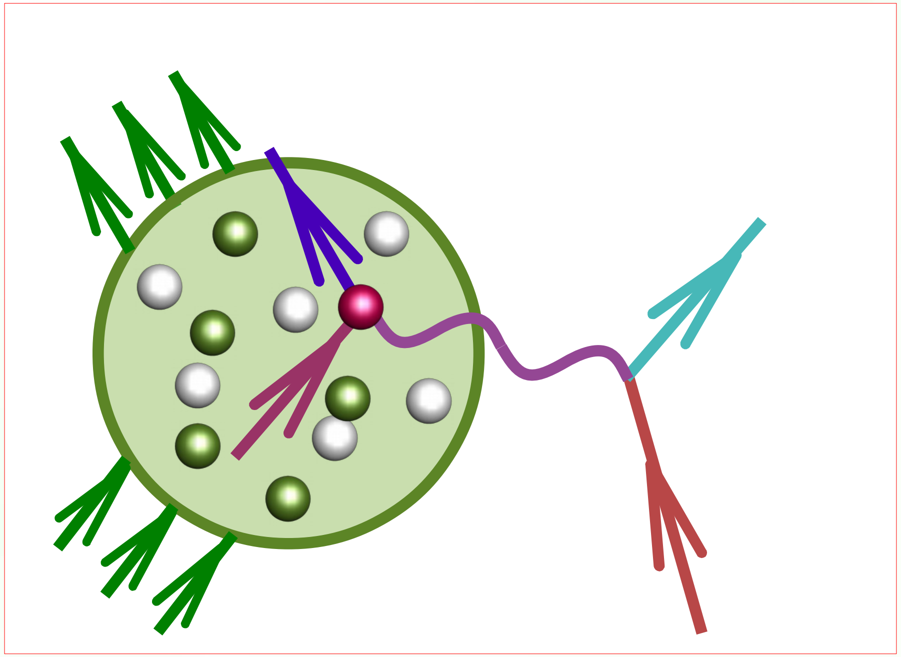

Energy conservation

$$E_{\mathbf{k}} + M_A = E_{\mathbf{k}'} + E_{A-1} + E_{\mathbf{p}'}$$

$$E_{\mathbf{k}} + M_A \boxed{\sim} E_{\mathbf{k}'} + E_{A-1} + E_{\mathbf{p}'} + U_V(\mathbf{p}')$$

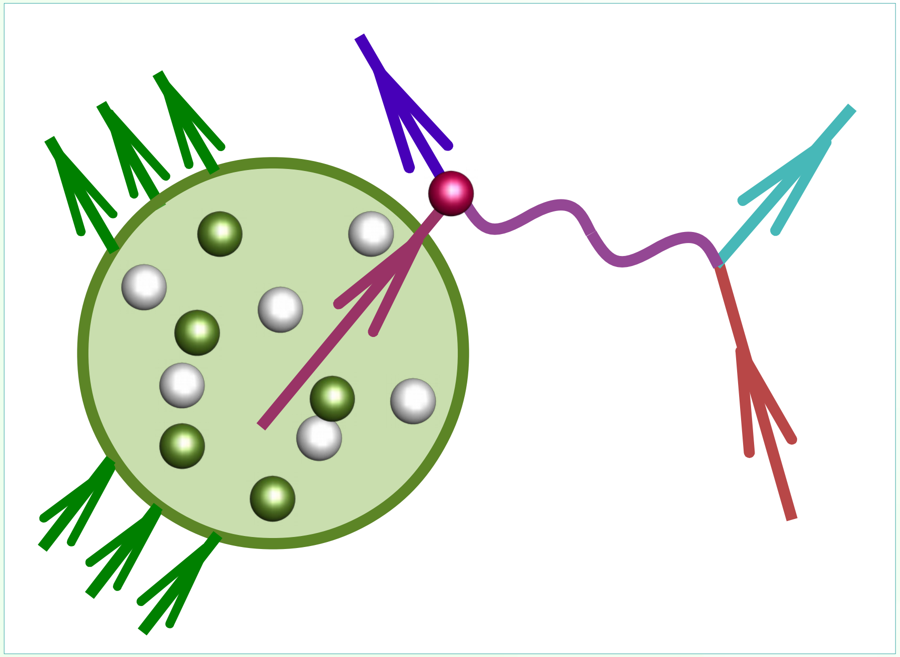

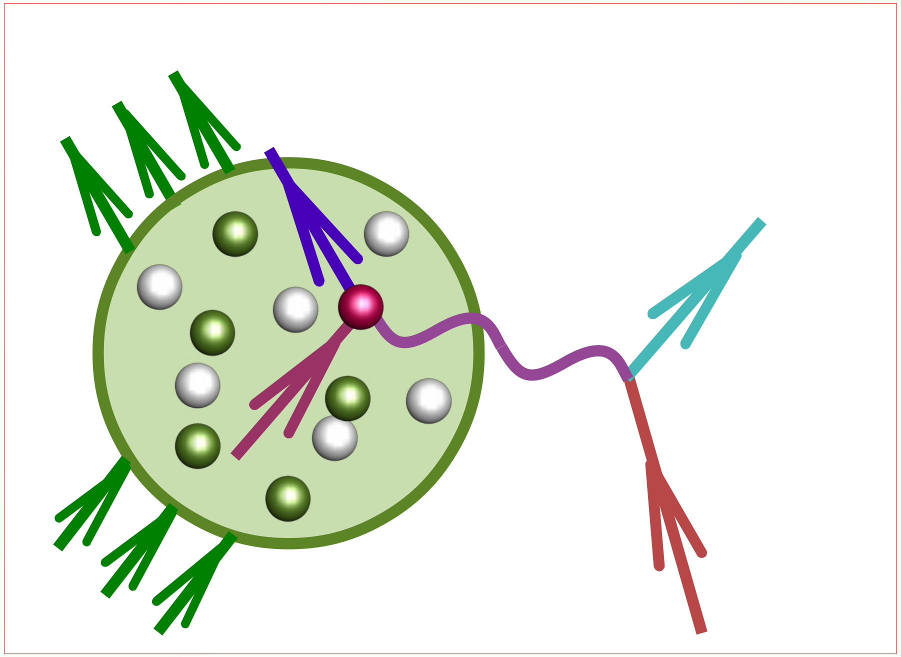

Final-state interactions

Their effect on the cross section is easy to understand in terms of the complex optical potential:

- the **real part** modifies the struck nucleon's energy spectrum: it differes from $\sqrt{M^2 + \boldsymbol{p}'^2}$
- the **imaginary part** reduces the single-nucleon final states and produces multinucleon final states

$$\boxed{e^{i(E+U)t} = e^{i(E+U_V)t} e^{-U_W t}}$$

Horikawa *et al.*, PRC 22, 1680 (1980)

Final-state interactions

In the convolution approach,

$$\frac{d\sigma^{\mathrm{FSI}}}{d\omega d\Omega} = \int d\omega' f_{\mathbf{q}}(\omega - \omega') \frac{d\sigma^{\mathrm{IA}}}{d\omega' d\Omega},$$

with the folding function

$$f_{\mathbf{q}}(\omega) = \delta(\omega)\sqrt{T_A} + \left(1 - \sqrt{T_A}\right) F_{\mathbf{q}}(\omega),$$

Nucl. transparency

$F_q(\omega)$

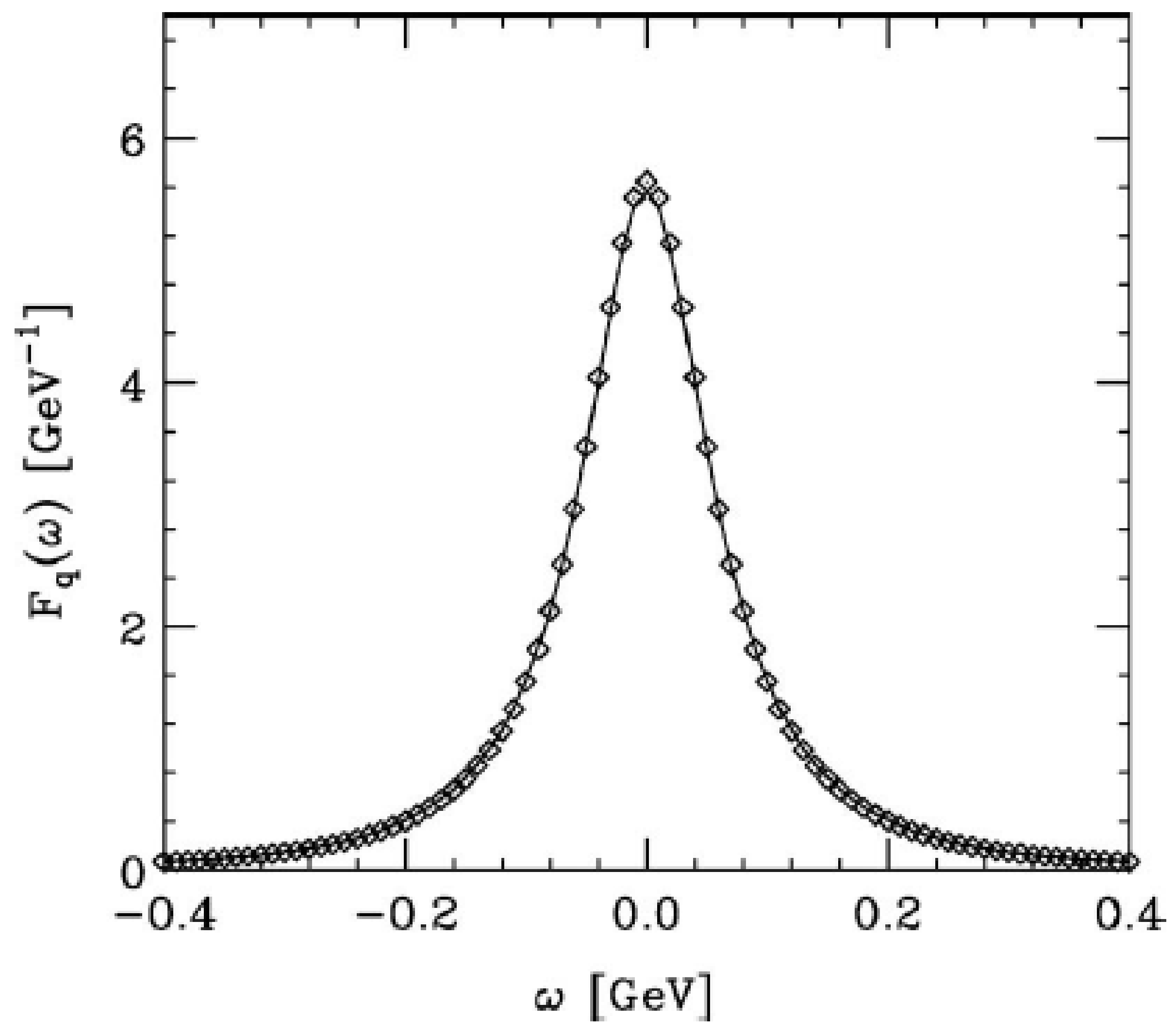

Nuclear transparency

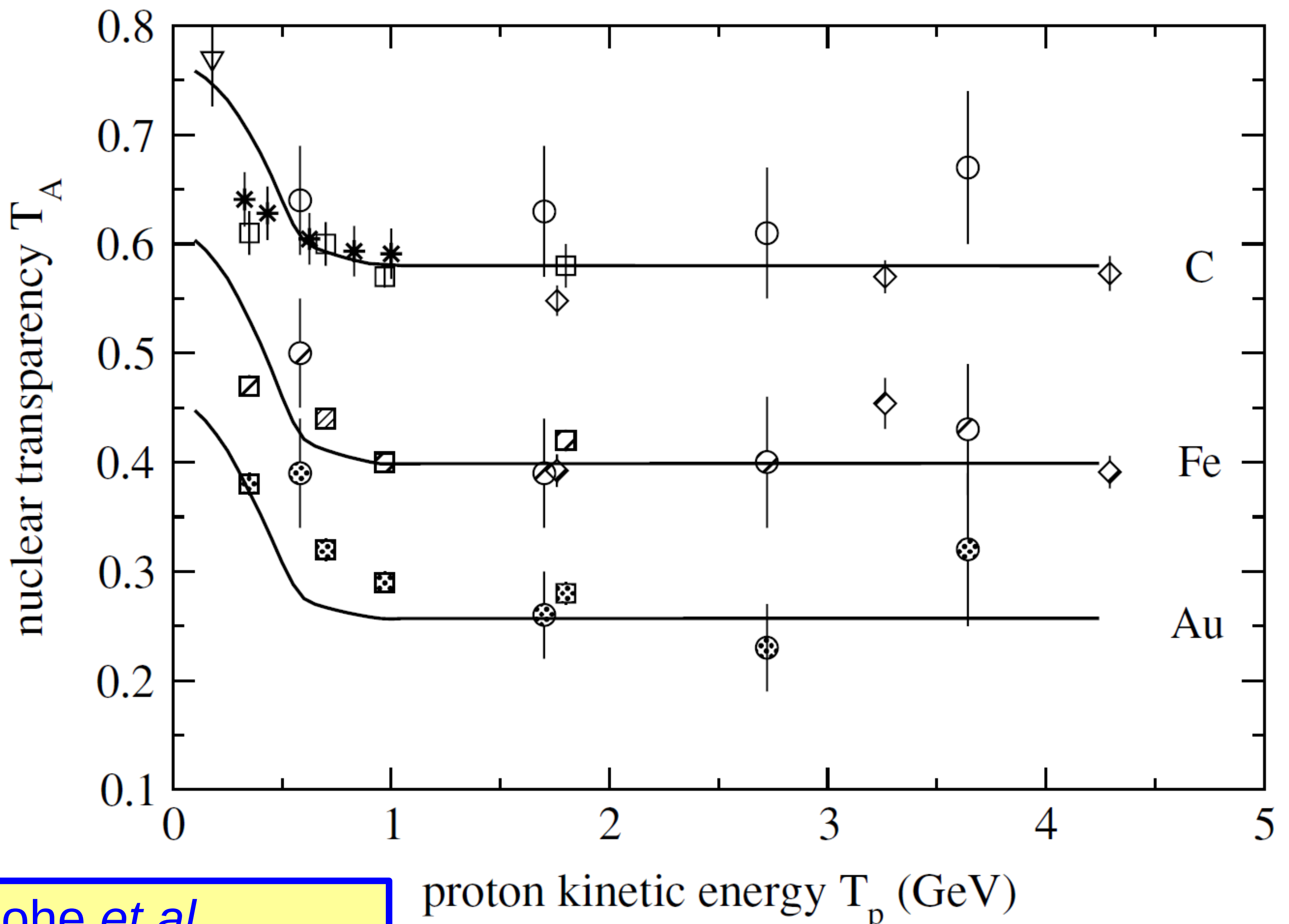

Rohe *et al.*,
PRC 72, 054602 (2005)

Nuclear transparency

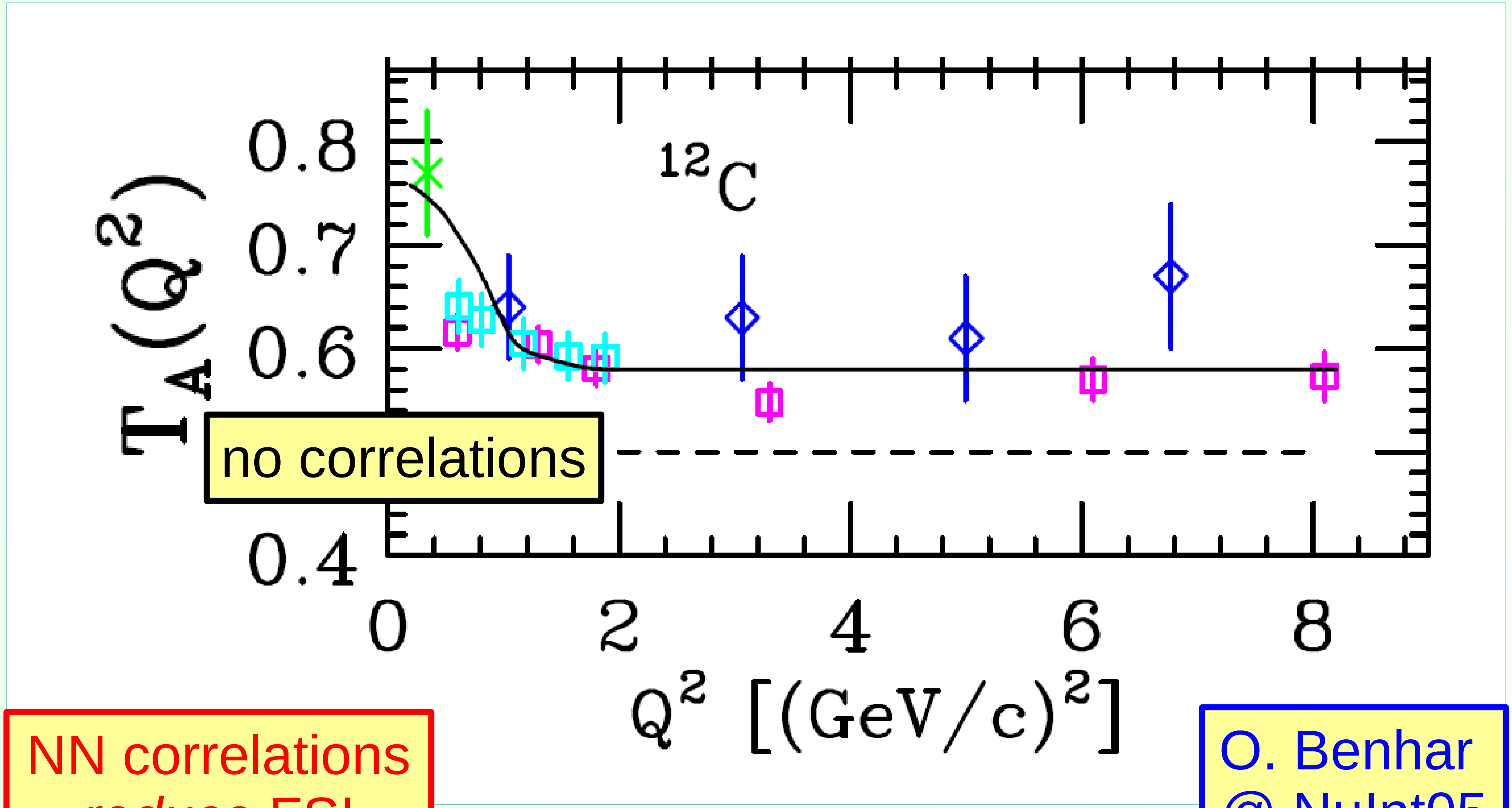

NN correlations
reduce FSI

O. Benhar
@ NuInt05

Short-range correlations

Pair distribution function of NM

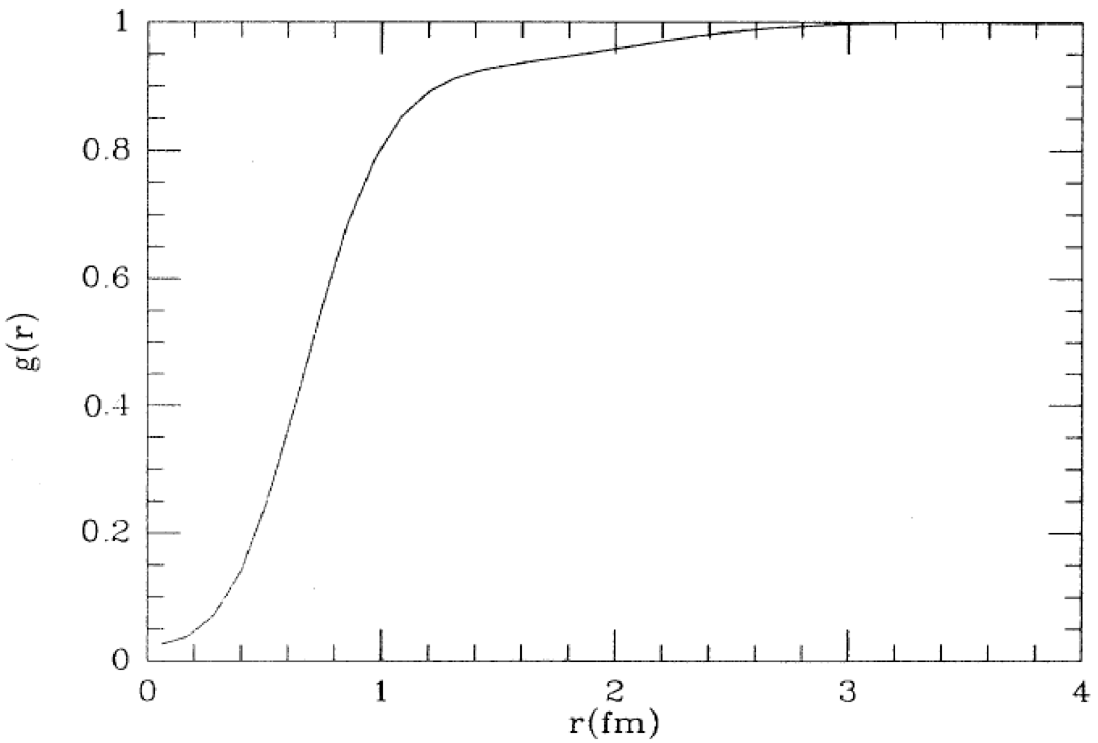

Benhar *et al.*, PRC 44, 2328 (1991)

Real part of the optical potential

We account for the spectrum modification by

$$f_{\mathbf{q}}(\omega - \omega') \to f_{\mathbf{q}}(\omega - \omega' - U_V).$$

This procedure is similar to that from the Fermi gas model to introduce the binding energy in the argument of δ(...).

$$U_V = U_V(t_{\text{kin}})$$

$$t_{\text{kin}} = \frac{E_{\mathbf{k}}^2(1-\cos\theta)}{M + E_{\mathbf{k}}(1-\cos\theta)}$$

Optical potential by Cooper *et al.*

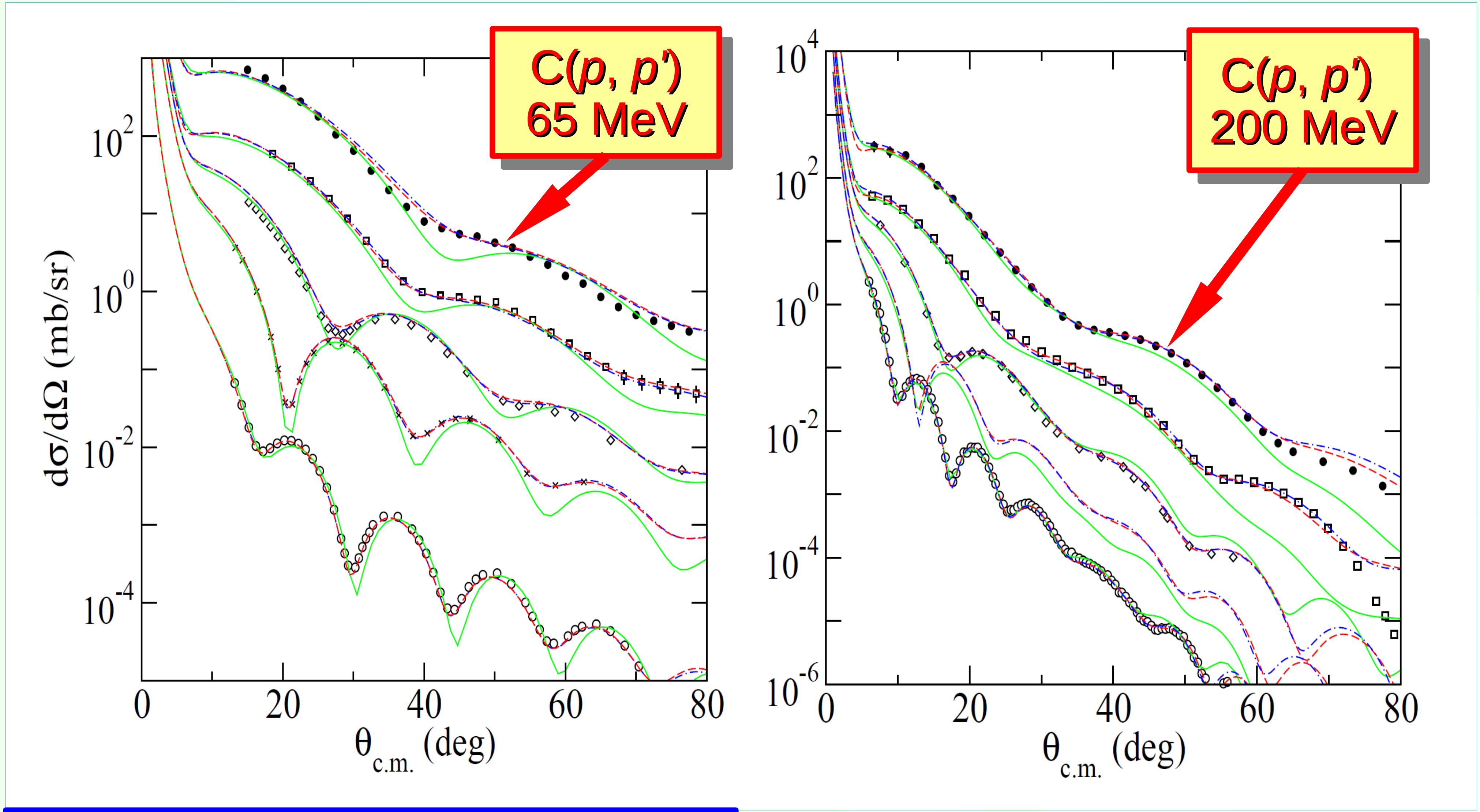

Deb *et al.*, PRC 72, 014608 (2005)

Optical potential by Cooper *et al.*

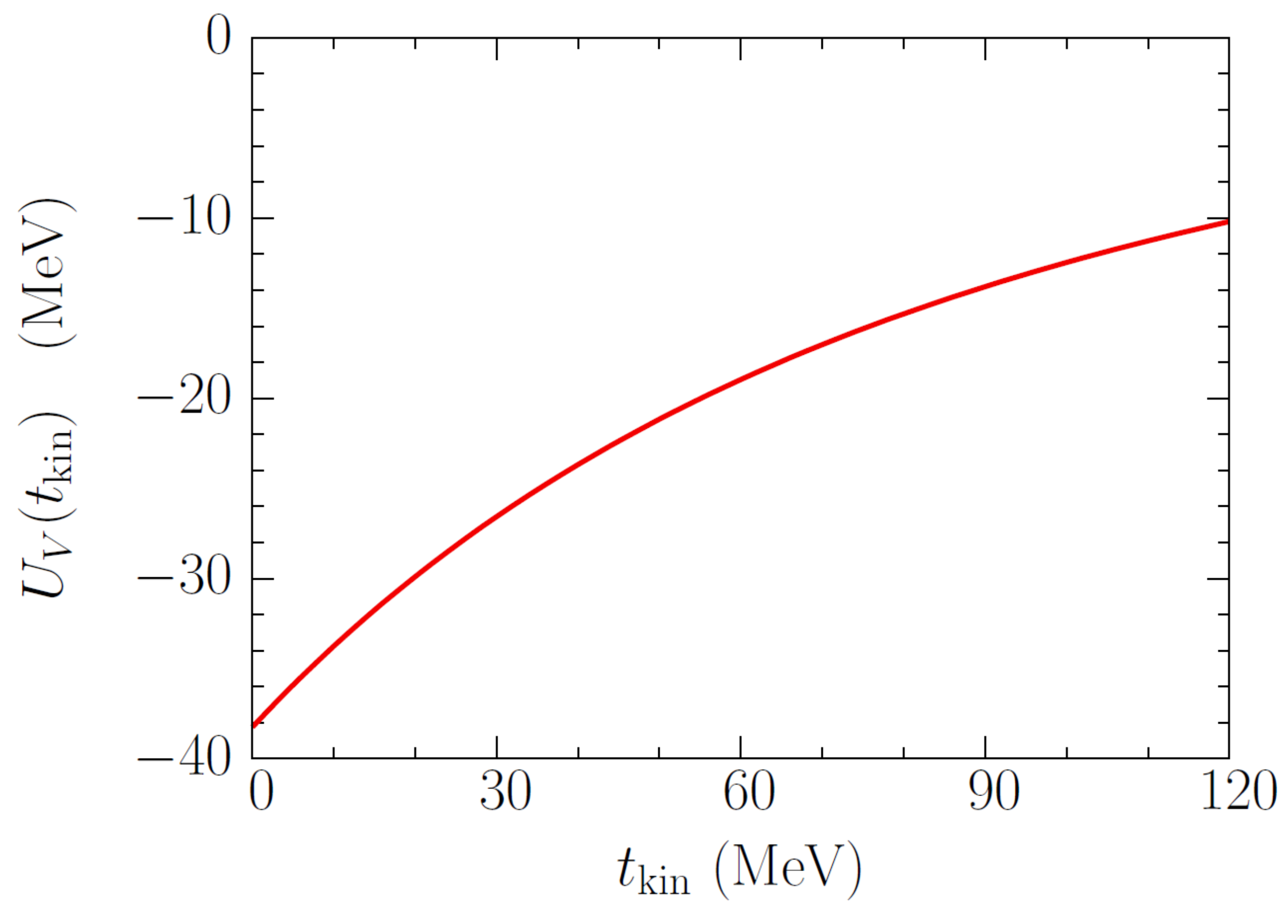

obtained from
Cooper *et al.*, PRC 47, 297 (1993)

Simple comparison

Real part of the OP

- acts in the final state
- shifts the QE peak
  to low ω at low $|\mathbf{q}|$
  (to high ω at high $|\mathbf{q}|$)

Binding energy in RFG

- acts in the initial state
- shifts the QE peak to high ω

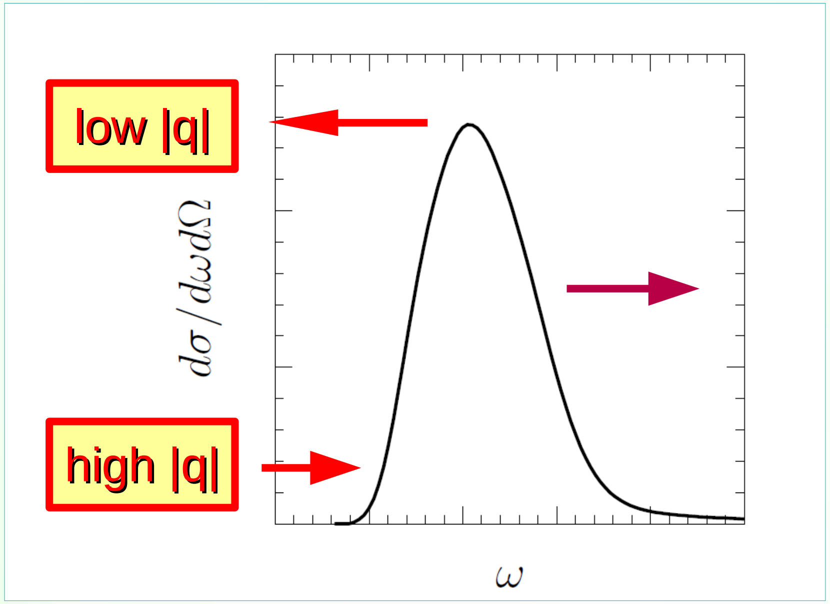

Comparison to C(*e*, *e*′) data

13.5°

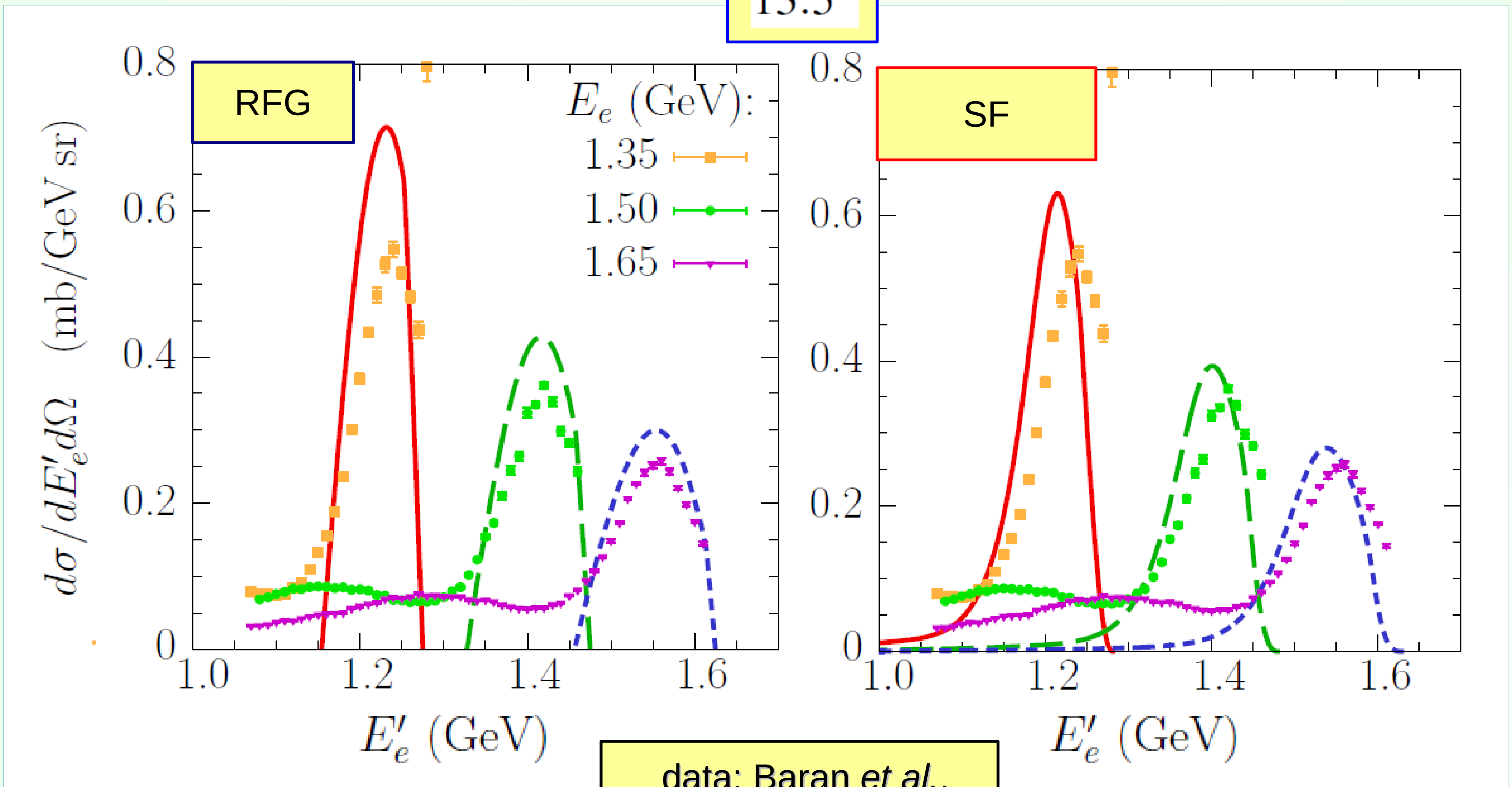

data: Baran *et al.*,
PRL 61, 400 (1988)

Comparison to C(e, e') data

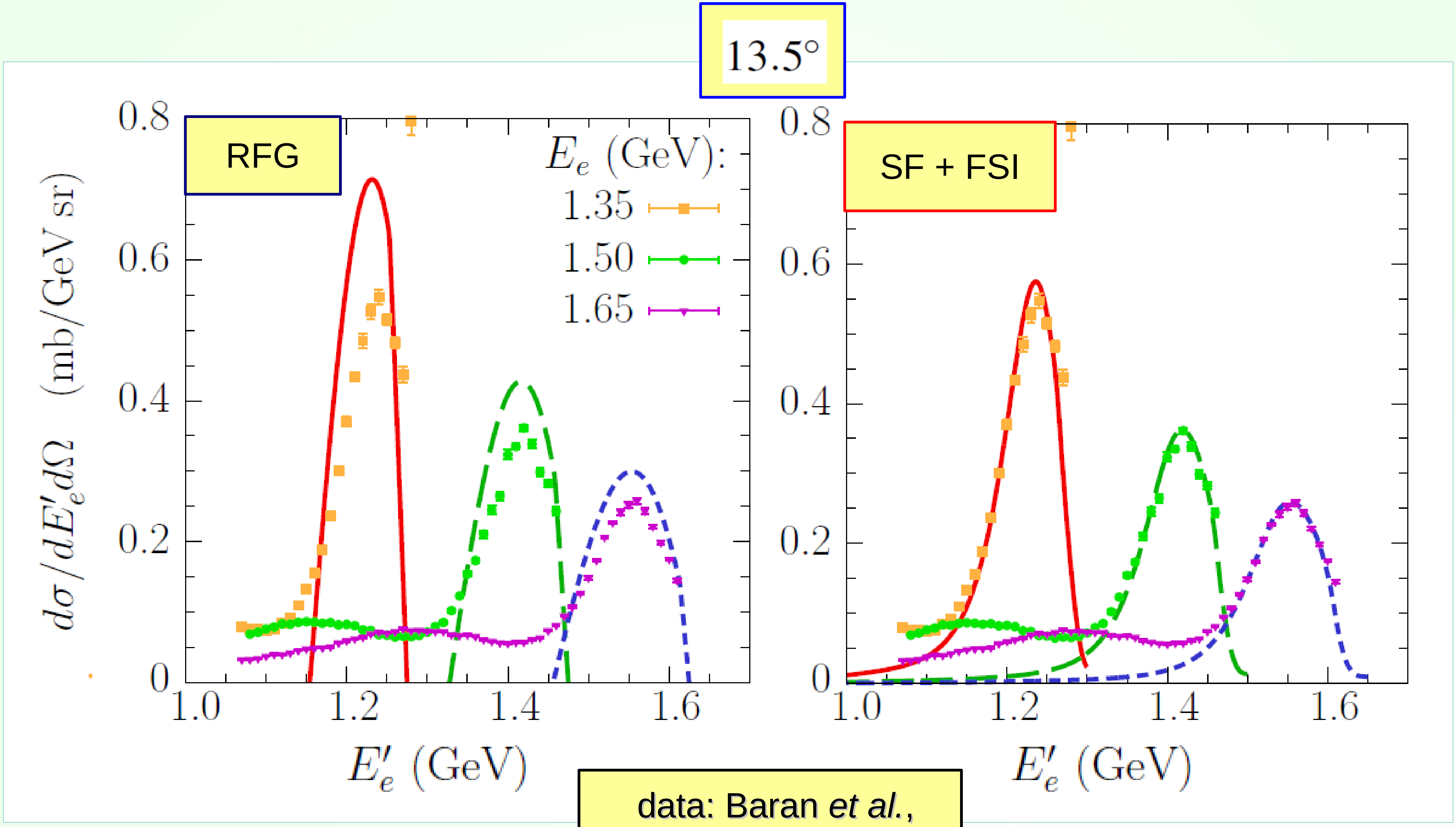

data: Baran *et al.*, PRL 61, 400 (1988)

Compared calculations

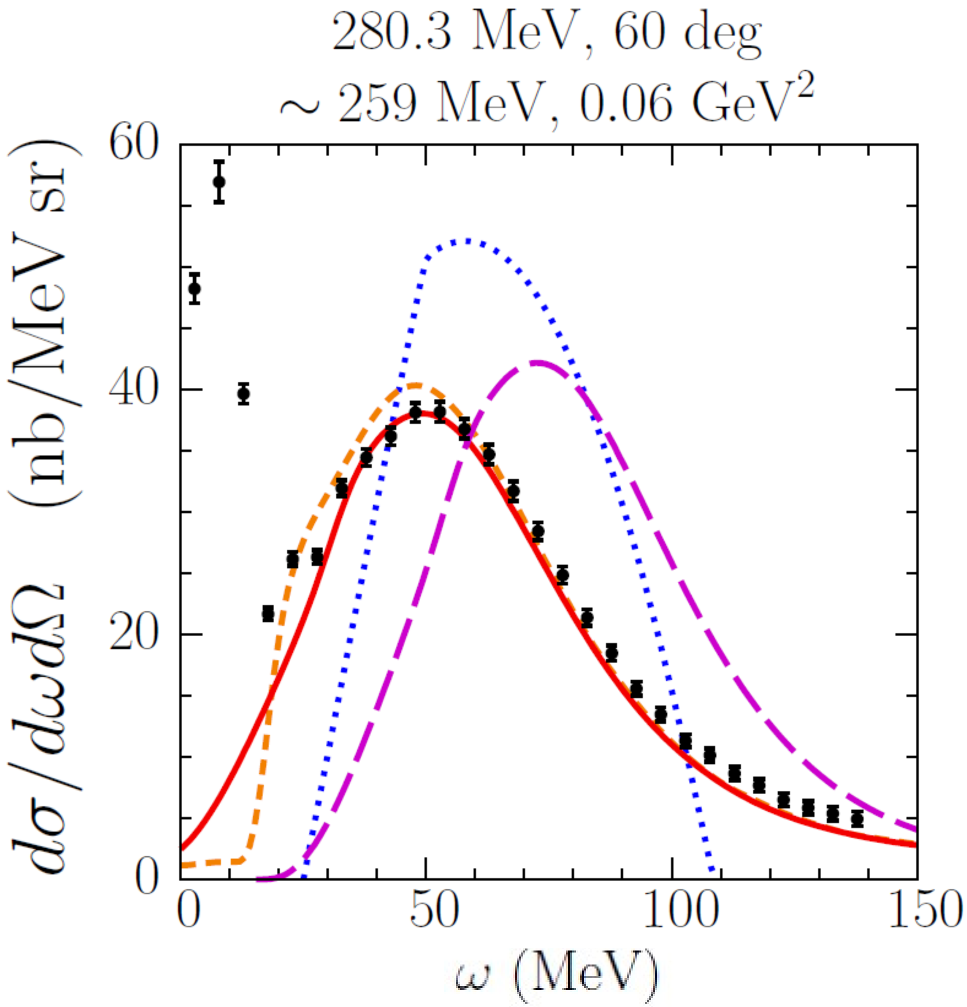

RFG model
ε = 25 MeV
p_F = 221 MeV

SF calculation without FSI

SF calculation, LDA treatment of Pauli blocking

SF calculation, step function

Compared calculations

Calcs. include QE by 1-body current only

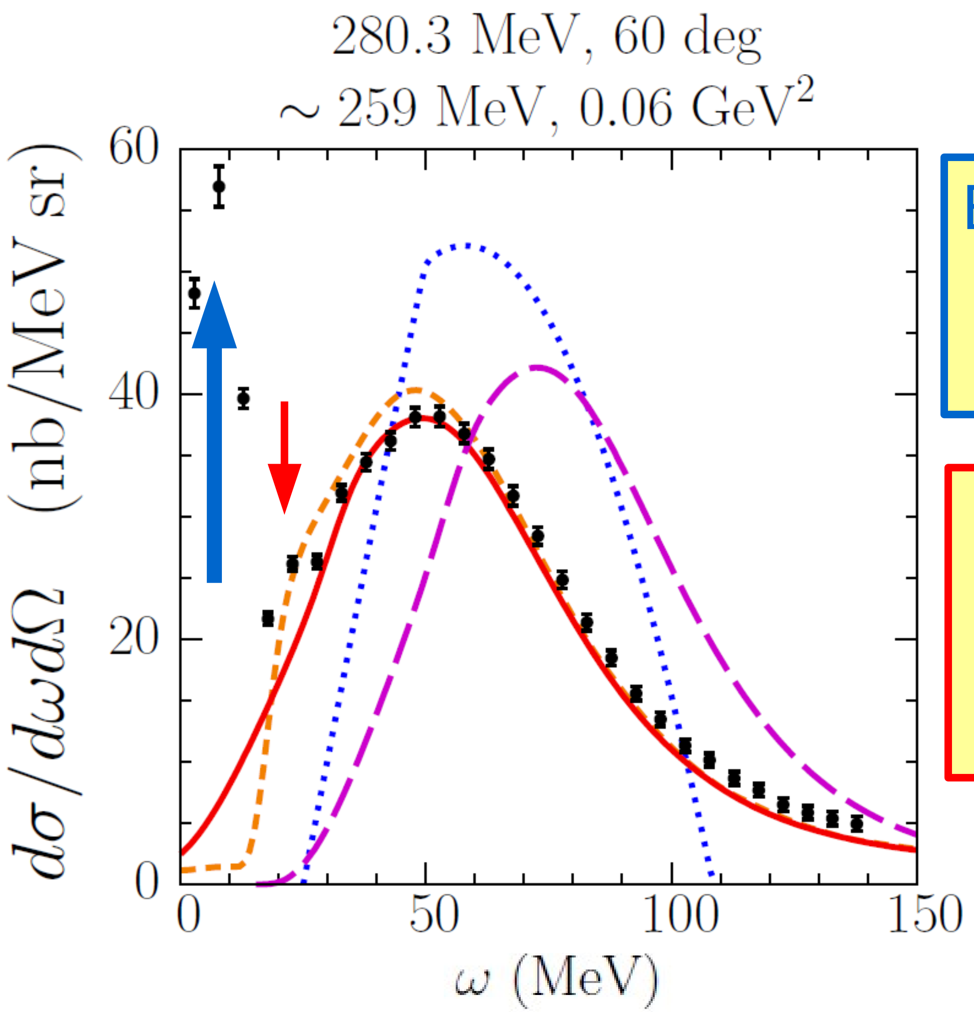

Elastic scattering and excitation of low-E_x levels

Giant resonance
E_x = 22.6 MeV,
Γ = 3.2 MeV

Comparisons to C(*e*,*e*′) data

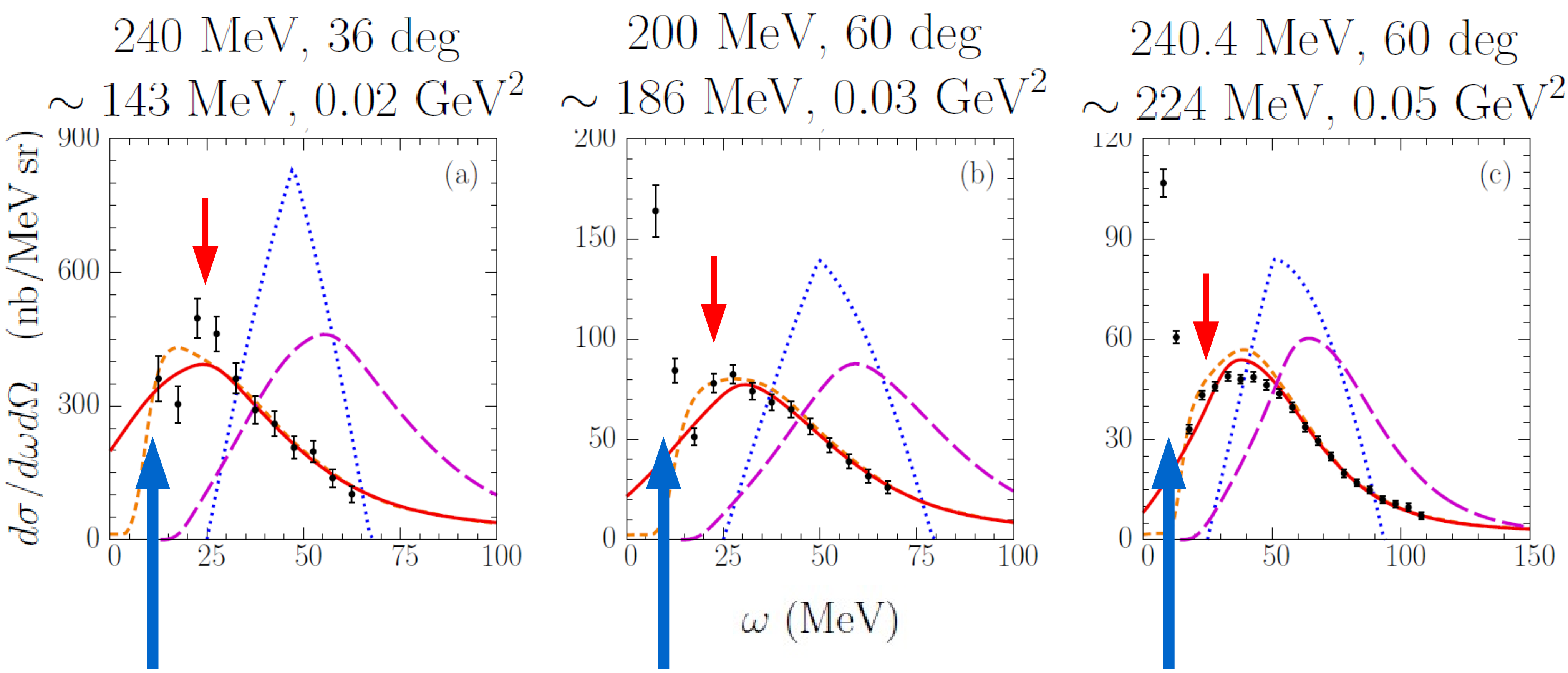

Barreau *et al.*,
NPA 402, 515 (1983)

Comparisons to C(*e*,*e*′) data

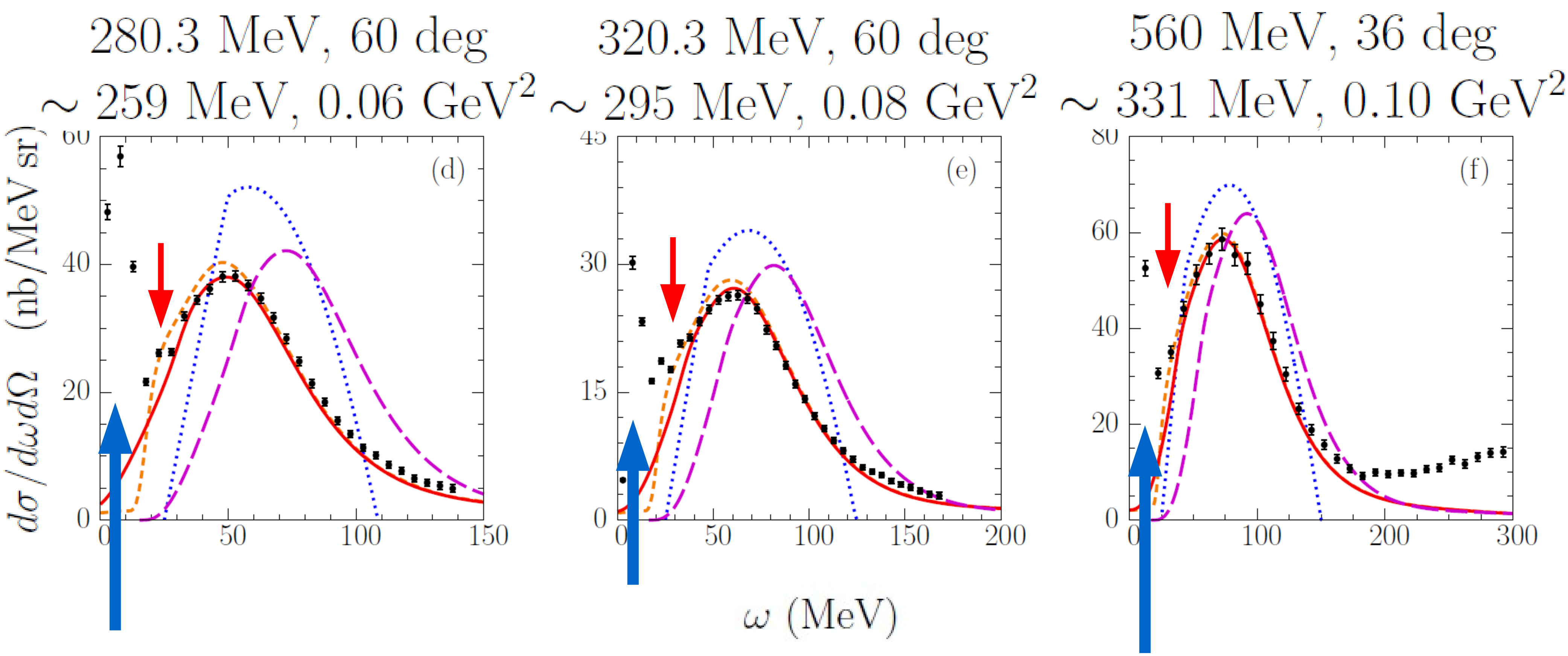

Barreau *et al.*,
NPA 402, 515 (1983)

Comparisons to C(*e*,*e'*) data

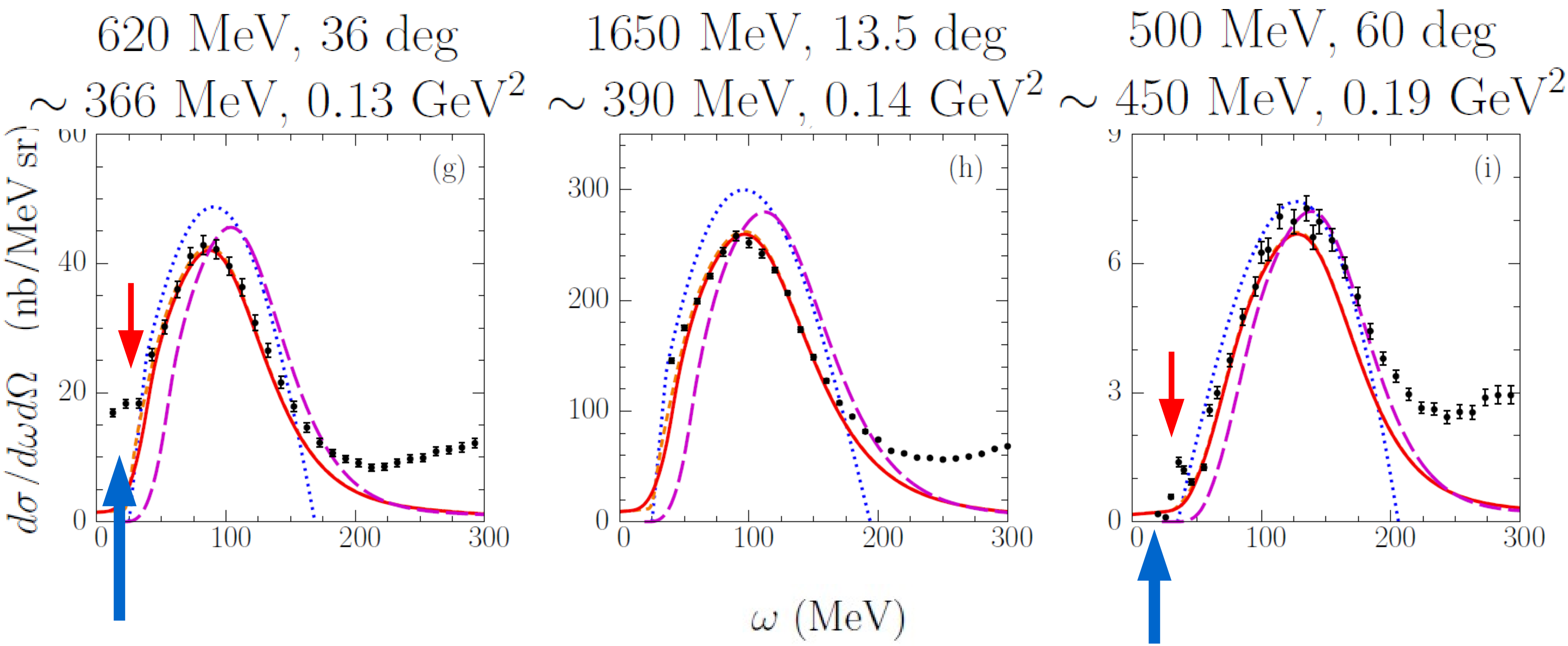

Barreau *et al.*,
NPA 402, 515 (1983)

Baran *et al.*,
PRL 61, 400 (1988)

Whitney *et al.*,
PRC 9, 2230 (1974)

Comparisons to C(*e*,*e'*) data

The supplemental material of PRD 91,033005 (2015)

shows comparisons to the data sets collected

at **54 kinematical setups**

- energies from ~160 MeV to ~4 GeV,
- angles from 12 to 145 degrees,
- at the QE peak, the values of momentum transfer from ~145 to ~1060 MeV/*c* and $0.02 \leq Q^2 \leq 0.86$ (GeV/*c*)^2 .

CCQE MINERvA data

SF calculations with FSI

vs.

SF calculation without FSI

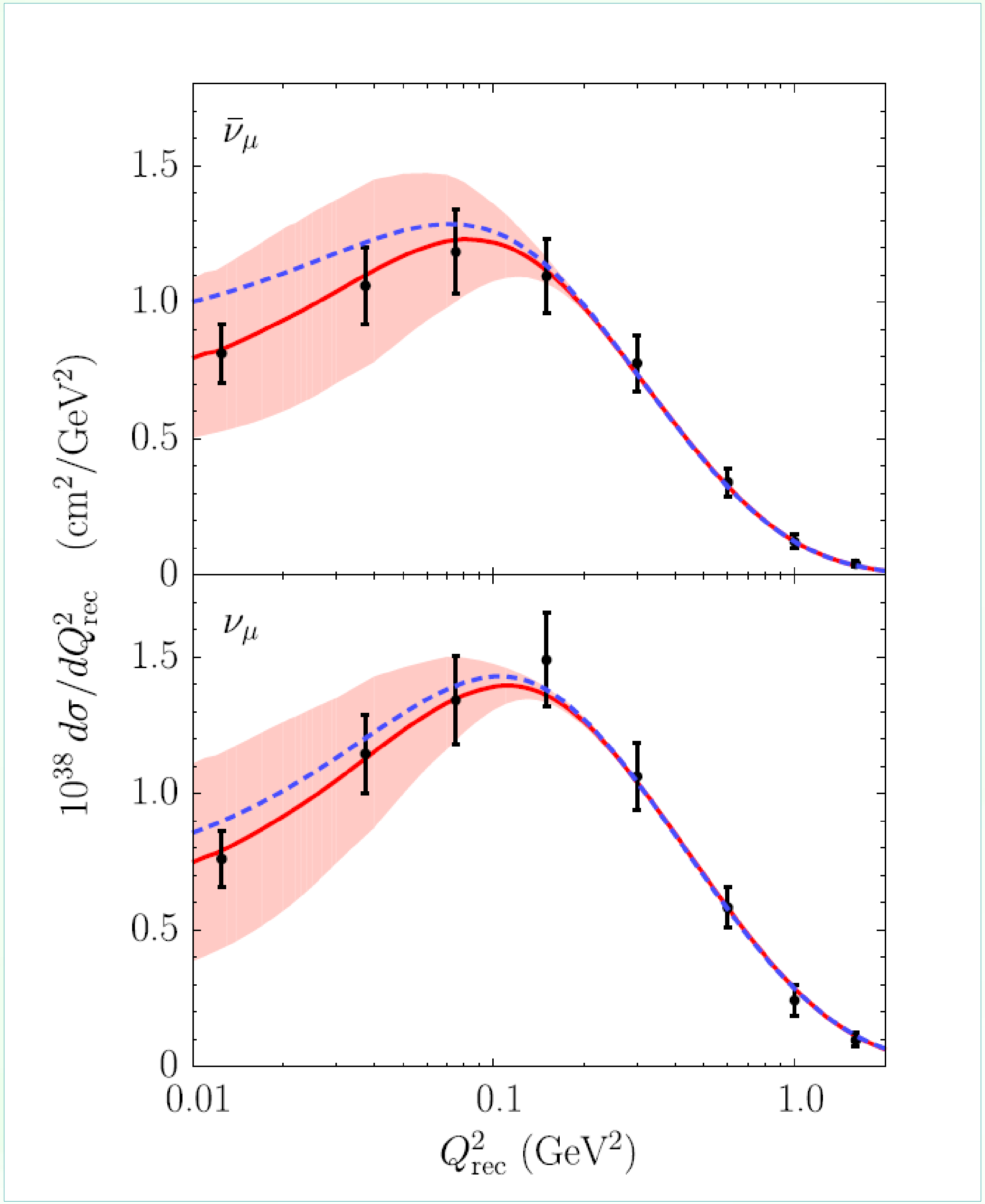

Fields *et al.*, PRL 111, 022501 (2013)

A. M. A., PRD 92, 013007 (2015)

Fiorentini *et al.*, PRL 111, 022502 (2013)

CCQE MINERvA data

TABLE I. Fit results to the CC QE MINERvA data.

	antineutrino	neutrino	combined fit
	including theoretical uncertainties:		
M_A (GeV)	1.16 ± 0.06	1.17 ± 0.06	1.16 ± 0.06
$\chi^2/\text{d.o.f.}$	0.38	1.33	0.93
	neglecting theoretical uncertainties:		
M_A (GeV)	1.15 ± 0.10	1.15 ± 0.07	1.13 ± 0.06
$\chi^2/\text{d.o.f.}$	0.44	1.38	1.00
	neglecting FSI ($M_A = 1.16$ GeV):		
$\chi^2/\text{d.o.f.}$	2.49	2.45	2.42

Measurement of the spectral function of argon in JLab

What do we know about Ar?

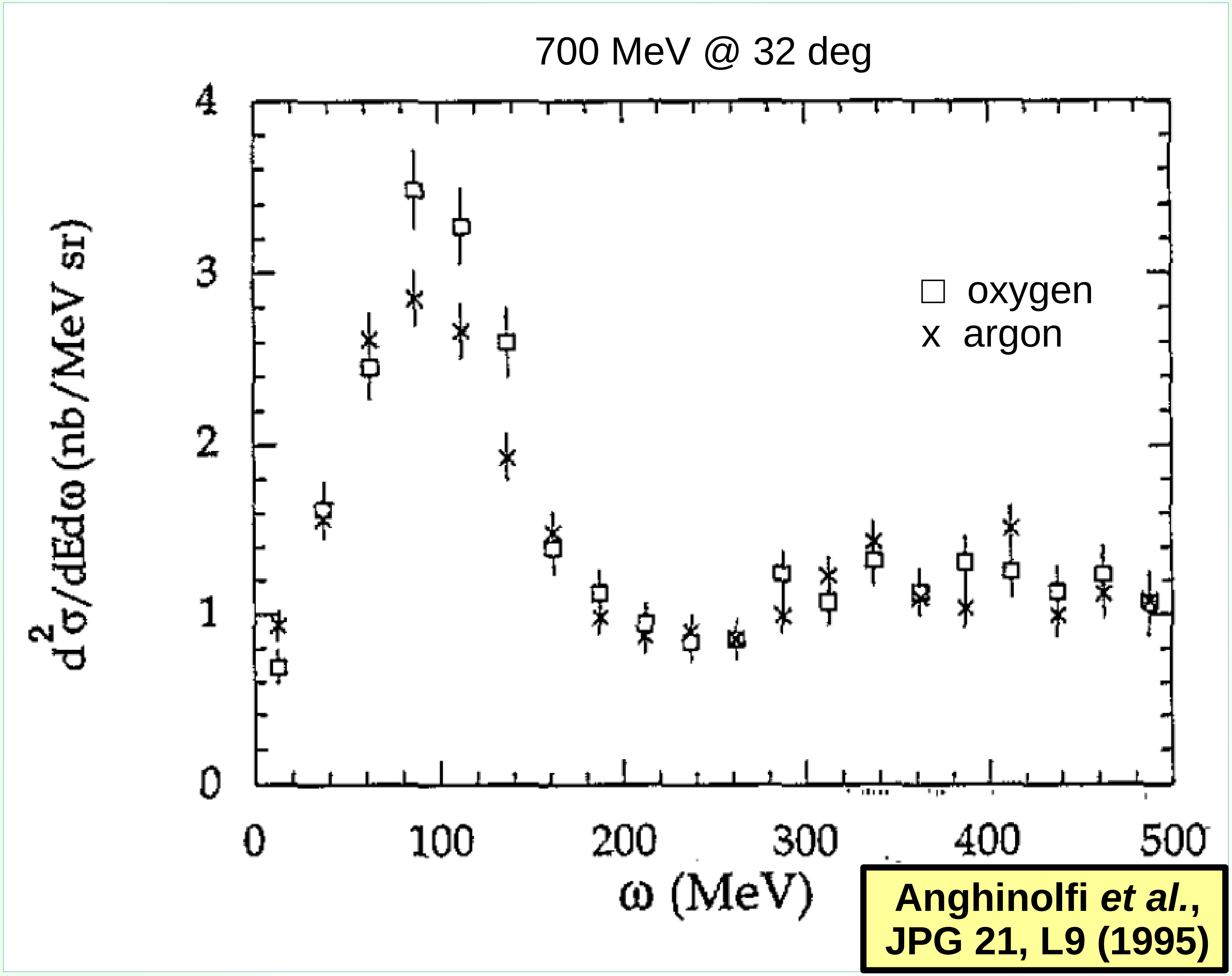

Anghinolfi *et al.*, JPG 21, L9 (1995)

What do we know about Ar?

- nuclear excitations by up to ~11 MeV

  Cameron & Singh, Nucl. Data Sheets **102**, 293 (2004)

- angular distributions of ^{40}Ar(p, p') for a few excitation lvls.

  Fabrici *et al.*, PRC **21**, 830 & 844 (1980); De Leo *et al.*, PRC **31**, 362 (1985); Blanpied *et al.*, PRC **37**, 1304 (1988)

- angular distributions of ^{40}Ar(p ,d)^{39}Ar

  Tonn *et al.*, PRC **16**, 1357 (1977)

What do we know about Ar?

- *n*-Ar total cross section for energies < 50 MeV

  Winters *et al.*, PRC **43**, 492 (1991)
- ^{40}Ar(ν_e ,*e*) cross section from the mirror ^{40}Ti$\rightarrow$^{40}Sc decay

  Bhattacharya *et al.*, PRC **58**, 3677 (1998)
- Gammov-Teller strength distrib. for ^{40}Ar$\rightarrow$^{40}K from 0°(*p, n*)

  Bhattacharya *et al.*, PRC **80**, 055501 (2009)
- ^{40}Ar(*n, p*)^{40}Cl cross section between 9 and 15 MeV

  Bhattacharya *et al.*, PRC **86**, 041602(R) (2012)

Spectral function of ^{40}Ca

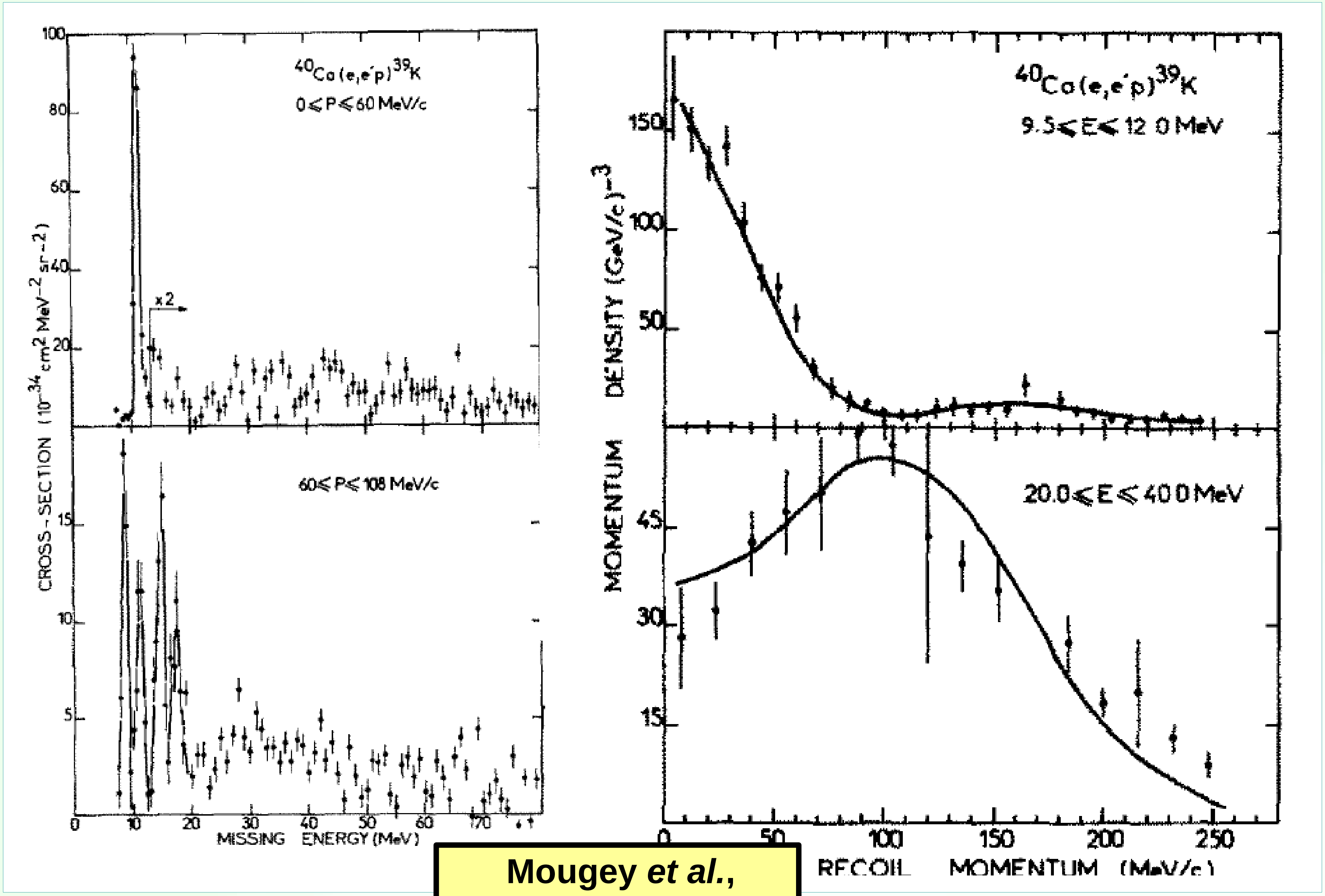

Mougey *et al.*,
NPA 262, 461 (1976)

Approximated SF of ^{40}Ar

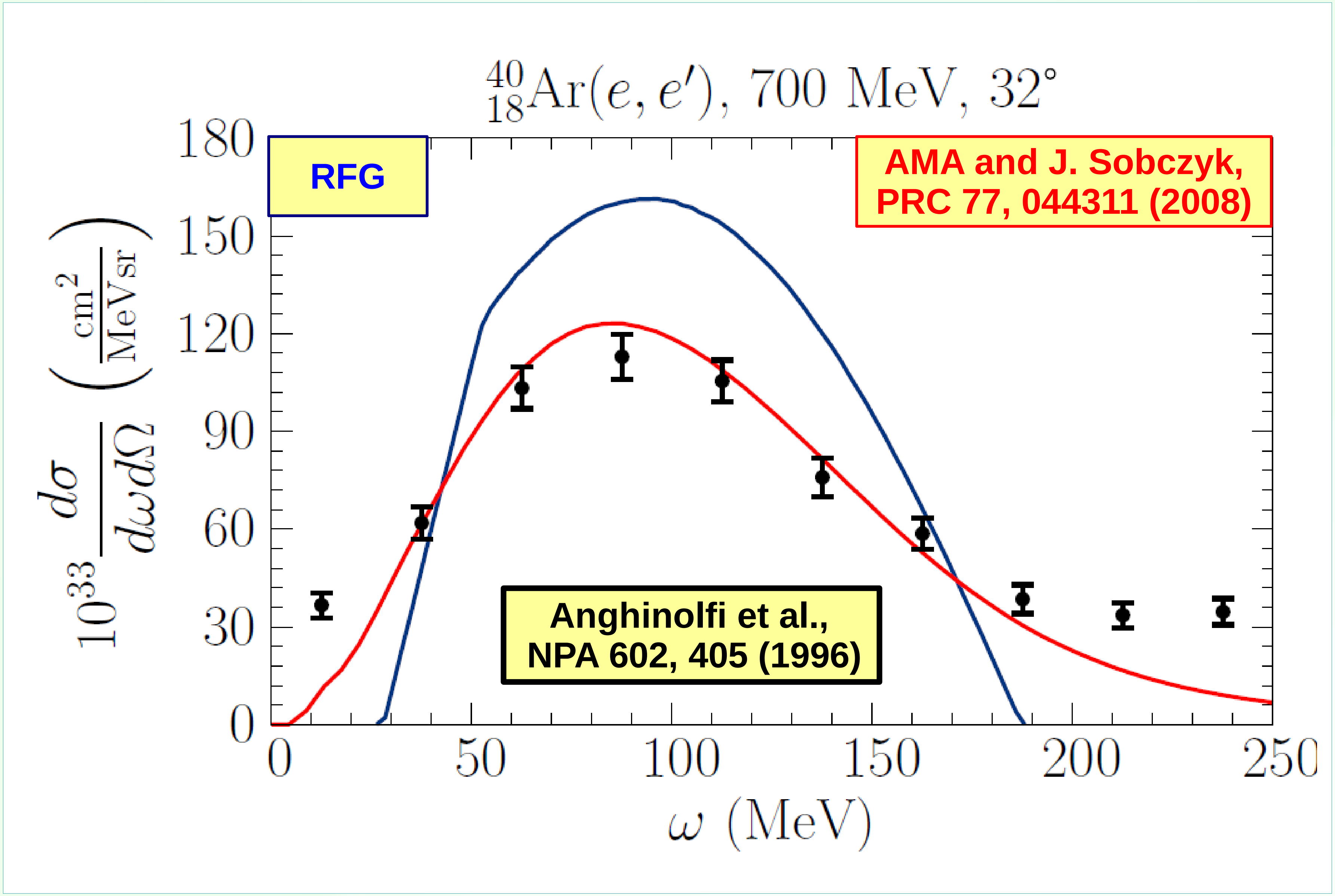

Experiment E12-14-012 at JLab

"We propose a measurement of the coincidence (e,e'p) cross section on argon. This data will provide the experimental input indispensable to construct the argon spectral function, thus paving the way for a reliable estimate of the neutrino cross sections."

Benhar *et al.*, arXiv:1406.4080

Experiment E12-14-012 at JLab

Primary goal: extraction of the proton shell structure of ^{40}Ar from $(e,e'p)$ scattering

- spectroscopic factors,
- energy distributions,
- momentum distributions.

Secondary goal: improved description of final-state interactions in the argon nucleus.

Relevance for DUNE

- Neutrino oscillations
  Reduction of systematic uncertainties from nuclear effects, especially for the 2nd oscillation maximum.

- Proton decay
  Probed lifetime affected by the partial depletion of the shell-model states.

- Supernova neutrinos
  Information on the valence shells essential for accurate simulations and detector design.

Impulse approximation

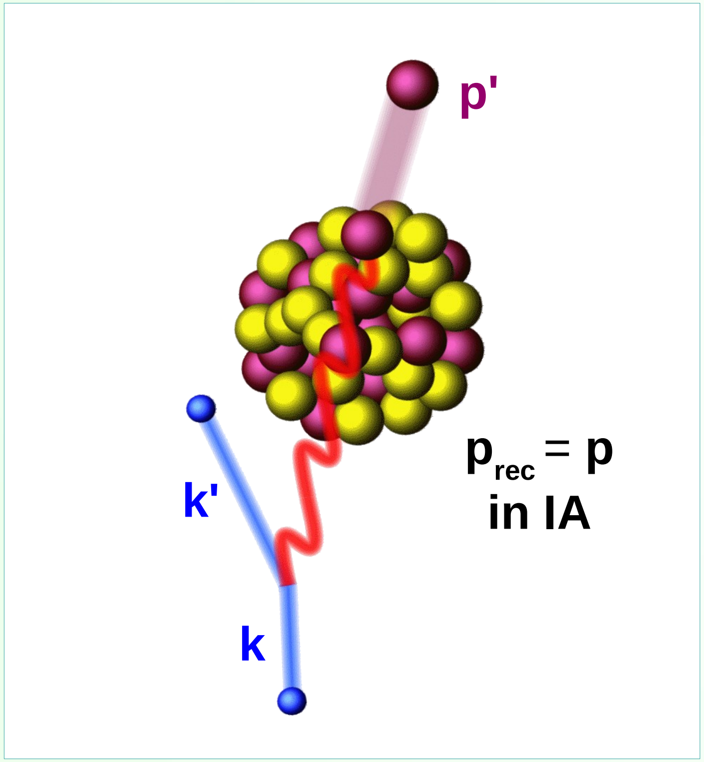

$$\frac{d^6\sigma_{\mathrm{IA}}}{d\Omega_{k'}dE_{k'}d\Omega_{p'}dE_{p'}} \propto \sigma_{ep}\, S(\mathbf{p}, E)\, T_A(E_{p'})$$

σ_{ep} elementary cross section

$S(\mathbf{p}, E)$ spectral function

$T_A(E_{p'})$ nuclear transparency

(Anti)parallel kinematics, p' ∥ q

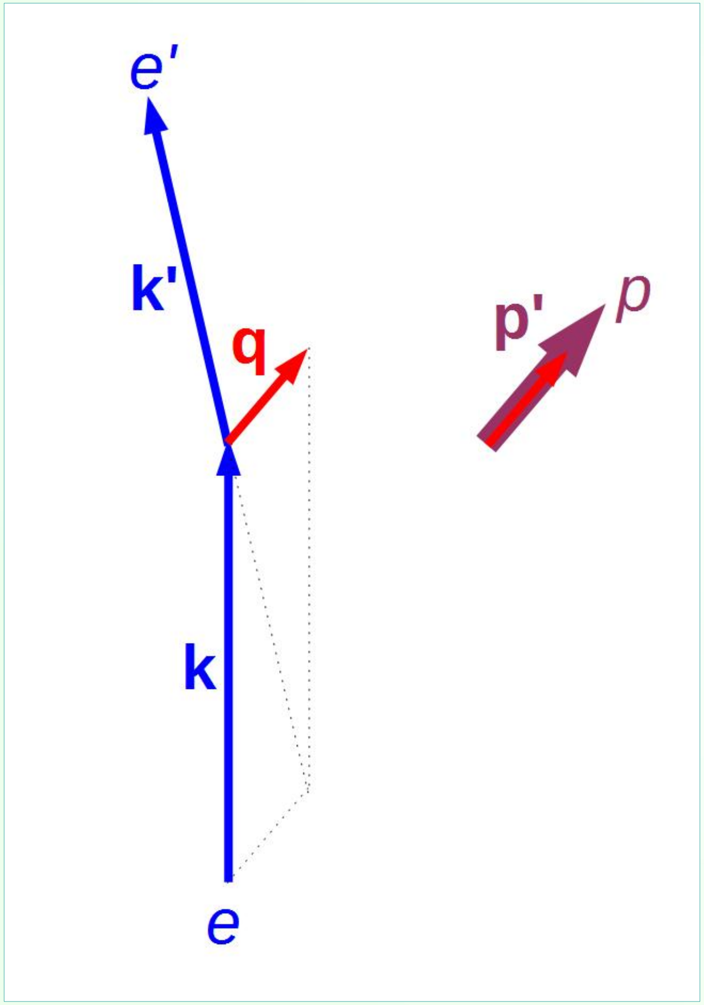

Energy conservation

$$E_{\mathbf{k}} + M_A = E_{\mathbf{k}'} + E_{\mathbf{p}'} + \sqrt{(M_A - M + E)^2 + \mathbf{p}_{\mathrm{rec}}^2}$$

Momentum conservation

$$\mathbf{q} = \mathbf{p}' + \mathbf{p}_{\mathrm{rec}} \to |\mathbf{q}| = |\mathbf{p}'| + |\mathbf{p}_{\mathrm{rec}}|$$

$$\mathbf{q} = \mathbf{p}' + \mathbf{p}_{\mathrm{rec}} \to |\mathbf{q}| = |\mathbf{p}'| - |\mathbf{p}_{\mathrm{rec}}|$$

Impulse Approximation, $|p_{rec}| = |p|$

Neutron spectral function of ^{40}Ar

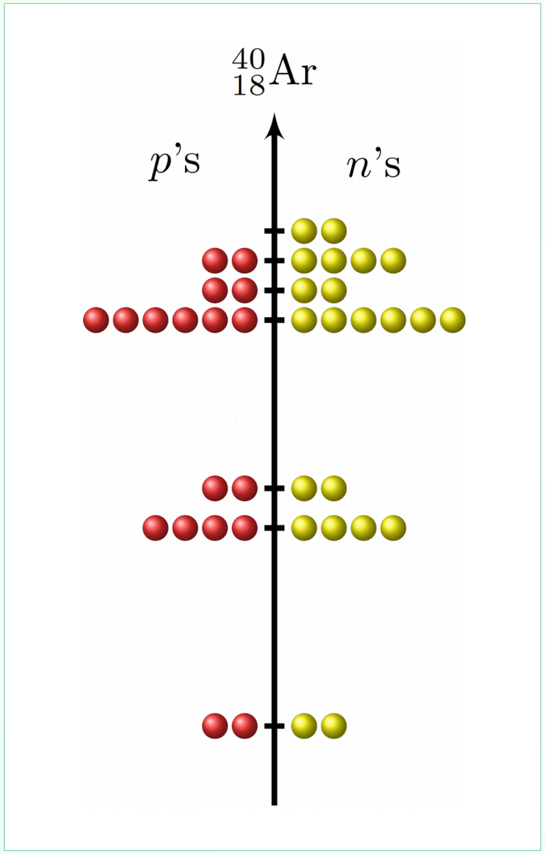

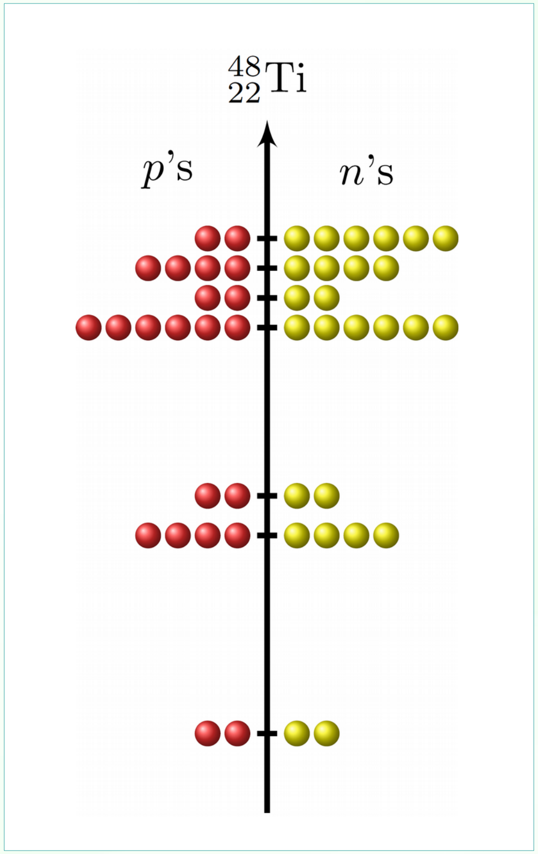

Kinematic settings

	E_e MeV	$E_{e'}$ MeV	θ_e deg	P_p MeV/c	θ_p deg	$\lvert\mathbf{q}\rvert$ MeV/c	p_m MeV/c	Ar events	Ti events
kin1	2222	1799	21.5	915	−50.0	857.5	57.7	44M	13M
kin2	2222	1716	20.0	1030	−44.0	846.1	183.9	63M	21M
kin3	2222	1799	17.5	915	−47.0	740.9	174.1	73M	28M
kin4	2222	1799	15.5	915	−44.5	658.5	229.7	159M	113M
kin5	2222	1716	15.5	1030	−39.0	730.3	299.7	45M	61k
(e, e')	2222		15.5					3M	3M

Data collected Feb - Mar 2017

Expected energy distributions

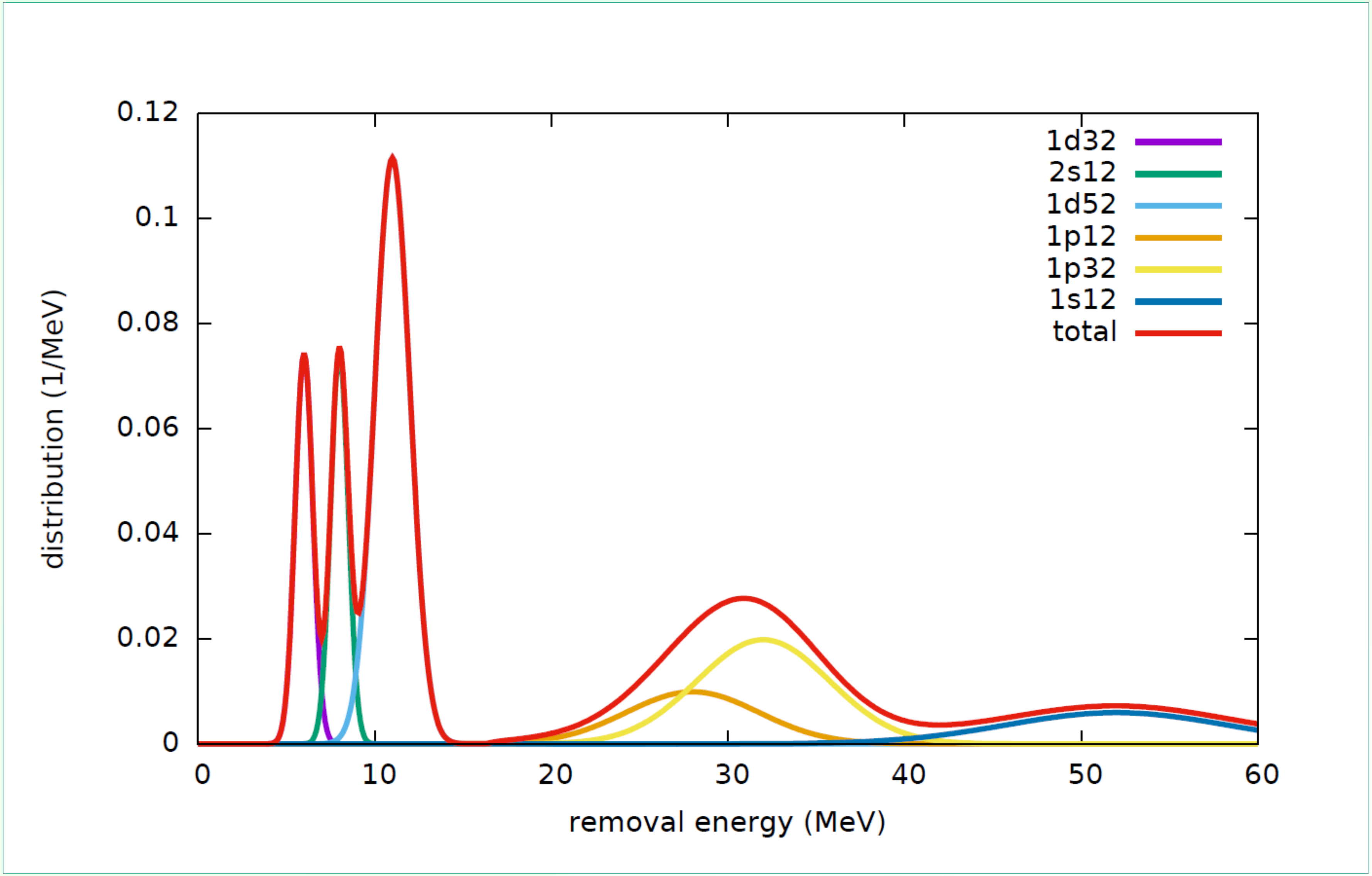

Momentum distributions

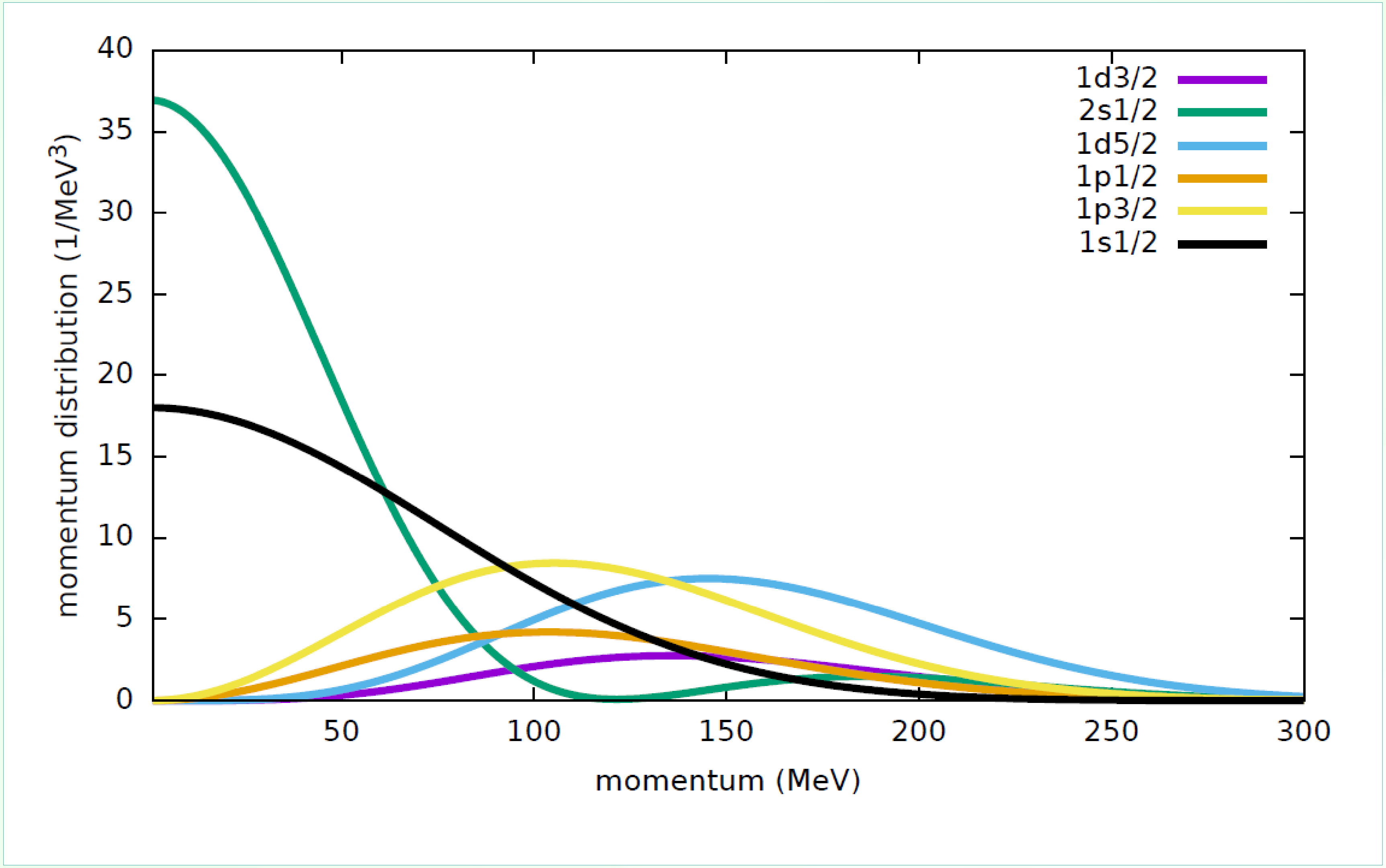

Summary

- An accurate description of nuclear effects, including final-state interactions, is crucial for an **accurate reconstruction of neutrino energy**.

- Theoretical models **must be validated** against (e,e') data to estimate their uncertainties.

- The spectral function formalism can be used in Monte Carlo simulations to **improve the accuracy** of description of nuclear effects.

Backup slides

Why the beam energy ~2 GeV?

	E_e MeV	$E_{e'}$ MeV	θ_e deg	P_p MeV/c	θ_p deg	$\lvert\mathbf{q}\rvert$ MeV/c	p_m MeV/c
A	2200	1777	23.01	915	−50.9	895	20
B	2200	1777	21.66	915	−50.1	855	60
C	2200	1777	20.29	915	−49.1	815	100
D	2200	1777	18.90	915	−48.0	775	140
E	2200	1777	17.49	915	−46.6	735	180
F	2200	1777	16.03	915	−44.9	695	220
G	2200	1777	14.53	915	−42.9	655	260
H	2200	1777	12.96	915	−40.4	615	300
I	2200	1777	11.30	915	−37.3	575	340
J	2200	1777	27.64	915	−52.8	1035	−120

Why the beam energy ~2 GeV?

	E_e MeV	$E_{e'}$ MeV	θ_e deg	P_p MeV/c	θ_p deg	$\|\mathbf{q}\|$ MeV/c	p_m MeV/c
A	4400	3977	10.82	915	-56.5	895	20
B	4400	3977	10.19	915	-55.4	855	60
C	4400	3977	9.55	915	-54.1	815	100
D	4400	3977	8.90	915	-52.6	775	140
E	4400	3977	8.24	915	-50.8	735	180
F	4400	3977	7.56	915	-48.8	695	220
G	4400	3977	6.85	915	-46.4	655	260
H	4400	3977	6.12	915	-43.6	615	300
I	4400	3977	5.34	915	-40.1	575	340
J	4400	3977	12.97	915	-59.6	1035	-120

Hall A

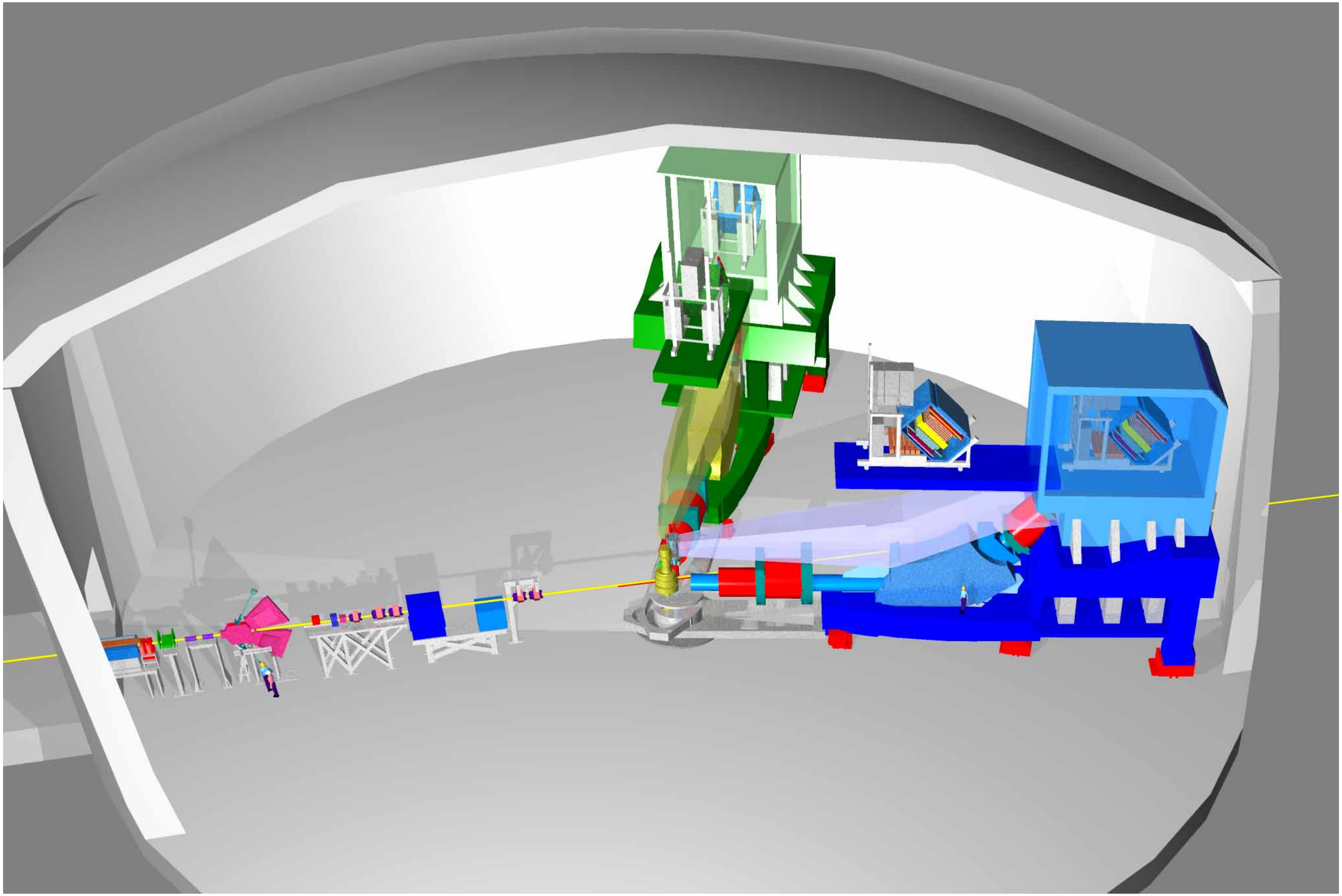

Argon cell

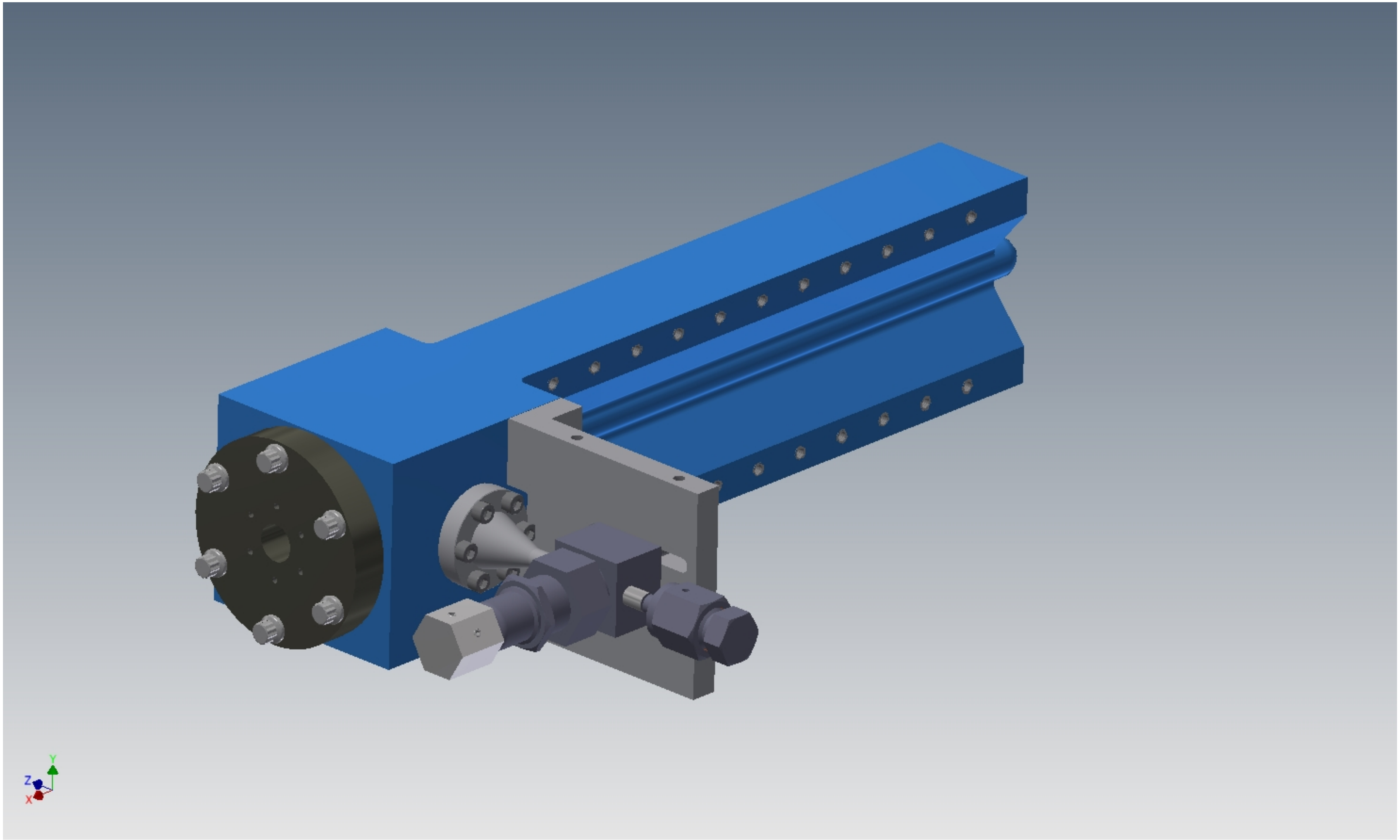

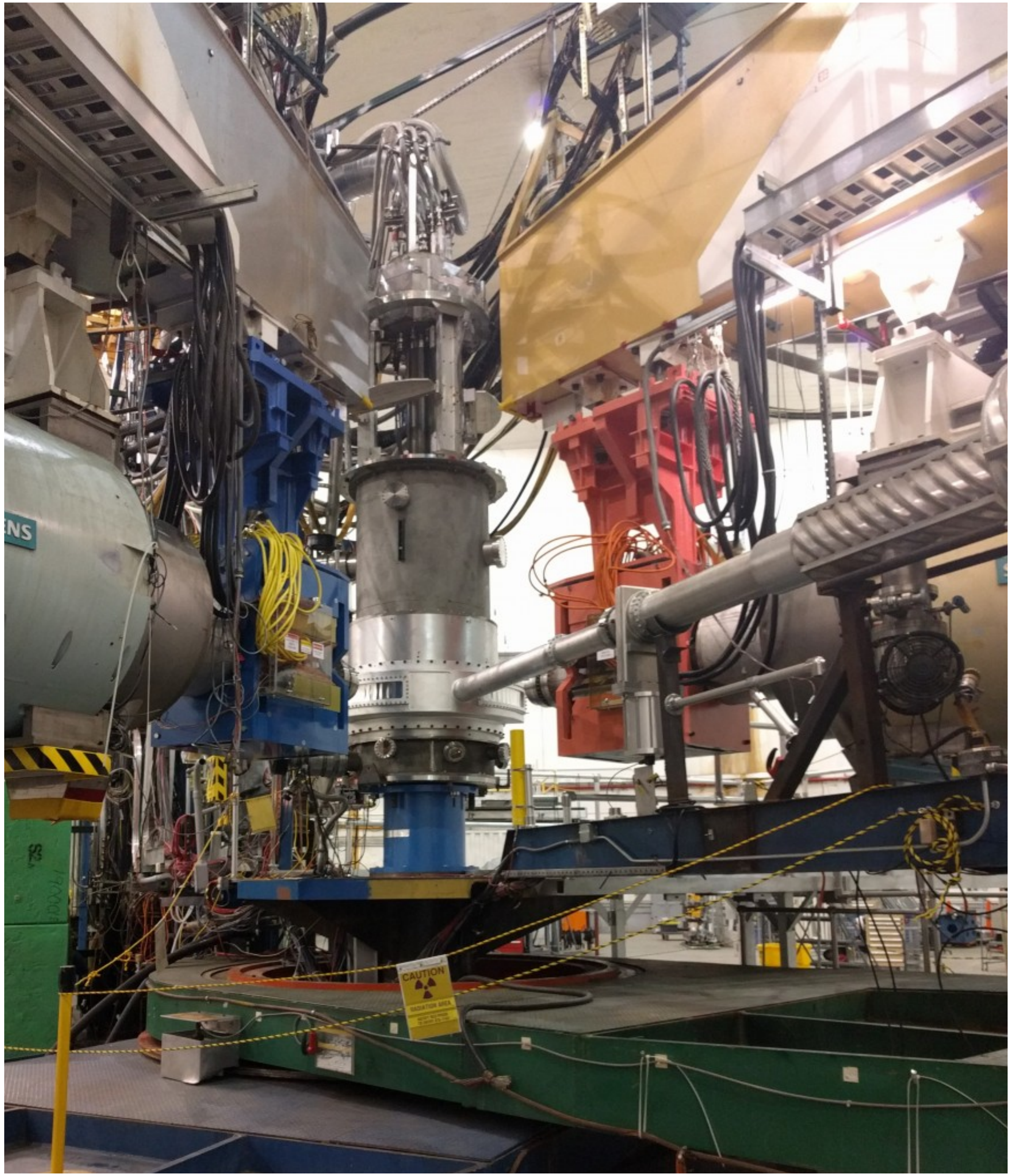
CAUTION

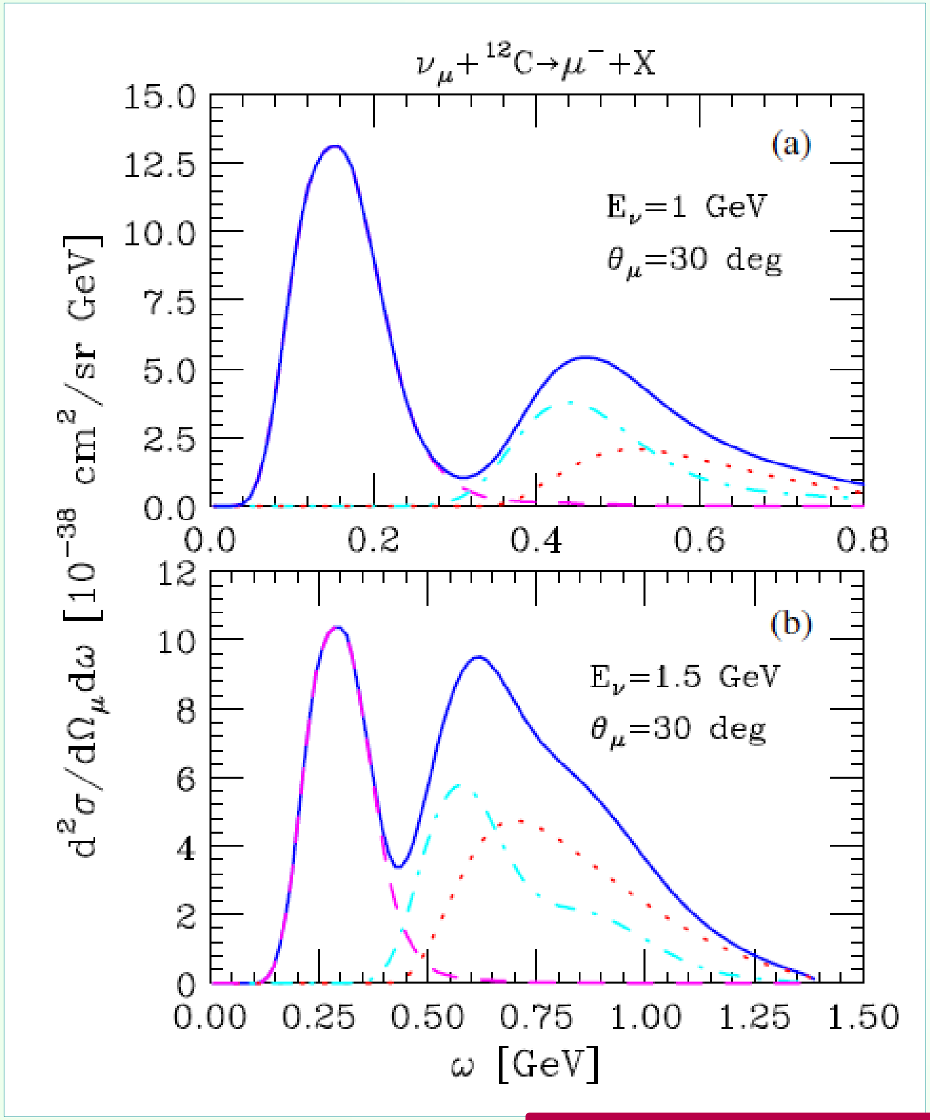

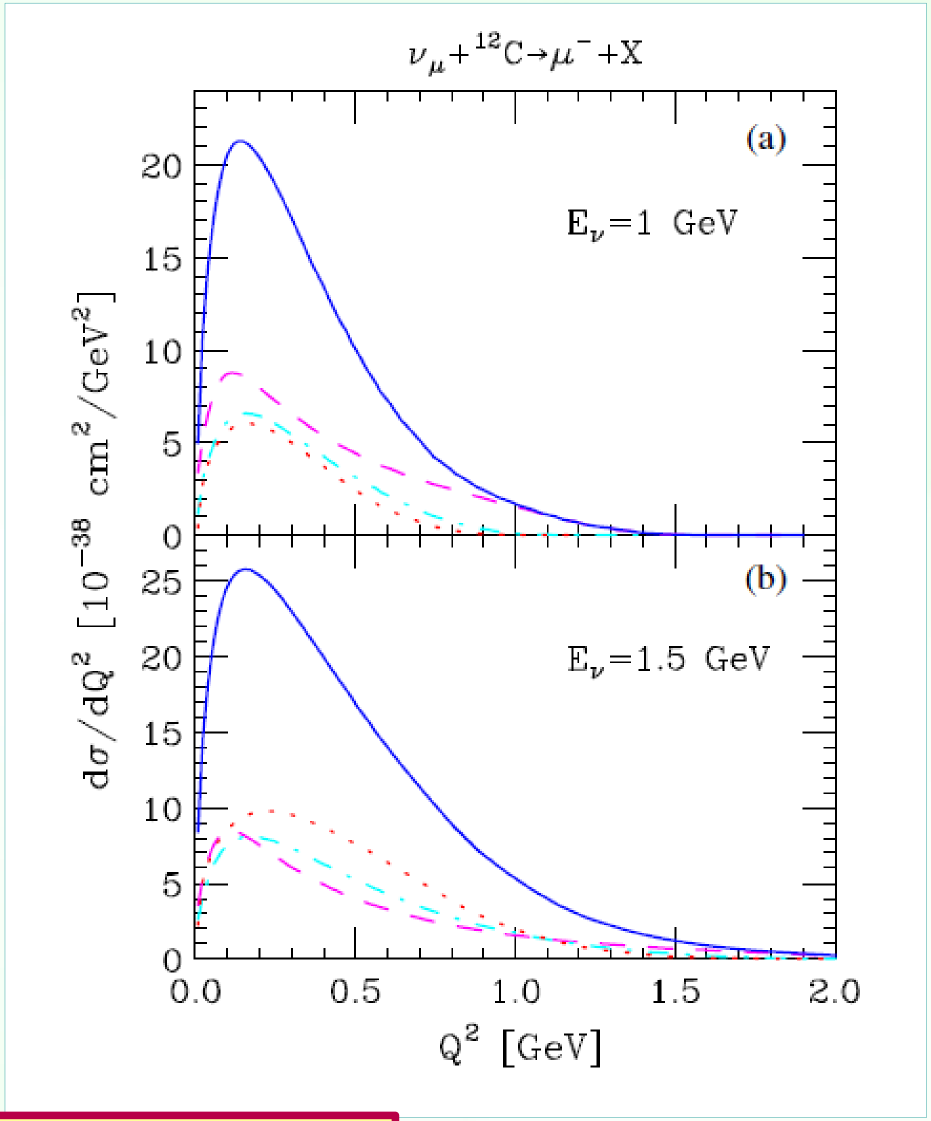

Vagnoni *et al.*, PRL 118, 142502 (2017)

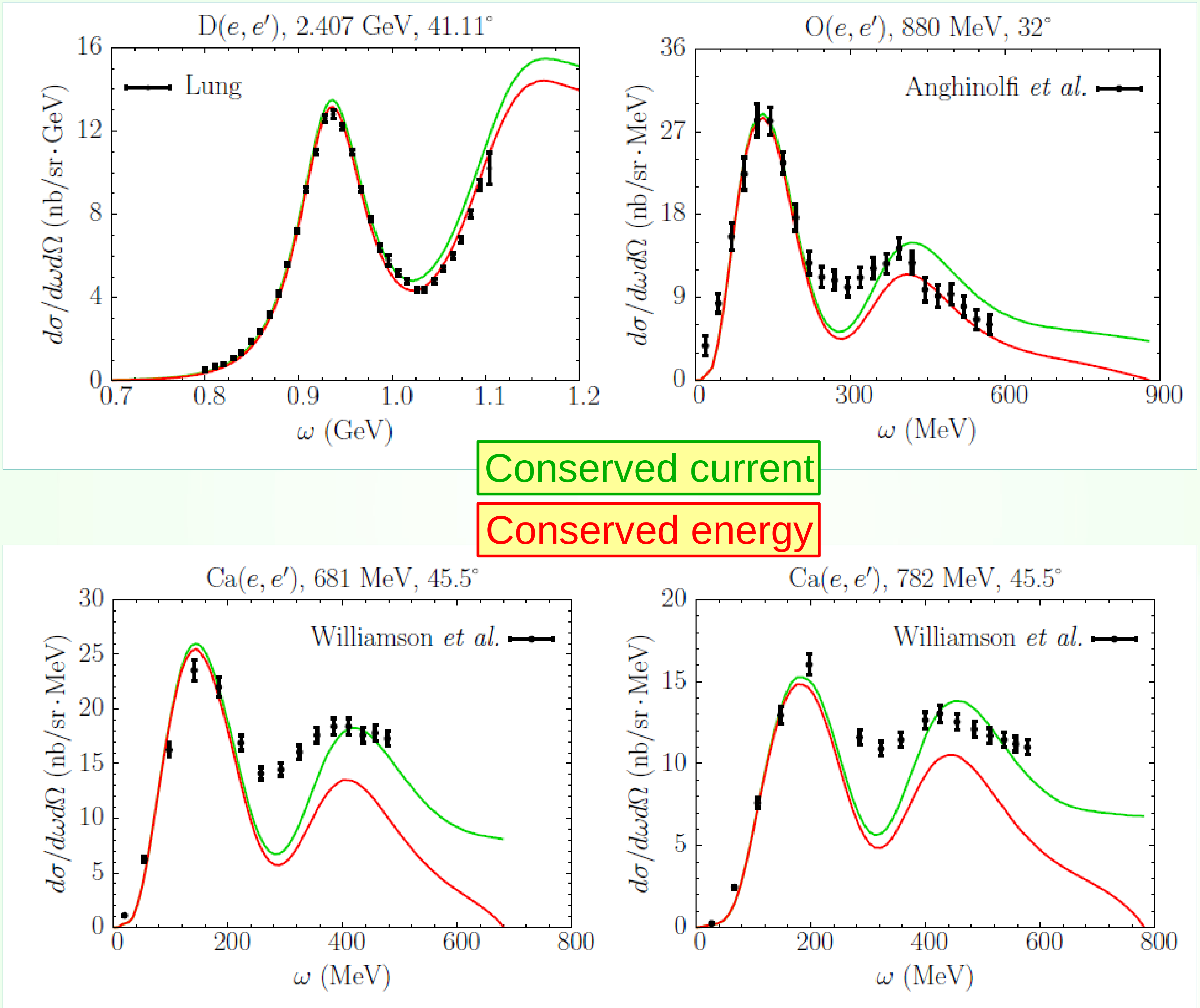

D(e, e′), 2.407 GeV, 41.11°
Lung
dσ/dωdΩ (nb/sr·GeV)
ω (GeV)
O(e, e′), 880 MeV, 32°
Anghinolfi et al.
dσ/dωdΩ (nb/sr·MeV)
ω (MeV)
Conserved current
Conserved energy
Ca(e, e′), 681 MeV, 45.5°
Williamson et al.
dσ/dωdΩ (nb/sr·MeV)
ω (MeV)
Ca(e, e′), 782 MeV, 45.5°
Williamson et al.
dσ/dωdΩ (nb/sr·MeV)
ω (MeV)

Other NC and CC QE data

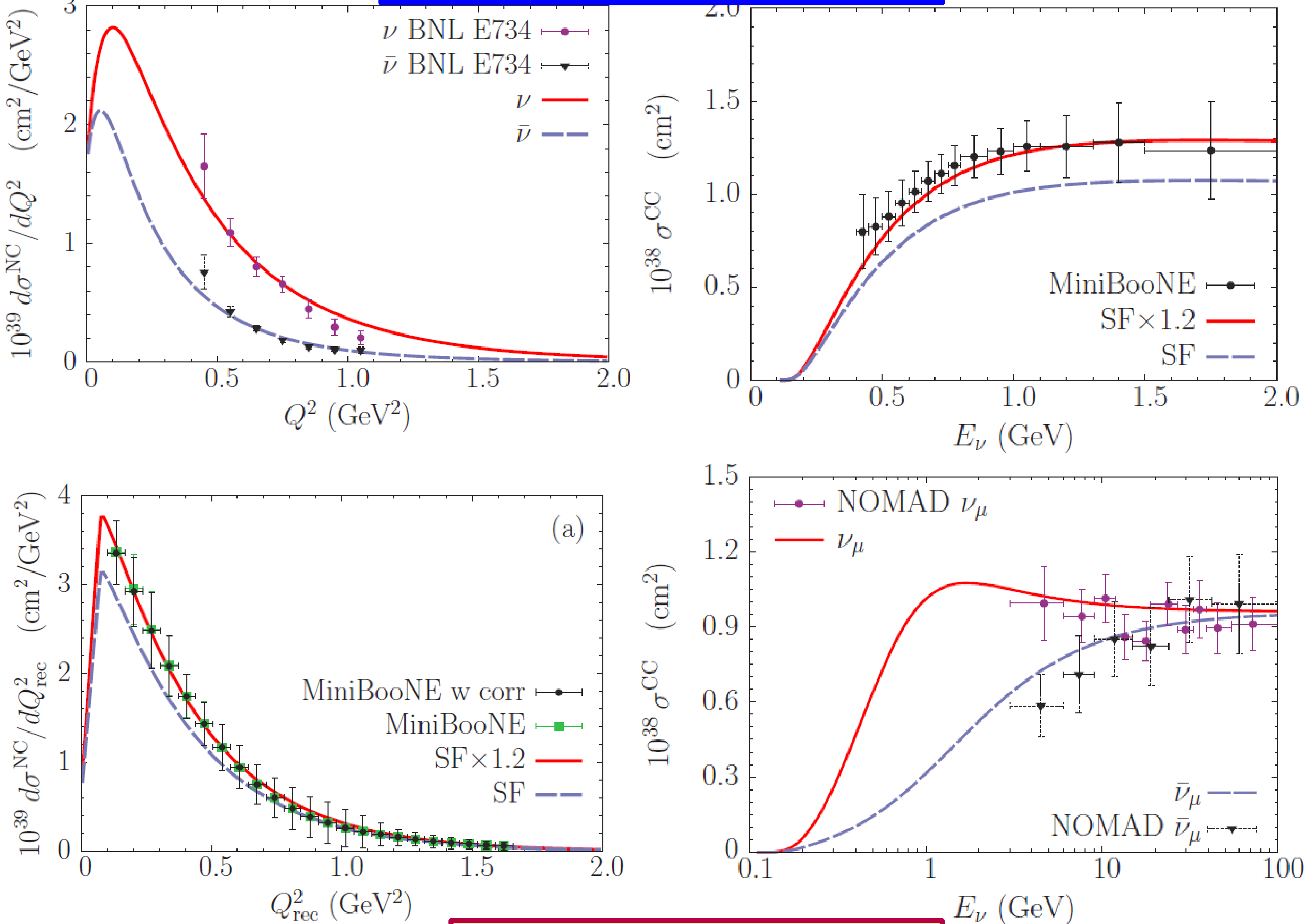

A. M. A, PRC 86, 024616 (2012)